JPRS-CST-87-004

10 FEBRUARY 1987

China Report

SCIENCE AND TECHNOLOGY

FBIS FOREIGN BROADCAST INFORMATION SERVICE

NOTE

JPRS publications contain information primarily from foreign newspapers, periodicals and books, but also from news agency transmissions and broadcasts. Materials from foreign-language sources are translated; those from English-language sources are transcribed or reprinted, with the original phrasing and other characteristics retained.

Headlines, editorial reports, and material enclosed in brackets [] are supplied by JPRS. Processing indicators such as [Text] or [Excerpt] in the first line of each item, or following the last line of a brief, indicate how the original information was processed. Where no processing indicator is given, the information was summarized or extracted.

Unfamiliar names rendered phonetically or transliterated are enclosed in parentheses. Words or names preceded by a question mark and enclosed in parentheses were not clear in the original but have been supplied as appropriate in context. Other unattributed parenthetical notes within the body of an item originate with the source. Times within items are as given by source.

The contents of this publication in no way represent the policies, views or attitudes of the U.S. Government.

PROCUREMENT OF PUBLICATIONS

JPRS publications may be ordered from the National Technical Information Service, Springfield, Virginia 22161. In ordering, it is recommended that the JPRS number, title, date and author, if applicable, of publication be cited.

Current JPRS publications are announced in Government Reports Announcements issued semi-monthly by the National Technical Information Service, and are listed in the Monthly Catalog of U.S. Government Publications issued by the Superintendent of Documents, U.S. Government Printing Office, Washington, D.C. 20402.

Correspondence pertaining to matters other than procurement may be addressed to Joint Publications Research Service, 1000 North Glebe Road, Arlington, Virginia 22201.

JPRS-CST-87-004
10 FEBRUARY 1987

CHINA REPORT
SCIENCE AND TECHNOLOGY

CONTENTS

PEOPLE'S REPUBLIC OF CHINA

NATIONAL DEVELOPMENTS

/9987

STATE DESIGNATES 70 NEW TECHNOLOGIES FOR DISSEMINATION

Beijing RENMIN RIBAO OVERSEAS EDITION in Chinese 11 Oct 86 p 4

[Report by Li Dejin [2621 1795 6855]: "State Determines Dissemination of 70 Major New Technologies That Will Generate Great Effects for National Economic Construction"]

[Text] As learned from the State Economics Commission: during the period of the Seventh 5-Year Plan, we will in this country disseminate 70 major new technologies from science research that have outstanding economic and social results. Among them 20 have been selected from achievements in problem solving for national science and technology during the Sixth 5-Year Plan. Some of these new technologies are the first of their type in this country, and some are in foremost positions throughout the world or have attained advanced international levels. After they have been disseminated and applied, they are sure to play a promotional role in the four moderizations in this country and will lay a firm foundation for realizing the Seventh 5-Year Plan.

The state has determined that the principles for these major disseminated projects are: 1. that they be scientific and technical achievements that have outstanding economic and social results, technical advancement and maturity, large scale use of applications, and small investment and quick results; 2) that they be scientific and technical achievements that can improve quality, lower goods and materials consumption, and increase the capability of generating foreign exchange through exports for agriculture and forestry, light industry, energy resources, transportation, raw materials, and the electromechanical industries; 3) that they be scientific and technical achievements that can aid the strengthening of the capacity for new products and new technology development for traditional industries and be scientific and technical achievements with great adaptability for the technological transformation of enterprises.

At the top of the list of major projects for dissemination is a long-grained, non-glutinous hybridized type of rice, the high yield and superior breeding and cultivation techniques for which once won a special national prize for invention during the Sixth 5-Year Plan. Every technical index regarding the level of breeding, cereal rice quality, and economic results for this technology occupies a leading position in the world. Cultivation of more than 100 million mu during the period of the Sixth 5-Year Plan proved its

characteristics regarding high yield, superior quality, mixed resistances, and adaptability. Comparing it to conventional rice, yield can be increased by an average of 50 to 75 kg per mu, with a savings of 10 kg of rice seed. During the Seventh 5-Year Plan, this nation plans to extend this to 73,000 mu in 13 provinces and districts in the south, where it is estimated it could raise yields of paddy rice by 13 billion kg, save 1.73 billion kg of rice seed, and gross economic results could be in the billions of yuan.

On this occasion of nationally disseminating projects in major new technologies, there are 9 technologies involved with high-grade, high-yield, and freshness preservation in the industries of agriculture, animal husbandry, by-products, and fishing; 2 in afforestation technologies for national territory; 6 in light industries and technologies for medicine and health care; 11 high efficiency technologies for conserving energy resources and materials; 11 basic technologies for the electromechanical industries; 9 application technologies for new techniques and new materials; and 2 technologies for the transformation of traditional industries. In addition, there are also 20 other new technologies such as technologies for the production of new products in agricultural chemicals that are highly efficient and have low residue.

It has been said that a plan for guiding the dissemination of these 70 major new technologies has been drawn up to be implemented everywhere throughout the country.

12586
CSO: 4008/2012

WEAPONS SHOWN AT INTERNATIONAL TRADE EXHIBITION

Beijing RENMIN RIBAO OVERSEAS EDITION in Chinese 14 Nov 86 p 3

[Report by Liu Litian [0491 7787 1131]: "Cooperation in Military Technology Benefits Economic Construction"]

[Text] At the international exhibition of defense technology held not long ago in Beijing, 160 military-industrial enterprises from 12 nations and regions of 4 continents participated. Among the more than 1,000 products exhibited, there were both advanced military weapons systems that are well known far and near and highly effective and also unprecedented weaponry that embodies a refinement of the newest scientific and technical achievements. From the forms and substance of material objects, models, pictures, and video provided in the exhibition, this was the first time an international defense exhibition of such a scale had ever been held in China.

At this exhibition China broke from the examples of the past, and from Chinese modern-era companies, such as NORINCO, CATIC, China Precision Machinery Import Export Company, the China Electronics Import Export Corporation, and the China Atomic Energy Industrial Company, formed a strong line-up of Chinese exhibitors to participate in the exhibition. In systems were presented Army-Navy-Air Force tri-service equipment and the newest weapons systems, all designed and built by China, as well as carrier rockets and communications satellites representative of China's highly sophisticated scientific and technical equipment technology. More than 300 products fully displayed the newest accomplishments of Chinese national defense modernization. The infantry fighting vehicle exhibited for the first time in the China pavilion, cooperatively produced and improved by Chinese military-industrial enterprises together with foreign military-industrial firms such as the American FMC Corporation and the British Vickers Company, drew the most attention. From this exhibition, many foreign firms came to understand the true power of China, they sought a basis for cooperation, and in great numbers indicated their hopes for broad exchanges.

Premier Zhao Ziyang has recently emphasized that in the areas of developing weaponry and weapons technology, China will continue to be self-reliant, but at the same time will develop cooperation and exchanges abroad, which will include the development of trade in military goods. The exhibition of military goods jointly produced by China and foreign interests have clarified the fact that exchanges and cooperation with foreign interests in the field of defense technologies after industrial, agricultural, and scientific and

technical cooperation is very effective. Now, China has already developed exchanges and cooperation with more than 10 countries in dozens of products.

The goals for exchanges of military technology and trade in military goods are to promote the progressive modernization of weaponry, to improve self-defense capabilities, to import advanced technologies on this account, and by which may also be improved the levels of national economic construction. Defensive tactical guided missiles, tanks and armored vehicles, nuclear technology and equipment, military naval vessels, aircraft, and radar facilities are all comprehensive weapons systems that are technology intensive. They make broad use of microelectronics, lasers, millimeter waves, optic fibers, and new materials and technologies, combining light, machinery, and electricity into the organic whole of modern technical products. The newest materials and modern technologies used in these military products, the problems involved with energy resources, transportation and shipping problems, and the automation, artificial intelligence, and remote control of aircraft, guided missiles, military naval vessels, and tanks are completely in keeping with the demands of modernization in each sector of the national economy. Consequently, we may completely use the essence of the science and technology that has been used in the human intelligence involved with military affairs in dealing with peacetime building and to enrich the people. China's use of the Long March No 3 carrier rocket to launch satellites for resource surveys, communications and television, and environmental protection in accordance with the wishes of any country in the world is the most obvious true example of using military technology to enrich mankind. China is definitely not involved in the arms race of the superpowers. Instead, its focus is on economic construction. In China, many military-industrial enterprises have changed to civilian ones, and countless munitions technologies have realized economic results in the national economy. As for example the timely use of imported nuclear technology to build the Daya Bay nuclear power plant, military-industrial enterprises manufacturing civilian aircraft, as well as the active use of tank tread technology in territorial exploitation and oil field communications and exploration, and to produce the sea and beach operations vehicles needed at the Shengli oilfields, the high powered bulldozers for the Xinjiang desert area oilfields, and household electrical appliances to enrich the people's lives.

Therefore, using the crystallization of scientific knowledge that is in military technology for economic construction has a broad development future in China, and China is an important marketplace that has great potential for foreign firms. Concerned leaders in China have said that China welcomes foreign military-industrial enterprises and civilian products companies coming to China to develop and expand jointly funded operations, cooperation production, compensation trade, and import processing. It invites them to initiate the development and production of military and civilian goods and to allow the friendly cooperation in opening up channels of information between industrial and trade circles in all countries, in freeing up routes for thinking, and in promoting the prosperity of science and of the economy to reach new extents.

12586
CSO: 4008/2017

CHINESE COOPERATION WITH GDR IN HEAVY EQUIPMENT NOTED

Beijing ZHONGGUO JIXIE BAO in Chinese 23 Sep 86 p 1

[Text] A few days ago, when the deputy minister of the GDR Ministry for Construction of Heavy Machinery and Equipment, (MA YI), was interviewed by reporters, he stressed that with the constant strengthening of friendship between the peoples of the two countries of Germany and China, the GDR would be enhancing its cooperation with China in the areas of provision of equipment and the transfer of rights to technology.

Vice minister (MA YI) said that the GDR Ministry for Construction of Heavy Machinery and Equipment primarily manufactures engines, diesel engines, power generation equipment, cement, rolled steel, sugar refining, and refrigeration equipment, complete sets of equipment for electric cable plants, as well as large scale equipment for deep-water ships; it is a major industrial department with 11 joint enterprises and 330,000 staff and workers. In recent years, many products have attained a higher reputation in international markets due to a widespread development of technological innovation and vigorous dissemination of applied new technologies.

When speaking of the traditional friendship with China, vice-minister (MA YI) said that as long ago as the 1950's the GDR has begun to provide equipment to China, over time providing China with power generation equipment, caterpillar-tread cranes, forklifts, cold storage vehicles, steel rolling equipment, grinding apparati and processing equipment. He said that through the mutual visits of ministers of heavy machinery ministries of the two countries both parties have determined the major points of cooperation. He indicated that they hoped to be carrying on cooperation with China in regard to many projects such as strip-mining equipment, harbor transformation projects, steel rolling equipment, cement equipment, and cold storage vehicles through means such as the provision of equipment and transfer of the rights to technology.

12586
CSO: 4008/2012

SHANGHAI ELECTRICAL PLANT EXCHANGES WITH GERMAN COMPANY

Beijing RENMIN RIBAO OVERSEAS EDITION in Chinese 15 Nov 86 p 3

[Report by Sun Lin [1327 2651]: "Two Electric Machinery Plants in China and West Germany Exchange Plant Directors to Improve Enterprise Quality by Personally Searching for Disparities"]

[Text] The Shanghai Electric Machinery Plant has exchanged factory directors with the generator plant of the Siemens Company of West Germany, and has imported modern management methods from them.

The first exchange has already been concluded. Factory director (AI XI TUO MA YA) of the generator plant came to this country to assume the post of advisor to the Shanghai Electric Machinery Plant director. After undertaking 4 weeks of surveys and observation, he recently presented an initial "diagnosis report" on the enterprise to Li Wenhua [2621 2429 5478], plant directory of the Shanghai Electric Machinery Plant, and has returned to his country.

In May of last year, the Shanghai Electric Machinery Plant signed an agreement with the Generator Plant whereby the plant directors of both plants would exchange positions. From November of last year to February of this year, factory director Li Wenhua of the Shanghai Electric Machinery Plant and 3 aides went to West Germany where they acted as aides to the generator plant director, learning management on the job for 3 months. At that time, Li Wenhua worked as an aide to the German factory director in the same office. They went together to visit the workshops, participated in conferences, listened to reports, and Li came to fully understand the modern management methods of this similar profession with very strong competitive capabilities in the international market. This ranged from the activities of entering bids, quoting prices, designing, and manufacture, all the way to sales and service. After plant director Li Wenhua returned to this country, he spoke to cadre and specialists throughout the plant on 9 occasions about his experiences, and established a working group to formulate plans and study the gradual learning from and application of the modern management methods of the generator plant.

This was the first time in this country that modern management methods were brought in through this kind of exchange of Chinese and foreign currently employed factory directors. The generator plant is one of the most famous

electrical machinery manufacturing plants in the world. Their products are very competitive in the international marketplace. The Shanghai Electric Machinery Plant is also one of the more advanced well-known enterprises in China, and their volume of medium to large scale electrical machinery production and labor productivity are in the forefront of those in this country. But there are still great disparities when compared with the generator plant. Labor productivity, for example, is only one-ninth of that of the generator plant. By exchanging current plant directors, the Shanghai Electric Machinery Plant brings in modern foreign management methods, which will improve labor productivity and at the same time will further promote a cooperative partnership relationship between the two plants.

Currently, the first round of exchanges of plant directors between the two plants has been completed. The Shanghai Electric Machinery Plant is summing up the results from the exchanges, will gradually implement them, will strive to obtain substantial results, and after that will continue in accordance with the original agreement, implementing the second round of plant director exchanges.

12586
CSO: 4008/2017

SHIPYARD MAKES GOOD USE OF HIGH EFFICIENCY WELDING

Beijing CHUANBO SHIJIE [SHIPPING WORLD] in Chinese 12 Sep 86 p 4

[Text] Welding is one of the important work processes in ship construction, and the work time for welding is 30-40 percent of the total time to build a ship. Therefore, the level of welding technology and of productivity is directly related to the quality of shipbuilding and the construction process. As annual shipbuilding tonnage at the Jiangnan Shipyard continues to rise (this year, annual shipbuilding production can be expected to exceed 150,000 tons), individual vessel tonnage has gone from the 10-20,000 tons of the past toward the current 30-60,000. That means that in both quality and quantity, the demands on welding are increasing. In such a situation, to actively use various high efficiency and specialized welding technology has become the key to advancing shipbuilding manufacturing trends in the directions they must go.

In recent years, the Jiangnan Shipyard has paid special attention to the approval of welding methods and the approval of welding testing and qualifications, as well as to basic work in documents on welding construction techniques and on welding technology management. They have energetically disseminated the six highly efficient welding techniques of gravity welding, CO2 shielded welding, descending welding, FAB gasket welding, iron powder welding, and submerged arc welding. Last year, 38.46 percent of welding equipment at the Jiangnan Shipyard was specialized, average consumption of welding materials for welding per day per man was 6.97 kg, which was foremost among shipyard enterprises affiliated with shipping industrial corporations in China.

In the process of disseminating applications for highly efficient welding, the Jiangnan Shipyard both improved the quality of hull construction and reduced time and lowered costs, all through attention from leadership, clarification of goals, organizational strengthening, and the implementation of measures. This allowed highly efficient welding to expand annually in the scope of applications in shipbuilding production. For example, on the 65,000 ton oil tanker "Liu He" that was recently launched, the CO2 single surface welding technique was applied in the construction of 48 middle closing-up segments. According to statistics, in 1985 the Jiangnan Shipyard saved more than 90,000 hours in welding time because of the dissemination of high efficiency welding and saved more than 33 tons of welding materials, which amounts to a total of more than 400,000 yuan. In the construction of 6 20,000-ton class cargo ships

last year, the berth period was reduced an average of 15 days for each vessel, which allowed the construction time for all vessels to be reduced a total of 90 days and produced better economic results.

This year, in its plans for annual technology advancement at the factory, the Jiangnan Shipyard has integrated practices in shipbuilding production to continue to focus on the active dissemination and application of high efficiency welding. Because of this, hull workshops have specifically formulated "Schedules for the Dissemination of High Efficiency Specialized Welding Methods," and have striven to bring new breakthroughs to proficiency indexes for welding specialization.

12586
CSO: 4008/2012

AERONAUTICS INDUSTRY DEVELOPS CIVILIAN PRODUCTS

Beijing ZHONGGUO JIXIE BAO in Chinese 23 Sep 86 p 1

[Text] Since the April conversations between ministers of the Ministry of the Machine Building Industry and the Ministry of Aeronautics, inter-ministry relations have improved, which has promoted cooperation between the military and civilian sectors. The first group of enterprises and factories of the Ministry of Aeronautics have striven to develop key parts and components and basic components for civilian-use machinery in accordance with the needs of the marketplace and their own characteristics, from which they have obtained excellent economic results.

In hydraulics, pneumatics, and hermetics, the Liaoyuan Machinery Plant has the upper hand. As of now, this plant has developed 5 large categories of products in a complementary series, and its output value for civilian products has reached 8 million yuan. Some of those basic components such as hydraulic assemblies and an engineering mechanical hydraulic oil cylinder have been broadly adopted by several motor vehicle plants such as Erqi, Jiqi, and Shanqi and by fork lift plants in Baoming, Guangzhou, and Jingjiang in Jiangsu Province. Among the equipment imported by the Wuhan Iron and Steel Mill was a type of balance cylinder that the Japanese would only guarantee for 6 months use, while the balance cylinder developed by this plant has a life expectancy several times that of the Japanese product after supply by the Whan Iron and Steel Mill.

The Qunfeng Machinery Plant has made use of forging specialties to develop industrial tools for charged operation on high-voltage power lines. These completely aluminum industrial tools are strong, light, small and flexible, and have been well received by operational workers.

12586
CSO: 4008/2012

EFFORTS TO INDIGENIZE VEHICLE PRODUCTION REPORTED

Beijing RENMIN RIBAO OVERSEAS EDITION in Chinese 15 Nov 86 p 1

[Text] Beijing, 14 Nov XINHUA--From now on, vehicles cooperatively produced by China and foreign interests will not concentrate on importing assembly lines for component assembly, but instead will to the greatest degree possible use advanced foreign technology to arrange for the production of parts and components or for assembly. There will also be a number of products that can be exported.

Chen Zutao [7115 4371 3447], general manager of the China Automotive Industries Company, today described this method as an "important principle" for the Chinese-foreign cooperative production of vehicles as he was interviewed by reporters from this news service.

He said that from now on, for vehicles produced by new jointly funded enterprises, their primary components should be made in China.

Currently, China is running some jointly funded enterprises with vehicle production plants from the United States, West Germany, and France.

Chen Zutao said that "to improve the environment for investment by foreign firms in these enterprises, we are in the process of making reasonable arrangements. But the distinguishing feature of these enterprises has been that they have first imported assembly lines to assemble foreign vehicle components, and progress in the indigenization of the production of parts and components has been slow, quite unsatisfactory."

He said that "some foreign firms are selling components and parts, then selling the entire vehicle after assembly in China. The Chinese side allows foreign firms to earn money in this way and also allows the release of a portion for domestic markets, the goal being to master the technology. But if some cooperative partners do not see to the interests and demands of China, but plan only the interests of one side, intentionally delaying the Chinese nationalization of parts and component production, that would then not be fitting with what we have expected."

Chen Zutao said that China is the broadest market for the automotive industry. Within 10 years from now, the production of ordinary car models will be on the

agenda, and if there is only 1 vehicle for every 100 households, the total quantity needed could reach 2 million vehicles. After 10 years, China will strive for at least 15 percent of domestically produced vehicles to be in international markets.

He said that to reach the aforementioned goals, the automotive industry will require a great deal of funding and advanced technology, and cooperation with foreign interests has a very broad future.

According to what this general manager has said, firms from the United States, Japan, West Germany, France, Italy, Brazil, Chile, Spain, and some countries in Eastern Europe are currently in contact with China, and some countries are preparing to provide long term low interest loans for the development of China's automotive industry.

12586
CSO: 4008/2017

SHANGHAI INDUSTRIAL TECHNOLOGY LEVELS EVALUATED

Beijing RENMIN RIBAO OVERSEAS EDITION in Chinese 14 Nov 86 p 3

[Report by Xu Jiazhu [1776 1367 2691]: "The Level of Industrial Technology Determines Scientific Methods to be Used"]

[Text] Shanghai, 10 Nov (XINHUA)--The city of Shanghai has successfully completed studies into using scientific methods to comprehensively determine the level of technology for every industry and profession in this country, and recently this has been evaluated by the municipal science and technology commission.

Because these kinds of studies affect the selection of overall decision making, investment directions, projects, and levels of technology, they have attracted the attention of industries, science and technology circles, and some provinces and cities in this country.

To scientifically evaluate a level of technology is to determine an important premise for dealing with technological progress. But at present when many industries and enterprises in this country evaluate their levels of technology, they still focus on empirical appraisals or look only at a few technical indices, and therefore lack standardization and comprehensiveness. More than 40 specialists from units such as the Shanghai Foundation for Advances in Industrial Technology pointed out for the first time in their study "A Representative Survey and Projected Plan for Shanghai Industrial Levels of Technology" methods and standards for a systematic review of the levels of industrial technology in terms of 3 administrative levels and 4 aspects. They determined the levels of technology for a particular industry and other industries considered as a group through the three levels of analyzing products, related products, and related products in other industries; then, through the four aspects of analyzing the levels attained by products, the levels of key technologies for products, the levels achieved by production technology, and the levels of key technologies for production technologies, they were able to determine product levels and levels of technique and technology.

Those specialists participating in this evaluation felt that this method of projection that is a system having a set of standards can distinctly display through data and graphics the current state and the dynamic state of each

important aspect in an industry or the level of technology for an industry. This can consequently help people see their own gaps, for which they can take appropriate measures and strive to reduce these gaps. This will both help the progress as enterprises take control of advances in technology and can also provide a basis for overall policy making.

12586
CSO: 4008/2017

OVERVIEW OF DRUG QUALITY CONTROL

Beijing YAOXUE TONGBAO [CHINESE PHARMACEUTICAL BULLETIN] in Chinese Vol 21, No 6, 8 Jun 86 pp 323-327

[Article by Zhou Haijun [0719 3189 6874], Chinese Bureau of Drug and Biological-product Control]

[Text] The promulgation of the "Drug Administration Bill of the PRC" marks the legalization of China's drug control and management. This is an important decision made by the state and the party to improve and strengthen drug administration in order to protect the health of the public. How do we, as workers in the field of drug control, implement and gradually perfect the drug control bill to serve better the public's need for an effective and safe application of drugs? Based on the actual situation in China, it is likely that, for a rather extended period, the further integration of drug administration and drug control and the combination of management and technology have to be dealt with properly so that drug control can play an even more significant role in overall drug quality assurance and clinical pharmacology. Looking into the future with these understandings, I am going to discuss some personal observations on the developing trend of drug control.

Quality As Top Priority and Comprehensive Quality Control

Drugs are special commodities that mankind uses to prevent and cure diseases. The manufacture of drugs is both a social and economic activity and a business of social welfare. When there are conflicts between the two, the protection of the people's health and lives must be the prime consideration. Only by protecting the labor force and ensuring that the masses possess the energy and vigor to be dedicated to the cause of socialism can the maximum macroscopic economic benefits be realized. This is the most significant contribution the health profession can make to the socialist modernization constructions. Therefore, one cannot simply look at the output, output values, and profits when assessing the importance of an enterprise or a product. It is more appropriate to look at its impact and role in the prevention and treatment of diseases.

In the concepts of modern management, the quality assessment of a drug is no longer confined to checking whether it meets the specifications or not. Rather it involves the quality assurance of all segments from R&D, production, quality

control, and distribution to clinical application. It can be done only through the joint efforts and close cooperation of all departments. In the comprehensive quality control effort, the drug administration and drug control departments exercise their authority only over approval, supervision, testing, and monitoring as well as in the area of administrative discipline. Likewise, the production and management departments have to treat the implementation of the drug bill as their own responsibilities, establish a comprehensive quality control concept, and improve quality control. Only through coordination, and with each discharging his own responsibilities, can the gradual improvement of China's drug quality be assured. In the effort to carry out the comprehensive quality control, I believe the following areas have to be handled properly.

1. Improve the Examination and Approval of New Drugs

Evaluating a new drug means assessing the quality of a new drug's R&D efforts and determining, through clinical tests, whether the new drug is beneficial to the health of people. This is an important first step in the assurance of the product's quality. Therefore, the bill mandates that all new drugs be examined and approved only through the Ministry of Health. Fifty-five medical and pharmacological experts have been invited to join the Drug Evaluation Committee of the Ministry of Health. The Office of the Drug Evaluation Committee has been established to serve as a technical consulting body in helping the ministry carry out the examination and approval of drugs.

For the proper execution of new drug evaluations, the Ministry of Health has formulated the New Drug Examination and Approval Measures with detailed rules and regulations. New drugs are defined in it as those that have never been manufactured in China. For the drugs already in production, expanded application and changes in the method of administration and in drug formulations all qualify as a new drug. For management purposes, it is necessary to divide Chinese and Western medicines into five categories. Each category has different requirements for data submitted with its application and has different clinical regulations. There are also explicit rules for new biological products. Thus, the past situation where examination and approval was done separately by the provincial governments, autonomous regions, and municipalities directly under the central government has changed, in which the chaos and confusion resulting from different products sharing a same name or the same product having different names. The problem of insufficient data for quality control resulting from variations in technical capabilities of each location and differences in the strictness of standards have been overcome. It can be envisioned that, through stringent evaluation of new drugs and the improvement of legal procedures and technical requirements; the scientific level of drug research will be raised; that laboratory research, clinical tests, development and production, and clinical applications will be better integrated; that the competition between institutions and projects will be livelier; and that conditions for stepping up to the advanced domestic or international level will be created.

The key to conducting proper examinations and approvals of new drugs lies in science and technology. Advanced experiences abroad should be absorbed and the situation of China be taken into account in determining the requirements for

new drug approvals. Under the premise of assuring effectiveness and safety, an appropriate balance should be reached. To accomplish this depends on the drug administration and control departments of every province, autonomous region, and municipality directly under the central government to handle properly the preliminary evaluations in accordance with the measures formulated by the Ministry of Health, and on the collective wisdom and strength of the Drug Evaluation Committee of the Ministry to handle properly the examinations and approvals. It is also necessary to review constantly past experiences so that the New Drug Examination and Approval Measure is gradually improved and perfected.

2. Production Departments' Active Implementation of GMP

GMP (good manufacturing practice) means the quality control of the whole production process of a drug. The quality of a product can be assured only by adhering strictly to the requirements and specifications for every step from raw-material purchase, storage, testing, processing technology, and product testing up to the delivery of the product. The most vigorous measure in drug quality assurance is implementation of the GMP system. Its purpose is prevention. In theory, the quality of a drug is established during the production process by the technical staff and production workers rather than by testing and monitoring. Product testing only locates problems but cannot solve them. Once a product fails to pass, the loss to the state becomes a fact. Therefore, the most vigorous measure to assure the quality of drugs starts with following closely the basic requirements and operational standards of every step in the production process. For drug administration departments, the GMP should be regarded as the minimum standard a government proposes to the drug manufacturers and is the principal basis on which drug inspectors examine and monitor drug productions. For drug manufacturers, the GMP should be regarded as the technical level a factory is required to attain in its production and management. With the implementation of China's open-door policy, Chinese medical and pharmaceutical products are moving onto the international market and it is imperative under the circumstances that the GMP system be implemented. The National Bureau of Drug Administration is planning the GMP system and moving toward its implementation. Workers in the drug control area should earnestly acquire knowledge about the GMP, drop the idea of being responsible simply for product inspection, and be gradually geared toward the needs of comprehensive quality control. Only by doing so can we meet the needs of developing circumstances.

In order to speed up the pace of pursuing the GMP system, the Ministry of Health is actively working on the national GMP system. Supervisory and production departments should work together and coordinate with each other in training management and technical staff and production workers. First of all, the traditional idea of quality control, bad operational practices, and out-of-date production conditions ought to be changed. For the factories manufacturing preparations and products for export, for new plants, and for joint-venture plants involving foreign partners, strict inspection before acceptance and key transformations should be done according to the GMP requirements with the hope that, with 3 to 5 years of effort, a group of plants and workshops that meet the requirements of GMP will emerge so as to raise the level of the pharmaceutical industry.

3. Establish an Adverse-Effect Reporting System

In the process of preventing and treating diseases, drugs used often promote reactions that are not associated with their intended therapeutical purposes such as side effects, toxicity, allergies, complications, addiction, and the "three causes" reactions. These undesirable effects can be discovered only through the monitoring and reporting of any adverse effect after a drug is on the market. Furthermore, it has to be systematic in order to be able to carry out the monitoring more effectively and steadily. This is because before production, and particularly before approval, of a drug all the tests are done on animals. There are inherent differences between animals and humans and they do not respond to a drug in exactly the same way. In addition, clinical tests are done on a limited number of subjects and may not be able to detect rare clinical reactions. By simple probability, in order not to miss 1 case of abnormal reaction to a drug in 1,000 ($P = 0.95$), it is necessary to examine 3,026 clinical cases. This is hardly realistic in clinical trials of new drugs. Only by implementing the adverse-effect monitoring and reporting system can we forecast and give warnings about any serious adverse effect. It also enables us to provide guidelines with regard to the reasonable dosage in clinical applications, to correct the problem of insufficient data at the time of examination and approval, and to provide a basis for judging the overall merits and drawbacks of a drug and for banning the drugs with serious flaws. The Ministry of health in recent years has established over 10 clinical centers. Certain progress has been made in the constant improvement and reinforcement of the construction of these centers.

At present, a primary center at the national level for monitoring the adverse effects of drugs and its local counterparts should be established to form a network; more testing sites should be established and contact with the WHO monitoring center should be strengthened; a monitoring and reporting system should be formulated and issued; procedures for determining adverse effects should be formulated; an information exchange system should be established; and research should be carried out. Drug control departments should be actively involved in these tasks so as to raise the level of drug monitoring and testing and the level of drug standardization.

Quality Control of Biotechnology Products

Biotechnology products are those medical products manufactured on an industrial scale by a cell of tissue culture technology that employs new biological species whose functions have been altered through gene manipulations by taking advantage of the recent advances in modern biotechnology, cell biology, and molecular biology. Biotechnology has become an integrated science and technology system to achieve specific goals and includes genetic engineering, cellular engineering, enzyme engineering, and fermentation engineering.

Modern biotechnology was first used in the medical area. In the past decade, it has been actively applied in the health-related field, making up over 60 percent of all biotechnology R&D efforts. The United States has formally approved the production of genetically engineered human insulin and growth hormone releasing factor. We started late in China but a medical team has been

formed and some preliminary results have been accomplished. Hybridoma monoclonal antibody technology has been established and propagated, resulting in over 100 varieties of monoclonal antibodies being produced. The reaction of these monoclonals to antigens is highly specific, sensitive, and fast. They can be easily prepared in large quantities. Clinically, they can be used for specific diagnoses and for purifying products of low concentration. Advances in genetic engineering include the high titre or initial expression of such products as interferon, hepatitis-B virus, human insulin, and penicillinase. The industrial-scale culture of ginseng cells is awaiting scale-up.

Quality control of biotechnology products is a new subject that drug control departments have to begin studying because there are inherent differences in the quality standards and testing methods of these products when compared with the traditional methods. In the United States, several guidelines for the assurance of safety, high potency, and high purity have been proposed. Special emphasis has been placed on quality control at each step of the production process such as gene insertion, plasmid construction, cell culture, and purification. In product inspections, the emphasis is on the importance of checking the absence of host DNA because there are oncogenes in the DNA of animal germ cells. A purity check is particularly important to ascertain if the structure of the produced protein is identical with the natural product. It is recommended that 15 amino acids be sequenced from the N-terminal and the C-terminal amino acid be determined. In addition, methods to control biological potency and viral and nucleic acid contamination have to be established. In China, these new technologies and methodologies have to be studied and established in a planned manner so that the quality of new biotechnology products can be controlled in time after their introduction on the market.

Development and Applications of Computer Technology

The development and popular use of computer technology are two signs of a modern society. The State Council formed an electronics revitalization leadership group in 1984 to strengthen leadership in the electronics enterprise and information business and to set the strategy, direction, policy, and measures for their development. The Ministry of Health also proposed the establishment of a national computer network. Controlling the quality of drugs is an important part of the effort in the health area and computer technology should be gradually employed. There are 1 billion people in China who consume over 10,000 varieties of drugs manufactured by 1,600 pharmaceutical companies. Using a computer system to establish a data bank on drug quality would be of tremendous value in helping the national- and local-level drug quality control departments, drug production and sales departments, and research and teaching departments understand and grasp the current situation of drug quality. Based on this, the popularization of computer equipment and the design and execution of data bank projects are currently underway. For those drug data banks that have been approved, including the ones with such subtitles as approved drugs, country of manufacture, drug standards, foreign standards, drug indications and actions, and U.S. FDA-approved drugs, data are being compiled. The design and planning of a quality status data bank for marketed drugs are also underway. Others such as the adverse-effect data bank and the sample management system also should be planned and established eventually.

Limited by current manpower and the financial situation, microcomputers should be emphasized as far as equipment is concerned. Software design should be practical and single machine applications should be implemented first before networking. In the meantime, consideration should be given to the compatibility and matchup between a single machine and the system's mainframe, the feasibility of linking individual machines, the feasibility of advancing from single-item management to comprehensive management, and the standardization and normalization of software design and data bank planning.

The applications of computer technology can be extended to other areas of drug testing. Because the data processing and statistical analysis of biological products are included in the 1985 edition of the Chinese Pharmacopeia, the use of a computer will be advantageous in terms of savings in time, labor, and improved accuracy. Along with the planned development role in the development of the drug control system, the computer will play a significant role in the development of automatic analysis, data processing, and the graphical analysis of a single product. Besides, it has great potential in the task of modern management.

Quality Control of Chinese Medicine

China has an abundant number of traditional medicines. Chinese medicines are particularly effective in treating heart and cerebral diseases, tumors, and hepatitis as well as preventing chronic diseases and slowing down the aging process. Along with increasing awareness of the harmful effects of chemicals and the increasing drug resistance of pathological organisms, more and more attention is being shifted to natural products.

There are many problems facing the development and utilization of Chinese medicines. The demand is increasing and the disparity between supply and demand is getting worse. The supply and quality of Chinese medicines face serious challenges because of insufficient policy studies, management's lagging behind, and a persistently low level of research.

Chinese medicines can be divided into two categories: crude drugs and drug preparations. For crude drugs, items should be selected, through investigation and research and based on the materials doctors of traditional medicine often prescribe, to compile a common Chinese crude-drug catalog of the centrally controlled items. For these items, scientific specifications that truly reflect their quality should be formulated gradually, starting from their sources. Policies should be implemented to guarantee a normal supply. Along with R&D in the principles of traditional medicine, the catalog should be carefully revised. For drug preparations, there are over 6,000 items on the market and it is commonplace that different drugs have a common name and that a drug has many different names. Many of these preparations are based on historical experience. There is an insufficient number of systematic laboratory studies and clinical trials. They need to be included in the national planning and be reorganized through investigation and research. Those institutions with necessary expertise can be organized to evaluate these preparations according to traditional-medicine criteria. Those proved safe and effective should be listed as national standards and a Chinese traditional-

medicine manual should be compiled so that the information can be passed on promptly to traditional-medicine practitioners. Policymaking and other forms of support should be given to the production of these preparations. An effective control measure should be established to eliminate those varieties that are ineffective and whose safe use cannot be guaranteed.

The quality assurance of traditional medicines is manifested in scientific standards and specifications. The bases for the formulation of these standards are laborious investigations and data organization as well as extensive scientific research. The 1985 edition of Chinese Pharmacopeia has 207 items of traditional drug preparations, over 85 percent of which include physicochemical characterizations and microanalyses. But few have the strong scientific specifications that truly reflect their intrinsic qualities. Therefore, the scientific studies of traditional medicine ought to be strengthened. At present, there are two approaches to the study of traditional medicine. One is conducted according to the principles of modern pharamcology. Traditional medicines are treated as natural products and analyses are carried out by using the multiple criteria of the general pharmacology. The action of the drug is studied by using the new techniques and methodologies in biochemistry, immunology, and molecular biology. Or, in conjunction with pharmaceutical chemistry, the active ingredients are extracted, their structures elucidated, and their clinical efficacy observed. The other is to study traditional medicine according to the principles of traditional medicine, confirm the actions and clinical effects described by these principles, and eventually define the indications for each prescription. My personal view is that whichever approach is followed in these studies, they are helpful in improving the quality standards of traditional medicines. Workers in the drug control area not only should study the traditional medicines themselves in a planned and organized manner but should also watch closely trends in domestic and foreign research efforts and use the results of these efforts to improve the standards of traditional medicines. In the attempts to establish standards and determine quality indicators, for those whose effective ingredients are not clear, the overall number of major species or a certain indicator can be determined first for identification purposes. Further studies can then be done to develop methods to determine the content of active ingredients. Also indicators that can reflect the efficacy of a drug should be chosen from the published and established indicators for various pharmacological effects and biological testing methods can be established. Macroscopic control of the intrinsic quality is also an important approach.

Standardization Research

Standardization is a comprehensive task of fundamental importance and an important measure in putting together modernized production. It also plays a significant role in enhancing technological advancement and assuring the quality of products. The most fundamental in the context of standardization is the concept of standards. In order to optimize the national economy, a universal rule is made by a certain procedure and in a certain form, on the basis of scientific data and sufficient consultations. This is called a standard. Standardization implies all the activities involved in the process of setting up and implementing standards.

The extent that standardization is emphasized reflects the level of industrialization and the development of science and technology of a country. The goal of the research on the standardization of drug control is to ensure that the test results are authoritative and reproducible so that accurate and reliable conclusions can be made. The gradual implementation of "good laboratory practices" (GLP) in drug testing is a powerful measure for the standardization of laboratories. It proposes a set of specific requirements for the scientific management of every step, starting from sample collection down to the assessment of experimental results, so as to ensure the quality of the testing. In addition, because there are drug control agencies from the central government down to the provincial, regional, and some county governments in the Chinese system, there must be a guided and gradual implementation of the external quality assessment schemes in order to improve the quality of tests done by authorized testing organizations all over the country. An organizer will give out known or unknown samples to a number of prearranged laboratories for analysis. Each laboratory will carry out the analysis by a specified procedure within a specified time period. All the data will be handled by the organizer and the results from each laboratory will be assessed. To realize standardization, the quality of testing in an individual laboratory will be gradually improved through consultations, training, and comparative appraisals.

The World Health Organization has paid attention to the task of standardization and has established the Department of Biological Standardization and the Department of Specifications and Pharmaceutical Preparations in the Prevention, Diagnosis, and Treatment Section. The goal of standardization is realized through the formulation of specifications and the establishment of standards and references. In the area of hormone assay kits, it has organized, through its coordination center, laboratories at many countries to develop programs for external and internal quality assessment in order to raise the accuracy of each country's assay results. In China, standardization research has not received the proper attention of the leadership. As a result, many achievements of scientific research cannot be translated into social and economic benefits. For example, immunoassay kits have been used in clinical research for over 10 years. They are widely used because they are fast, sensitive, and highly specific. But there is no systematic research on standardization in our scientific research efforts and the quality of each manufacturer's testing kits cannot be guaranteed. There are substantial variations from lot to lot and from one manufacturer to another. Beginning in 1982, the Chinese authority has worked on the assay kits for T_3 (Triiodothyroxine) and T_4 (Thyroxine). Through various measures of standardization, a collection of sera for quality control purposes has been prepared, which is used to monitor production, and the kits produced in several factories have been found to display systematic errors due to mistakes in the preparation of references. The random errors of the tests have been contained through internal quality assessment. Thus the quality of the products has been improved, the test results from different laboratories are comparable, and the measured values are closer to the true values. I wish the related authorities would tackle the large-volume radioimmunoassay kits such as those for hepatitis-B and push for organized research on their standardization.

Pyrogen is a problem that has raised the concerns in the pharmacological field. Because there are certain drawbacks in the rabbit pyrogen test, the study of horseshoe crab (limulus polyphemus) based testing has drawn attention recently in China. The limulus amebocyte lysate (LAL) test is rapid, simple, and sensitive. Research on and the production of LAL kits have been done at locations in Fujian, Zhejiang, Shanghai, and Guangxi. The emphasis is on raising the sensitivity and reducing the non-specific cross reactions. This is certainly beneficial for the rapid clinical testing of endotoxin-tainted blood, bacteriuria, and gram-positive meningitis. However, the pyrogen test described in the Pharmacopeia is actually a positive or negative test. If it is not sensitive enough, it defeats the purpose of the test; if oversensitive, it will increase the chance of false positive results. Also at each production and application stage, contamination by different bacteria occurs. The molecular structures of the endotoxins produced by these bacteria are not exactly identical and the minimum concentration of the toxins to induce response in human varies widely. Therefore, the LAL test standardization efforts involve an array of subjects including the logical selection of endotoxin references, uniformity in the sensitivity of LAL kits, standardization of the LAL test procedure, and the scientific assessment of the standards.

An effective measure for the reasonable use of antibiotics is to check the sensitivity of the bacteria in patients to various antibiotics. This is a gradually accepted practice at some larger hospitals in China. However, because the sensitivity tests adopted by individual hospitals are different and the paper and culture media necessary for the tests are not standardized, the test results are not reproducible and there is no basis for comparing the results from different locations. Now the state has decided to establish a national bacteria drug-resistance monitor center in order to enhance, through standardization, the hospital's bacteria testing and diagnosis as well as the quality of drug sensitivity tests and to provide guidance to the reasonable clinical application of antibiotics.

There is an urgent need to carry out standardization research on Chinese and Western medicines, sera, vaccines, polymers for medical applications, various diagnostic kits, and testing reagents. We should fully exploit the superiority of the socialist system to strengthen close coordination among departments, make use of the standardization accomplished by the International Organization for Standardization (ISO) and World Health Organization, take China's real situation into consideration, and push forward standardization research so as to serve the four modernizations.

Acknowledgement: The author wants to thank Comrades Wang Kaimin [3076 7030 2404] and Zhang Jingbao [1728 2529 0202] for their valuable comments.

12922/12379
CSO: 4008/3002

BRIEFS

BEIJING S&T LABORATORIES NOTED--Statistics from the Beijing Office of Higher Education, show that more than 1,300 institutions of higher learning in the city have laboratories. Some among these laboratories are at or approach advanced international standards, and investment in instrumentation and equipment is now over 749 million yuan, the highest in the nation. There are nearly 10,000 laboratory instructors and laboratory technicians. During the "cultural revolution," laboratories in the higher institutions were damaged severely. After 1978, rebuilding of the laboratories at all schools developed quickly. The general physics laboratory of Beijing University has over recent years designed and built more than 10 of its own instruments, has written more than 100 papers and laboratory materials of all sorts, which has hastened the development of the laboratory. Now, the number of students this laboratory accepts each year for laboratory classes exceeds 50,000. When the Hydraulic Drive and Control Laboratory of the Beijing Industrial Academy was checking a complete hydraulic center facility for acceptance as imported from Japan on behalf of the Liaoning Yingkou Chemical Fiber Plant, they did hundreds of examinations and tests on the exterior, construction, functions, and characteristics, recording a hundred test curves, and wrote a 80-page report on the check before acceptance and experiments, which verified serious quality problems in the product, prompting the Japanese to replace it. [Text] [Beijing RENMIN RIBAO OVERSEAS EDITION in Chinese 7 Nov 86 p 4] 12586

S&T RESULTS ATTRACT FOREIGN NOTICE--Science research achievements from various Shanghai higher institutions having been going abroad to technology markets in recent years. According to incomplete statistics from 49 higher institutions, the number of science research topics jointly developed by these higher institutions and foreign interests and technical achievements shifted abroad have reached more than 160. Among these projects, international cooperative projects in applied technology have increased greatly in recent years. The programmed switchboard cooperatively developed by the Shanghai Railway Institute and the Japanese Okidenki Kabushiki Kaisha, the studies jointly completed with Darmstadt University of West Germany regarding technical standards for road routes, the plant gene engineering technology developed jointly with the American Interferon Sciences Company, and the computers, laser photographic composition, and biological and medical instrumentation developed and funded jointly by the Shanghai Jiaotong University and pertinent national and local jointly run companies have all attracted wide-spread interest in foreign technology markets. At the upcoming Guangzhou Export Commodities Fair, higher institutions in Shanghai will have more than 60 scientific achievements on exhibit for sale. [Text] [Beijing RENMIN RIBAO OVERSEAS EDITION in Chinese 1 Oct 86 p 4] 12586

CSO: 4008/2012

FRONTS OF HUANGHAI SEA COLD WATER MASS INDUCED BY TIDAL MIXING

Beijing HAIYANG YU HUZHAO [OCEANOLOGIA ET LIMNOLOGIA SINICA] in Chinese
Vol 16, No 6, Nov 85 pp 451-460

[Article by Zhao Baoren [6392 0202 0088], Institute of Oceanology, Chinese Academy of Sciences, Qingdao: "The Fronts of the Huanghai Sea Cold Water Mass Induced by Tidal Mixing"; Institute of Oceanology, Chinese Academy of Sciences, Institute of Oceanology Report 1241; paper received 10 May 1984; first two paragraphs are source-supplied English abstract]

[Text] Abstract: Since Simpson and Hunter proposed the idea that shallow water fronts were induced by tidal mixing in 1974, many authors have investigated the tidal induced shallow water fronts in various areas. It was generally assumed that a critical value of the stratified parameter $K = \log_{10}(H/U^3)$ may be used to identify the location of these fronts. Here, H means the depth of sea water, U denotes the characteristic velocity of tidal current, and the critical value of K is generally taken as 1.8-2.0.

In this paper, Simpson-Hunter's stratified parameter K was calculated by using quasi-maximum current velocity (which consists of the six main tidal constituents, i.e., M_2, S_2, O_1, K_1, M_4, and MS_4) in Huanghai Sea (Yellow Sea) and in the northern East China Sea as well. Calculated results show that the areas of the Subei (the northern part of Jiangsu) Shoal, off the mouth area of the Changjiang River, along the coast of Shandong Peninsula and along the western coast of Korea, the tidal mixing is strong. Calculations also show that along the whole boundary of HCWM and also along the western boundary of the cyclonic eddy in northern East China Sea, i.e., along the fronts, the value of K is found to be very close to the critical value 1.8. It is also to be noted that at these locations, the temperature of surface water is very low. These clearly show that shallow water fronts in Huanghai Sea and in the northern East China Sea as well, are induced by tidal mixing.

Huanghai Sea is a semienclosed marginal sea surrounded by land on three sides, the bathymetric contours generally run parallel to the seacoast, and the water in the central part is rather deep but generally does not exceed 80 m. Its important hydrographic phenomena are: For the entire warm half of the year, below the seasonal temperature jumps there is a cold water block of broad scope--the Huanghai Sea cold water mass--which is renewed during the winter, and every summer has a similar boundary position and temperature and salinity composition.

Chinese scholars have done a great deal of work in research on the temperature and salinity characteristics, causes of formation, circulation characteristics, and thermal structure of the Huanghai Sea cold water mass. He Chongben [6378 1504 2609], et al.[8] discussed the formation process and the basic characteristics of the Huanghai Sea cold water mass. Guan Bingxian[7] [4619 4426 6343] discussed the water temperature changes in the Huanghai Sea cold water mass and the basic characteristics of cold water mass circulation. On the basis of the basic characteristics of the Huanghai Sea cold water mass water temperature structure, Yuan Yeli[6] [5913 2814 4539] established a strict shallow sea thermal production and circulation model, stressed the thermal structure and circulation characteristics of the central part of the cold water mass and obtained some results which conform to the actual situation quite well. Yet none of these studies touched on why there are frequently slight intermediate depressed platform-shaped structures in the cross-section diagram of Huanghai Sea cold water mass temperature and salinity and what dynamic factors control the boundary position of the Huanghai Sea cold water mass. This paper explains the process of generating the rising temperature seasonal Huanghai Sea cold water mass front from the perspective of tidal mixing and interprets the above questions satisfactorily.

I. Basic Concept of Shallow Water Fronts Produced by Tidal Mixing

On the topic of shallow water fronts induced by tidal mixing, since Simpson and Hunter[16] first proposed that summer shallow water fronts in the Irish Sea were structures induced by tidal mixing, there have been many definitive discussions and reports.[9-16] Simpson, et al.[15] further pointed out that summer shallow water fronts in the continental seas surrounding England were induced by tidal mixing and studied in detail the sea hydrographic features in the area of the fronts. Garrett, et al.[11] studied the tide-produced shallow water fronts in the Bay of Fundy and the Gulf of Maine. Griffiths, et al.[12] pointed out that the shallow water fronts in Hudson's Bay and other Canadian polar seas were caused by tidal mixing.

Just how does tidal mixing form shallow water fronts? As is illustrated in Figure 1a, if we consider only wind mixing, then the seasonal temperature jumps produced by solar radiation will generally exhibit a horizontal distribution. But, since there are sea currents and tidal currents in the ocean, and due to bottom friction, the average kinetic energy of tidal current (or sea current) movement will be converted into turbulence and consumed. When sea water is stratified by solar radiation on the sea surface, turbulence stress will act to overcome sea water buoyancy. The deeper the water, the stronger the turbulence, and when the turbulence increases to a certain degree, it can completely overcome the buoyancy produced by increasing temperature of the sea surface and cause the upper and low levels of the sea to tend toward uniformity, destroying the seasonal temperature jumps. Due to the break-up of the temperature jumps, the lower level cold water and the upper level warm water mix so that the water temperature of the coastal shallow water area is lower than the water temperature of the mixed level in the stratified off-shore sea area, and higher than the water temperature of the bottom level in the stratified area. At this time the direction of the isothermal lines no longer exhibits a horizontal extension, but has become

the platform-shaped structure illustrated in Figure 1b. Thus, between the coastal shallow water area generated by tidal mixing and far-shore stratified area where tidal mixing is weak a transitional area of concentrated isothermal lines is created, and this is the shallow water front produced by tidal mixing.

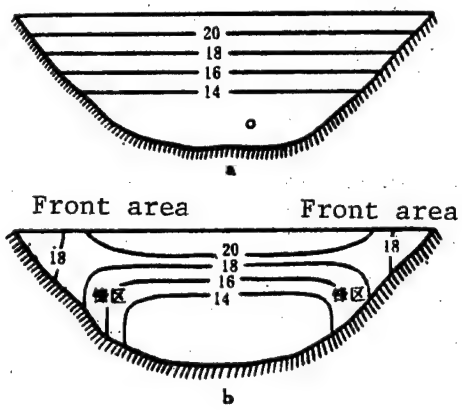

Figure 1. Shallow Water Fronts Formed by Tidal Mixing

a. Not considering temperature distribution of tidal mixing;
b. Considering temperature distribution of tidal mixing.

According to the analysis of Simpson and Hunter,[16] the position of the shallow water front induced by tidal mixing in the season of rising temperatures is determined by the characteristic value of the ratio of the potential energy which is increased by full tidal mixing vertically and the rate of consumption of the tidal current's kinetic energy. If the heat input rate of a unit sea surface is Q and the water depth is H, then the potential energy growth rate produced by vertical mixing is

$$B = \frac{1}{2} g\alpha QH/c_p \tag{1}$$

in which α is the heat expansion coefficient of sea water; c_p is specific heat. Concerning the question of consumption of tidal energy, it is difficult to be precise because the tides are made up of so many tidal constituents, but viewed simply, generally only the rate of energy consumption of characteristic tidal current velocity is considered. The energy consumption rate of a sine tidal wave of amplitude U

$$E = (4/3\pi)r\rho U^3 \tag{2}$$

in which r is the sea bottom friction coefficient; ρ is the sea water density. The ratio of potential energy growth rate (B) and kinetic energy consumption rate (E) is:

$$B/E = (3\pi/8)\cdot(g\alpha QH)/\rho c_p r U^3 \tag{3}$$

for a certain specific area, α, Q, ρ, c_p and r can be viewed as almost constants, thus the position of the front is determined by the specific value (critical value) of H/U^3, and the ratio H/U^3 or

$$K = \log_{10}(H/U^3) \tag{4}$$

is usually called the stratified parameter or the mixing parameter.

There are differences in the ways different authors take U when calculating the stratified parameter H/U^3. Some take the surface layer high tidal current velocity as U,[16] some take the large tidal vertical average velocity as U,[14] and still others take the amplitude of M_2 tidal constituent as U.[11,13] Because of the different methods of taking U, there are also differences in the thickness of the mixing layer in the sea areas,[10] thus the critical values which determine the position of the tide-produced shallow water front are also not very similar. A representative critical value is: $H/U^3 = 50\text{-}100\ m^{-2}s^3$ or $K = 1.7\text{-}2.0$. We proposed for the Huanghai Sea another characteristic velocity to determine the stratified parameter (K), and using the K value so derived to determine the position of the Huanghai Sea cold water mass front we obtained encouraging results.

II. Calculation of the Huanghai Sea Stratified Parameter

When discussing the matter of stratification of Changjiang River water dilution, Beardsley, et al.[9] calculated the stratified parameters (K) of the Huanghai Sea and Donghai Sea on the basis of the tidal current numerical calculation results, but did not take into account at all the related question of Huanghai Sea and Donghai Sea tide-generated shallow water fronts. In their calculations, they took the M_2 tidal constituent amplitude as U. In half-day tidal seas, using the M_2 tidal constituent amplitude as the U in the stratified parameter undoubtedly has a certain representative significance. But in full-day tidal and mixed tidal seas (such as the Bohai Gulf and part of the seas on the northern side of the Shandong Peninsula), using the M_2 tidal constituent amplitude as U, can introduce a substantial error in the calculation of the K value. For this reason, we adopted the vertical average quasi-maximum current velocity proposed by Ding Wenlan[1,2] to calculate the K value. The quasi-maximum current velocity is calculated from the harmonic constants of the six primary tidal constituents (O_1, K_1, M_2, S_2, M_4, MS_4), which can better represent the major tidal velocity in this sea area.

We calculated the K value of a total of 221 points in this sea area. A total of 132 of these points were in the sea area west of 124°E, and the quasi-maximum current velocity was calculated using the actually measured harmonic constants. A total of 89 points were in the sea area east of 124°E, and the quasi-maximum current velocity was calculated using the results of numerical calculation. Except for the central region of the northern part of the Huanghai Sea and individual areas on the west side of the Korean peninsula, the distribution of the K value calculated points in the entire sea area was very homogeneous. Thus, the calculation results of this paper can better reflect the tidal mixing of the Huanghai Sea.

Figure 2 gives the distribution of stratified parameter K greater than 1.4. From Figure 2 it can be seen that in the region from off northern Jiangsu to the shoal at the mouth of the Changjiang River, from Qingdao on the Shandong peninsula to the Weihai shore, the Bohai Gulf and along the western coast of the Korean peninsula are developed tidal mixing areas. On this basis we can predict that the water temperature in the above sea areas will tend toward a vertically homogeneous state, but in the central area of the Huanghai Sea, tidal mixing is rather weak and clear stratification will appear. Between developed tidal mixing areas and stratified areas there must be a transitional zone, and this is the interface of the Huanghai Sea cold water mass.

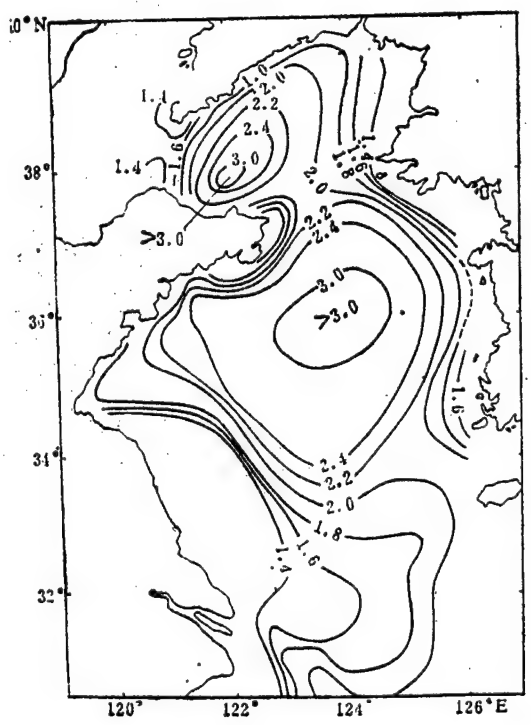

Figure 2. Distribution of Huanghai Sea Stratified Parameter K Value

To determine a critical value for the stratified parameter K, this paper takes the difference $\Delta\sigma_t$ between the bottom layer and surface layer σ_t of the southern and northern Huanghai Sea in June and August 1979, as the ordinate and the interpolated $\log_{10}(H/U^3)$ values of the corresponding points as the abscissa to form Figure 3. From the figure it can be seen that the overwhelming majority of points in the stratified area fall to the right of K = 1.8. This means that there is a critical value for the Huanghai Sea stratified parameter, therefore we can take the contour line K = 1.8 as the boundary between the stratified area and the vertically homogeneous area. Because the front face has a definite thickness, the location of the above-described temporary K value generally should be the outer front face of the Huanghai Sea cold water mass.

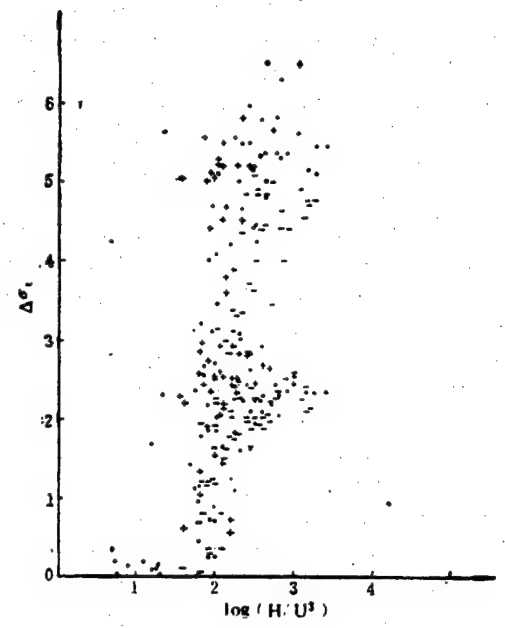

Figure 3. Relationship of Difference σ_t of Surface and Bottom Layer $\Delta\sigma_t$ and $\log_{10}(H/U^3)$
+ northern part of Huanghai Sea; • southern part of Huanghai Sea; - western coast of Korea

III. The Huanghai Sea Cold Water Mass Boundary, Shallow Water Fronts and Tidal Mixing

As described above shallow water fronts produced by tidal mixing exist in surface and bottom layers simultaneously. Since the sea bottom is little influenced by the outside and hydrologic conditions are comparatively stable, we first analyzed the relationship between the position of the Huanghai Sea cold water mass bottom layer front and the stratified parameter. According to the research of many scholars, the position of the boundary of the Huanghai Sea cold water mass in different summers is comparatively fixed. People often treat the area included inside 10°C or 8°C[3,7] isothermal lines as the range of the Huanghai Sea cold water mass, and treat 17°C as the boundary of the Huanghai Sea cold water mass and the surrounding seas.[4] Figures 4a and 4b give a distribution map of the range of bottom layer water temperature of the Huanghai Sea cold water mass in August 1979. (Footnote) (Figure 4a was drawn by Chinese scholars on the basis of materials from the thirties and forties (cited in Reference 8) and Figures 4b and 4c were drawn on the basis of August 1979 China and Korea materials.) To compare with the K value, we have also drawn with a dotted line the contour lines of K = 1.8 and K = 2.0 in the figure. From Figures 4a and 4b it can be seen that the distribution of Huanghai Sea bottom layer isothermal lines tend to be identical with the K value distribution given in Figure 2, in the boundary area of the cold water mass in particular the direction of the isothermal lines makes an even better fit with the K value lines. Thus we feel that the boundary of the bottom layer cold water mass is controlled by the critical stratified parameter. From Figures 4a and 4b it can also be seen that in the

outer side of the Subei Shoal, the western side of the Korean peninsula and the Bohai Gulf and the eastern coastal sea of the Shandong peninsula, the bottom layer isothermal lines are especially concentrated, and this is the transitional zone of the developed tidal mixing area and the stratified layer (see Figure 2). Thus it further explains that the tidal mixing is actually an important factor controlling the Huanghai Sea cold water mass boundary.

Now we will again analyze the Huanghai Sea surface layer shallow seas front which is produced by tidal mixing. Since the sea surface water temperature is comparatively homogeneous and the daily changes are clear, the run-off also has a definite influence on surface water temperature and stratification, and thus in conventional marine survey materials, shallow water fronts are not as clear and systematic as the bottom layer. Yet in areas where Huanghai Sea tidal mixing is severe, we still can discover its traces. Figure 4c portrays the horizontal distribution of August 1979 Huanghai Sea surface water temperature. From Figure 4c it can be seen that the water temperature of the Huanghai coastal area (except for areas where the water is especially shallow) is universally lower than the water temperature in the central area of the Huanghai Sea. It is most clear on the east side of the Shandong peninsula, the outer side of the Subei Shoal and the western side of the Korean peninsula. Between the near sea low temperature area and the outer sea high temperature area there clearly exists a transitional area where the water temperature steps are large, i.e., there is a sea surface temperature front.

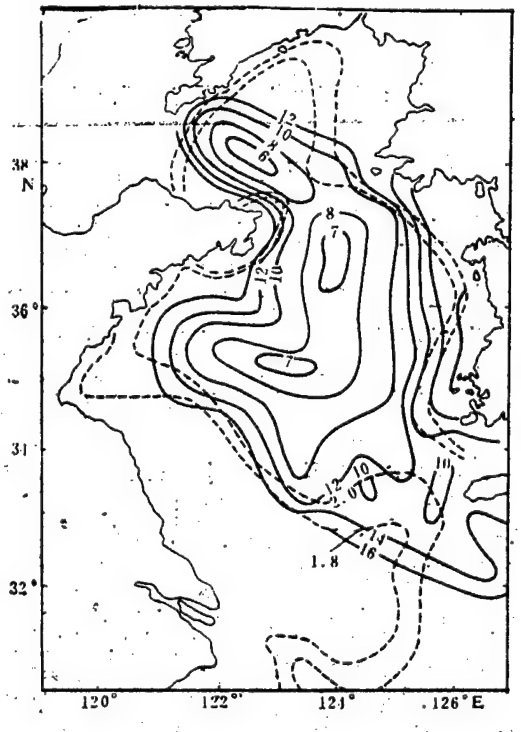

Figure 4a

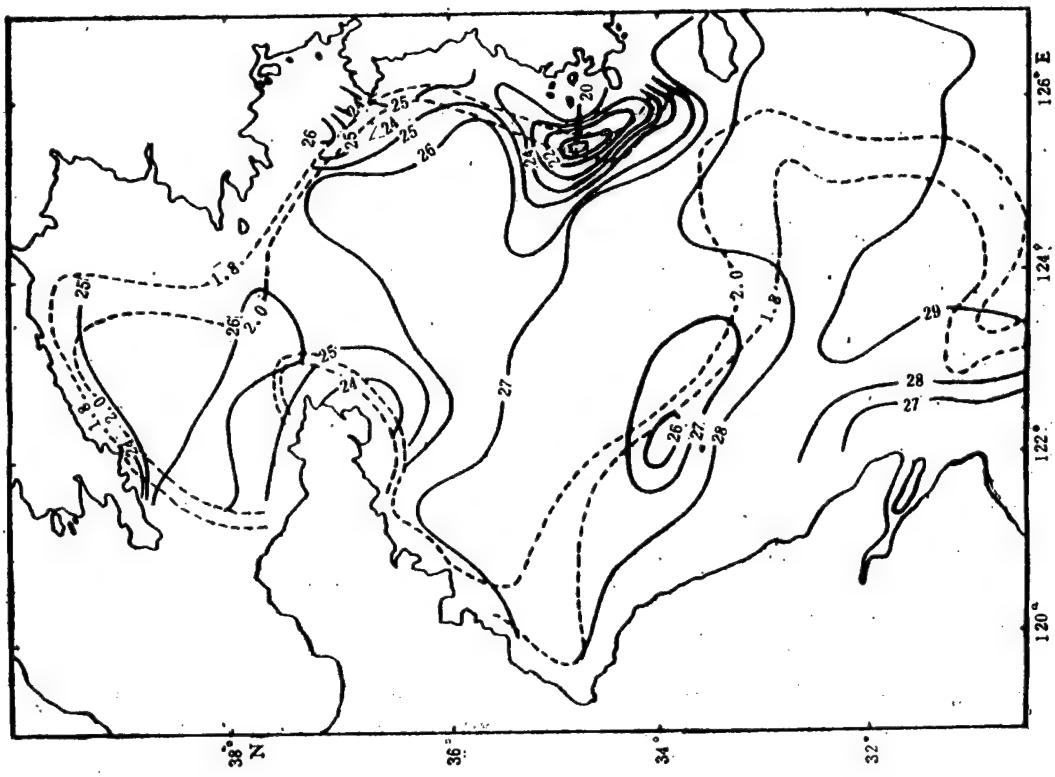

Figure 4c

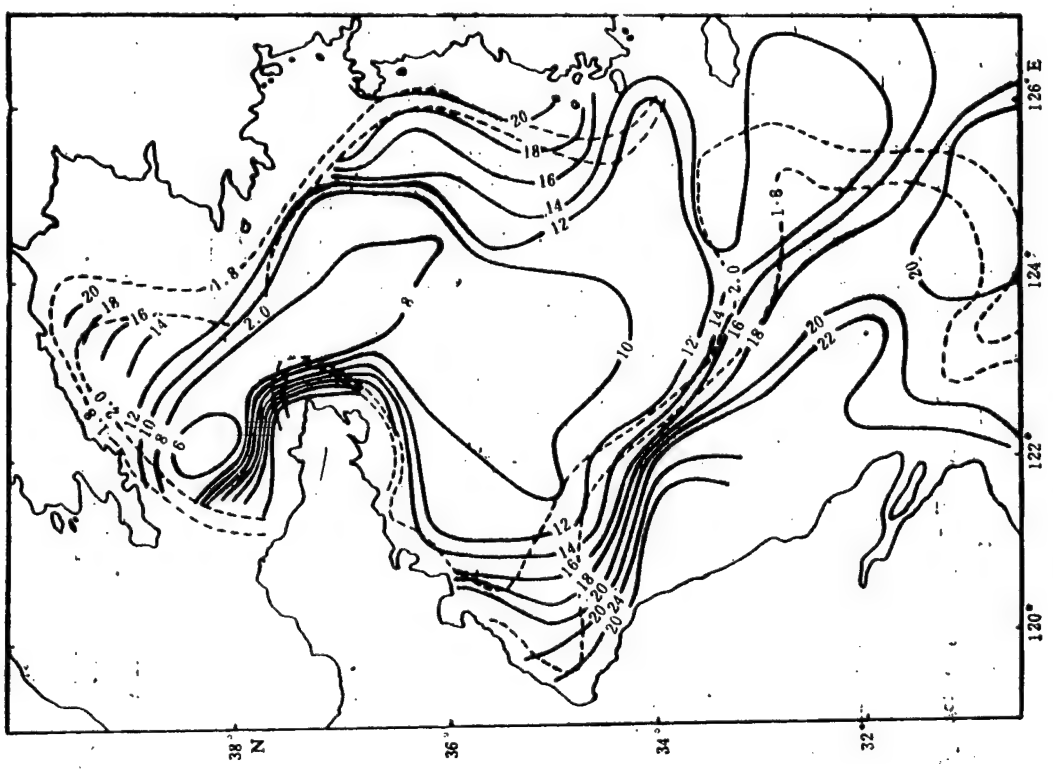

Figure 4b

Compared with Figure 2, the position of the sea surface temperature front is generally distributed along the K = 1.8-2.0 contour line (the dotted line in Figure 4c). Almost all the low temperature areas are on the coastal side of the K = 2.0 contour line. On this basis, we feel that the Huanghai surface layer shallow water front not only exists but also is controlled by the critical value of the tidal mixing stratified parameter.

To further clarify the controlling action of tidal mixing on the Huanghai Sea shallow water front, we drew a distribution map of the representative temperature cross sections (Figure 5) and indicated the position of K = 1.8 and 2.0 with arrows. As indicated in the map, the water temperature cross-section distribution of summer the Huanghai Sea cold water mass area has the platform structure illustrated in Figure 1b, and this indicates that the boundary of the Huanghai Sea cold water mass is controlled by tidal mixing. Figure 5a gives the temperature distribution of 36°N cross section in June 1979, and as the map shows, in the vicinity of 120°50'E off Qingdao below depths of 15 m, there is a vertically downward temperature front. In the vicinity of 121°05'E, the water temperature horizontal steps are large. The area of the above-described isothermal concentrations are extremely close to K = 2.0 positions. In the eastern part of the cross section, one side of the Korean peninsula near 125°55'E, on the sea surface and sea bottom there is a temperature front where the isothermal lines are concentrated, the K values of the corresponding location are 2.0, and the K values of the outer edge of the front area are 1.8. From Figure 5b it can be seen that the 123°E radial temperature cross section also has the platform structure illustrated in Figure 1, and the K values are in the vicinity of 1.8 (i.e., in the seas in the vicinity of 37°N, 33°20'N, and 31°15'N) the sea surface temperature is low, and the isothermal lines which are concentrated below the 10 m layer descend vertically. Figure 5c is the average Dalian-Chengshanjiao temperature cross section for many Augusts (cited from Reference 6). From the K value positions indicated in the figure it can be seen that in terms of the average situation over many years, the boundary of the temperature platform structure and the sea surface low temperature area both are controlled by the critical parameter K.

In summary, the distribution of the Huanghai Sea surface and bottom layer temperatures and the distribution of representative temperature cross sections indicates that the Huanghai Sea cold water mass bottom layer temperature distribution and the sea surface low temperatures area are controlled by tidal mixing. Contour lines of stratified parameter K equal to 1.8 and 2.0 generally are distributed in positions along the boundary of the Huanghai Sea cold water mass. This result is identical to the conclusion of Simpson, Garrett and others when researching the marine fronts in the continental seas surrounding England and the continental seas of the Bay of Fundy in North America.

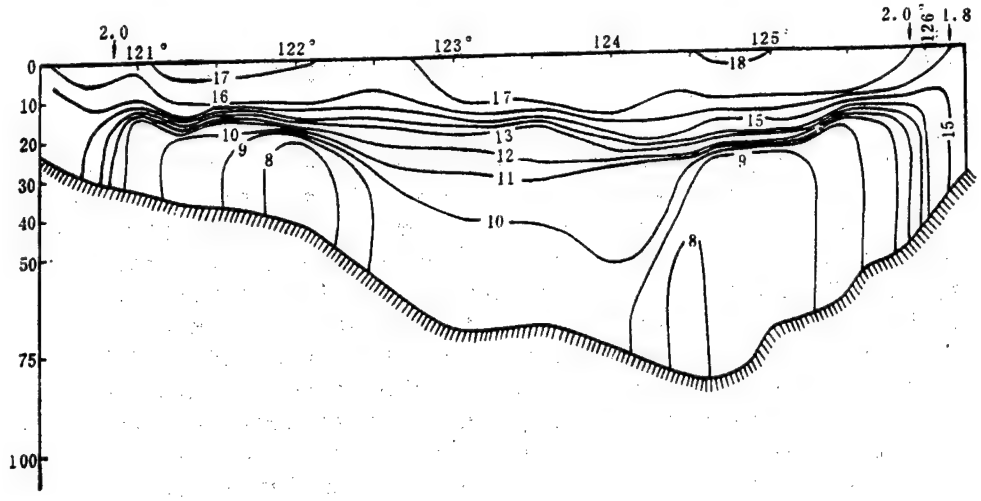

a

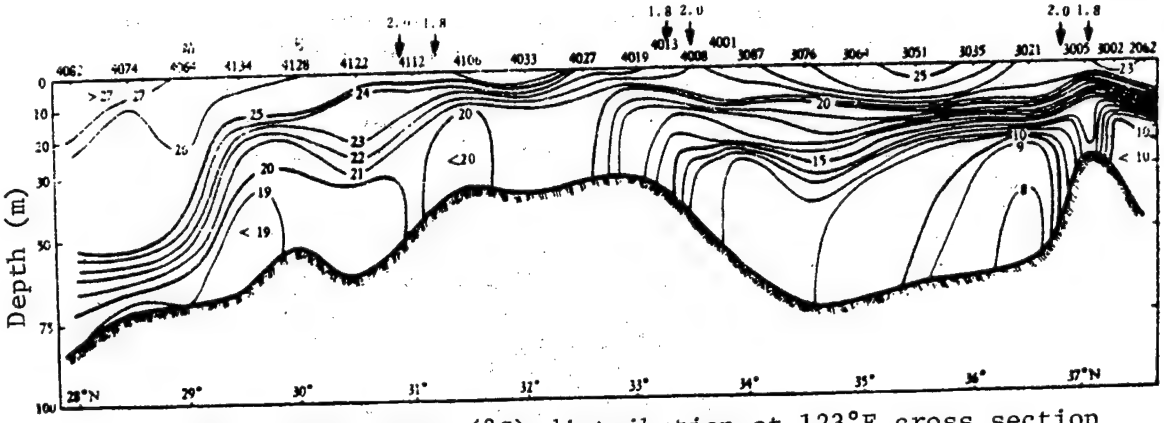

Water temperature (°C) distribution at 123°E cross section

b

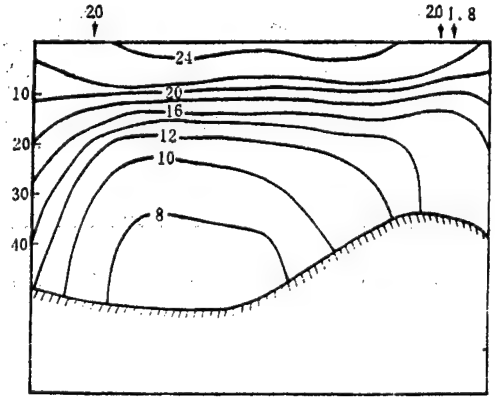

c

Figure 5. Map of Cold Water Mass Area Summer Temperature Cross-Section Distribution
a. 36°N June 1979 cross section; b. 123°E July 1959 cross section (cited from Mao Hanli et al.)[4]; c. Dalian-Chengshanjiao average temperature of August over many years' cross section (cited from Yuan Yeli)[6]

IV. Influence of Tidal Mixing on Cyclonic Eddy Boundaries in the Northern Part of the Donghai Sea

Research shows that the position of cyclonic eddies in the northern part of the Donghai Sea, with the western boundary in a position no further west than 124°30'E. And every summer there are similar thermal structures.[5] Since the boundary of the Huanghai Sea cold water mass is controlled by tidal mixing, is the boundary of the cyclonic eddy in the northern part of the Donghai Sea which is connected with the Huanghai Sea cold water mass with tidal mixing? From Figure 2 we can tell that the critical K value goes through the western boundary of this cyclonic eddy, thus the author feels that the western boundary of this eddy is also controlled to a considerable degree by tidal mixing. To further explain this question, we cite the temperature cross-section map (Figure 6) of Hu Dunxin [5170 2415 2946], et al.[5] and from the map it can be seen that the temperature structure of the western side of this cross section is extremely similar to the temperature cross-section distribution in Figure 5 in this article. Furthermore, the front position of sea surface low temperature area and sea bottom isothermal lines' concentration are both controlled by the critical K value. The 31°N cross section also has a similar temperature distribution. The above facts show that the western boundary of the cyclonic eddy is controlled by tidal mixing to a very large degree.

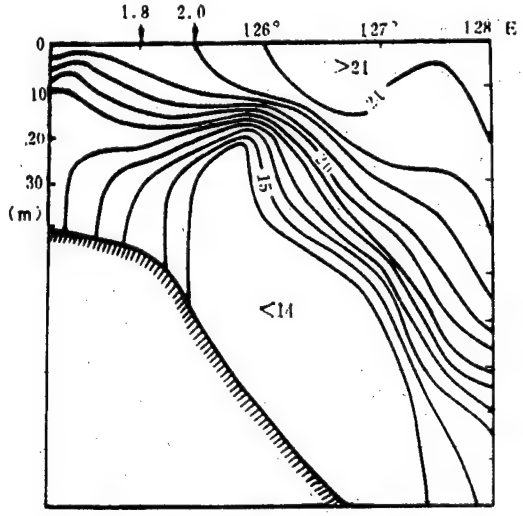

Figure 6. 32°N Cross Section July-August 1979 Temperature Distribution (cited from Hu Dunxin, et al.[5])

V. Conclusion

This paper used the quasi-maximum tidal current velocity to calculate the Simpson-Hunter stratified parameter $K = \log_{10}(H/U^3)$ to show the strength of tidal mixing in the Huanghai Sea and the northern part of the Donghai Sea. The results show that the Subei Shoal and Changjiang River plume, coastal seas of the eastern part of the Shandong peninsula, Bohai Gulf and the

coastal area of the western part of the entire Korean peninsula are strong tidal mixing areas. When calculating the stratified parameter K, using the quasi-maximum tidal current velocity as the characteristic velocity is clearly superior to using the amplitude of the M_2 tidal constituent as the characteristic current velocity. The critical value of the stratified parameter for these seas obtained according to the density materials of June and August 1979, was 1.8. From the plane distribution of bottom layer water temperature and the hydrologic distribution of several representative cross sections we can tell that the water temperature distribution of the Huanghai Sea cold water mass area is related to the strength of tidal mixing, and the boundary of the bottom layer of the Huanghai Sea cold water mass, i.e., the front, is controlled by the critical stratified parameter. The direction of the K = 1.8-2.0 stratified parameter contour lines is basically identical with the boundary of the entire bottom layer of the Huanghai Sea cold water mass, thus indicating that a strong tidal mixing action of sea surface rising temperature and alongshore areas is the basic thermodynamic-dynamic factor in the formation of the Huanghai Sea cold water mass. Calculations also showed that the western boundary of the cyclonic eddy of the northern part of the Donghai Sea in summer is also controlled by tidal mixing. From surface water temperature plane distribution and cross section water temperature distribution we can tell that in the above-described strong tidal mixing areas, the sea surface shallow seas temperature front clearly exists, and using satellite photographs to determine precisely the position of sea surface temperature fronts and establish concentrated marine hydrology measurement stations in the front areas to understand in detail the hydrologic structures of the front area is unusually significant.

This paper received the encouragement of Professor Mao Hanli [3029 3352 4409], Assistant Professor Fang Guohong [2455 0948 3163] read the paper and provided valuable opinions, Comrade Ding Wenlan [0002 2429 5695] provided the tidal materials, and Comrade Bai Shaoying [4101 1421 5391] drew the Chinese maps. I thank them all here.

REFERENCES

1. Ding Wenlan [0002 2429 5695], 1984. "Donghai Chaoxi He Chaoliu Tezheng De Yanjiu" [Research on Characteristics of Donghai Sea Tides and Tidal Currents], HAIYAN KEXUE JIKAN, 21: 135-148.

2. Ding Wenlan. "Bohai He Huanghai Chaoxi Chaoliu Fenbu De Jiben Tezheng" [Basic Characteristics of Bohai and Huanghai Tide and Tidal Current Distribution], HAIYAN KEXUE JIKAN, 25 (in press).

3. Mao Hanli [3029 3352 4409], Ren Yunwu [0117 0336 2976], Wan Guoming [8001 0948 6900], 1964. "Yingyong T-S Guanxi Dingliangdi Fenxi Qianhai Shuituan De Chubu Yanjiu" [Preliminary Research on Applying the T-S Relationship To Analyze Quantitatively Shallow Seas Water Masses], HAIYANG YU HUZHAO, 6(1): 1-22.

4. Mao Hanli, Ren Yunwu, Sun Guodong [1327 0948 2767], 1964. "Nan Huanghai He Donghai Beibu (28°-37°N) Xiaji De Shuiwen Tezheng Yiji Haishui Leixing (Shuixi) De Chubu Fenxi" [Preliminary Analysis of the Summer Hydrologic Characteristics and Seawater Type (Water System) in the Southern Huanghai Sea and Northern Part of the Donghai Sea (28°-37°N)], HAIYANG KEXUE JIKAN, 01: 23-77.

5. Hu Dunxin [5170 2415 2946], Ding Zongxin [0002 1350 0207], Xiong Qingcheng [3574 1987 2052], 1984. "Donghai Beibu Yige Xiaji Chixuanxing Woxuan De Chubu Fenxi" [Preliminary Analysis of a Summer Cyclonic Eddy in the Northern Part of the Donghai Sea], HAIYANG KEXUE JIKAN, 21: 87-100.

6. Yuan Yeli [5913 2814 4539], 1979. "Huanghai Lengshuituan Huanliu I. Lengshuituan Zhongxin Bufen De Rejiegou He Huanliu Tezheng" [Huanghai Sea Cold Water Mass Circulation I. Thermal Structure and Circulation Characteristics of the Central Part of the Cold Water Mass], HAIYANG YU HUZHAO, 10(3): 187-199.

7. Guan Bingxian [4619 4426 6343], 1963. "Huanghai Lengshuituan De Shuiwen Bianhua Yiji Huanliu Tezheng De Chubu Fenxi" [Preliminary Analysis of the Circulation Characteristics and Hydrological Variation in the Huanghai Sea Cold Water Mass], HAIYANG YU HUZHAO, 5(4): 255-284.

8. He Chongben [6378 1504 2609], Wang Yuanxiang [3076 0955 4382], Lei Zongyou [7191 1350 0645], Xu Si [1776 2448], 1959. "Huanghai Lengshuituan De Xingcheng Ji Qi Xingzhi De Chubu Taolun" [Preliminary Discussion of the Huanghai Sea Cold Water Mass Characteristics and Its Nature], HAIYANG YU HUZHAO, 2(1): 11-15.

9. Beardsley, R.C., R. Limeburner, Hu Dunxin, et al., 1983. "Structure of the Changjiang River Plume in the East China Sea During June 1980," Proceedings of the International Symposium on Sedimentation on the Continental Shelf, With Special Reference to the East China Sea. China Ocean Press, pp 265-284.

10. Fearnhead, P.G., 1975. "On the Formation of Fronts by Tidal Mixing Around the British Islands," DEEP-SEA RESEARCH, 22(5): 311-322.

11. Garrett, C.J.R., J.R. Keeley, and D.A. Greenbery, 1978. "Tidal Mixing Versus Thermal Stratification in Bay of Fundy and Gulf of Maine," ATMOSPHERE-OCEAN, 16(4): 403-423.

12. Griffiths, D.K., R.D. Pingree, and M. Sinclair, 1981. "Summer Tidal Fronts in the Near-Arctic Regions of Foxe Basin and Hudson Bay," DEEP-SEA RESEARCH, 28(8): 865-873.

13. Pingree, R.D., and D.K. Griffiths, 1978. "Tidal Fronts on the Shelf Seas Around the British Islands," JOURNAL OF GEOPHYSICAL RESEARCH (OCEANS AND ATMOSPHERES), 83(C9): 4615-4622.

14. Simpson, J.H., 1976. "A Boundary Front in the Summer Region of the Celtic Sea," ESTUARINE AND COASTAL MARINE SCIENCE, 4(1): 71-81.

15. Simpson, J.H., C.M. Allen, and C.G. Morris, 1978. "Fronts on the Continental Shelf," JOURNAL OF GEOPHYSICAL RESEARCH (OCEANS AND ATMOSPHERES), 83(C9): 4607-4614.

16. Simpson, J.H. and J.R. Hunter, 1974. "Fronts in the Irish Sea," NATURE, 250: 404-406.

17. Simpson, J.H., D.G. Hughes, and N.C.G. Morris, 1977. "The Relation of Seasonal Stratification to Tidal Mixing on the Continental Shelf," in "A Voyage of Discovery" (ed. M. Angel), Suppl. to DEEP-SEA RESEARCH, pp 327-340.

8226/6091
CSO: 4008/1004

FRONTS IN RISING CURRENT ZONES IN COASTAL ZHEJIANG WATERS

Beijing HAIYANG XUEBAO [ACTA OCEANOLOGICA SINICA] in Chinese Vol 7, No 4, 15 Jul 85 pp 401-411

[Article by Pan Yuqiu [3382 3768 3808], Xu Duanrong [1776 4551 5554], and Xu Jianping [6079 1696 1627], Second Oceanologic Institute, State Oceanologic Bureau, Hangzhou: "Front Structure, Variation and Its Causation of Rising Current Zone in Coastal Zhejiang Waters"; article received 10 August 1983, revised draft received 15 December 1984; first paragraph is source-supplied abstract]

[Text] Abstract: This paper applies 1980-1981 rising current survey data and related historical data to a discussion of the front features of structure characteristics, hybrid situation, and position variation of the rising current zone in coastal Zhejiang waters and their causation. This paper holds that positional variation of the Zhejiang coastal front and rising current front are largely attributable to the intensity and positional variation of the Taiwan warm current, though the wind is also an important factor. The rising current of the Zhejiang coastal waters is also influenced by Zhejiang offshore bottom topography and the Taiwan warm current. The theory proposed by Janowitz and others that rising current is caused by topography can be applied to Zhejiang offshore waters.

That there is a rising current in the coastal waters of Zhejiang is without question, our predecessors have verified this many times.[1-3] However, the explanations of the mechanism that forms it are not in agreement and still require further exploration.

In the summers in the Zhejiang offshore waters there are two qualitatively different fronts--coastal fronts and rising current fronts. The role of waters is central in the causation of the position, intensity and variation in these two types of fronts. From the angle of physical oceanology, although the formation of these two types of fronts has essential differences, they are both influenced by the rising of lower level water in the Zhejiang offshore waters, thus discussing the relationship between them is very important for the fishing industry. This paper uses historical data and survey data on rising currents obtained on many sailings in 1980-1981 by the Second Oceanology Institute of the State Oceanology Bureau to discuss the variations in the two types of fronts and also discusses the influence

of topography and the Taiwan warm current on the variation and height of the rising front layers. For the specific research area see Figure 1.

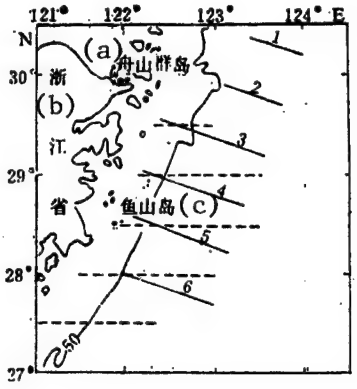

Figure 1. Distribution of Cross Sections Observed
—— June, August, October 1981 stations
---- July, August 1980 stations

Key:
a. Zhoushan Islands
b. Zhejiang
c. Yushan Island

I. Basic Hydrographic Conditions in Zhejiang Offshore Waters

There are three water masses in the Zhejiang offshore waters in summer and two in winter. Between April and October in the region studied there can appear the Zhejiang coastal water mass (C), the Taiwan warm current upper level water mass (M) and the Taiwan warm current deep water mass (K). The Taiwan warm current deep water mass appears in April, reaches its greatest intensity in July and August, retreats in October and after November disappears.[4] From November to March of the next year there are only the Zhejiang coastal water mass and the Taiwan warm current upper level water mass (see Figures 2 and 3).

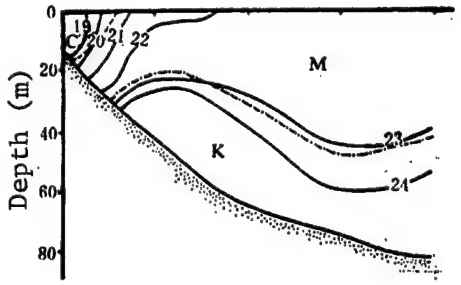

Figure 2. Cross Section Distribution of Zhejiang Offshore Summer Water Masses
_____ isopycnic line; ----- 31 salinity line; -·-·- 24°C isothermal line

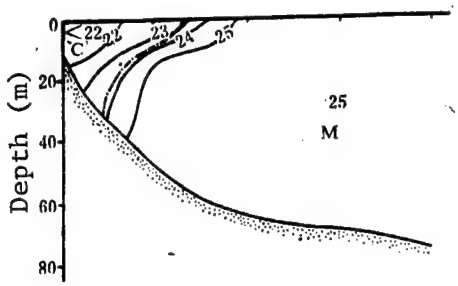

Figure 3. Cross Section Distribution of Zhejiang Offshore Winter Water Masses
_____ isopycnic line; -·-·- 31 salinity line

The temperature and salinity of the three water masses are: the primary characteristics of the Zhejiang coastal water mass is low salinity (salinity lower than 29), and the temperature varies with season. It is primarily made up of tepid water which flows into the sea in Jiangsu and Zhejiang coastal waters (primarily from the Changjiang). The primary characteristic of the Taiwan warm current upper level water mass is high temperature and high salinity: salinity is between 33 and 34. Temperature varies with seasons but since it is carried along by the Taiwan warm current, the temperature changes of this water mass are smaller than those of the Zhejiang coastal water mass. In the summer, there are constant seasonal jumps in the Taiwan warm current upper level water mass. In addition to high salinity (slightly higher than the Taiwan warm current upper level water), the Taiwan warm current deep level water mass is also characterized by low temperature, with core temperatures and salinity of t = 17-19°C and S = 34.5. The Taiwan warm current deep level water mass may originate in the secondary level water of the eastern side of the Kuroshio[4]; it forms a sharp transition with the Taiwan warm current upper level water mass.

In the study of this sea region there are two currents: one is the Taiwan warm current and the other is the East China Sea coastal current. The Taiwan warm current is the backbone of the Zhejiang offshore seas current, situated on the east side of the East China Sea coastal current. In the winter, the Taiwan warm current flows northward with the axis of the current situated in the summer from southwest to northeast, the axis in the winter tends more toward north-northeast along the coast. The velocity of the current is strong in summer and weak in winter, and magnitude of current is broad in summer and narrow in winter. The velocity of the Taiwan warm current in summer and winter is generally 15-40 cm/sec.[7] The East China Sea shore current is along the Zhejiang coast and constantly flows from north to south at an average velocity of 10 cm/sec.[5]

The distribution of the Zhejiang offshore coastal front can be seen in Figures 2 and 3. It is situated near the shore and is the boundary between the Zhejiang coastal water mass and the Taiwan warm current upper level water mass. The front inclination direction is the reverse of the offshore slope direction. The fishermen call it "liuge" [3177 7133]. Its salinity level increases by steps. The rising current front is on the outer lower side o:

the coastal front. The front inclination is the same as that of the slope inclination. When the upper level seas diverge and the Taiwan warm current deep level water rises, this front is formed by the inclination of the dense jumps toward the shore. The rising current front is mainly constructed of the interface between the Taiwan warm current upper level water and deep level water, manifested by the formation of a temperature front. See Figure 2 for its distribution position.

II. Distribution and Variation of Zhejiang Coastal Front and Coastal Fronts

From the perspective of the structure of the rising front layer, the rising front in the sea area under study clearly has two front structures (see Figure 4). Its north-south distributional characteristics are: the upper front (reflecting the seasonal jumps) is very similar in the degree of rise in each cross section, but the lower front (reflecting the boundary jumps between water masses) becomes gradually higher from south to north, and by the time it reaches the vicinity of 29°N it reaches the maximum and is one with the upper front level. Further north, the altitude of the lower front declines slightly and departs slightly from the upper front. We feel that this north-south distribution of the lower front is related to the marine topography of the Zhejiang offshore waters which is explained below.

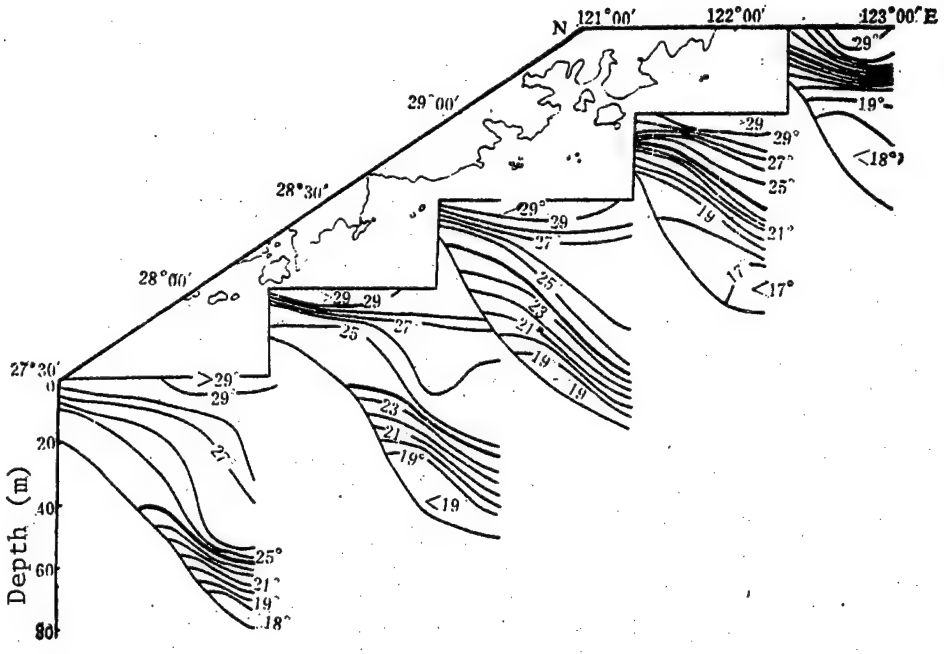

Figure 4. Temperature Cross Section Distribution at 27°30'-29°30'N on 22-25 July 1980
Heavy solid lines represent 24° isothermal lines

The level of the rising current front can be seen in Figures 5 and 6. From the figures it can be seen that in July 1980 the rising front of the Zhejiang coastal waters 20 meter level develops in a strip coastal slope. In

August 1981, the cold center of the 20 meter water level off the Zhejiang coast, i.e., the maximum cold water rising shifted to 29°N, 122°45'E, and the front around it stretched from southwest to northeast. The results of these two observations were obtained when the wind was southwest (wind velocity >6 m/sec) and northeast (wind velocity 6-8 m/sec) and this situation means that the distribution of the rising front on the Zhejiang coast is influenced by the wind.

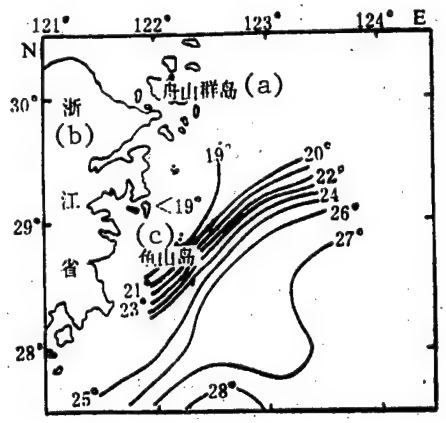

Figure 5. 20 m Layer Temperature Distribution on 22-25 July 1980

Key:
- a. Zhoushan Islands
- b. Zhejiang Province
- c. Yushan Island

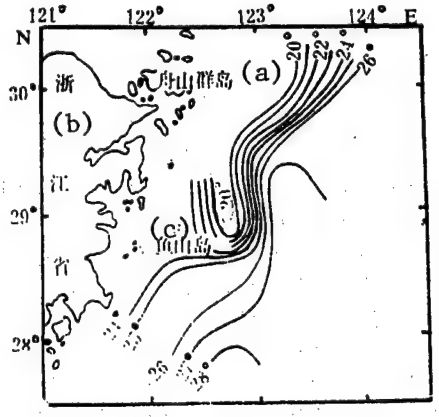

Figure 6. 20 m Layer Temperature Distribution on 5-8 August 1981

Key:
- a. Zhoushan Islands
- b. Zhejiang Province
- c. Yushan Island

We are not prepared here to give a water level distribution map of the rising current front in June and October 1981 because there were few measuring stations. However, from Figures 7 and 9 we can tell that the rising current front of this period could appear below the 25 m level and the direction of travel is similar to that in Figures 5 and 6.

The monthly variation characteristics of the rising current front level height are: in June it is inclined to be low, in July-August it is at its maximum, and in October it declines again. The navigational survey results make it clear that the thickness does not vary much. The overall characteristics of the monthly rising current front level's lateral distribution are: near the coast it rises the highest, and as the distance from the coast increases it drops, and the thickness increases gradually until a depth of 70 meters (see Figures 7-9). It should be noted that the rising current front level in the sea area studied generally did not intersect with the sea surface. This may be because the coastal front is its front part and the layering increases, keeping the Taiwan warm current deep layers from upwelling to the sea surface.

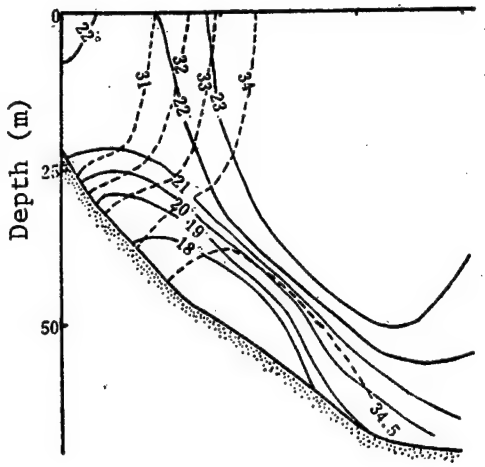

Figure 7. Temperature and Salinity Distribution of Cross Section No 4 on 17 June 1981

Dotted lines are salinity lines; Solid lines are isothermal lines

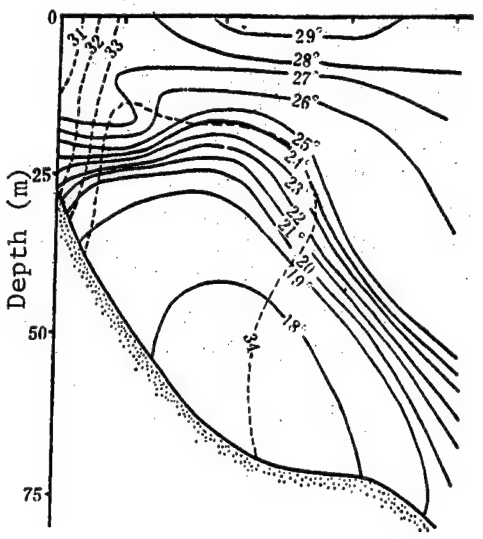

Figure 8. Temperature and Salinity Distribution of Cross Section No 4 on 12 August 1981

Dotted lines are salinity lines; Solid lines are isothermal lines

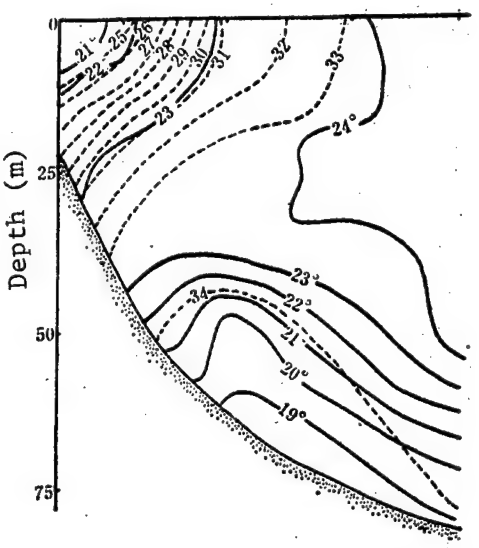

Figure 9. Temperature and Salinity Distribution of Cross Section No 4 on 17 October 1981

Dotted lines are salinity lines; Solid lines are isothermal lines

The structure of the coastal front can be clearly seen in Figures 7-9. This front was located at the nearshore side of cross-section No 4, and the 29-34 salinity lines are unusually dense. In the lateral cross-section, the front face exhibits a largely S shape, the Taiwan warm current upper layer highly

saline water wedges into the lower part of the Zhejiang coastal waters. The position of this front can be seen from Figures 7-9. In June it extends further to the east, but by July-August it is distributed close to the shore and by October it is even further from the shore than in June and the intensity is also greater than in June.

As far as the surface distribution characteristics of the coastal front, this paper deals only with the surface salinity distribution map for July 1980 and August 1981. From Figure 10 we can tell that in July 1980, the coastal front in the sea area studied appeared in the shape of a highly saline tongue. The tongue extended from the south toward the north. The tongue was situated between 28°40'-29°40'N and 122°-123°E, the broad part of the tongue was toward the south. The coastal front did not appear south of 28°30'N. The sea area south of it was completely occupied by the upper layer water of the Taiwan warm current, and the northern part was occupied by the Zhejiang coastal waters.

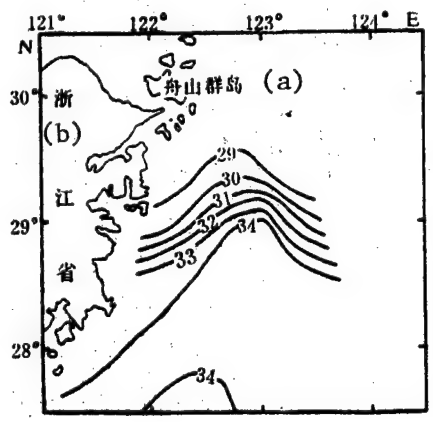

Figure 10. Surface Layer Salinity Plane Distribution on 22-25 July 1980

Key:
a. Zhoushan Islands
b. Zhejiang Province

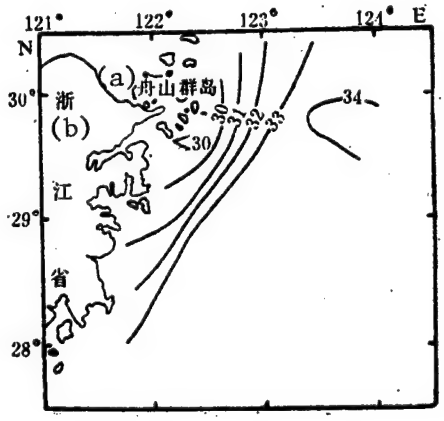

Figure 11. Surface Layer Salinity Plane Distribution on 5-8 August 1981

Key:
a. Zhoushan Islands
b. Zhejiang Province

The distributional shape of the Zhejiang coastal front in August 1981 was very different. From Figure 11 we can tell that the salinity front in this period revealed a slight arc shape, extending from 28°30'N, 122°E toward 30°N 123°E. The southern section is close to the shore, but the northern section is further from the shore. This feature clearly shows that the main body of the Zhejiang coastal front water mass in this period is at the mouth of Hangzhou Bay, the Taiwan warm current upper layer water extends further toward the north, and is on the right side of the coastal front. The greatest characteristic of the coastal front in this period is that the highly saline tongue does not appear in the sea area surveyed. The wind situation of the two examples is the same as the wind situation in Figures 5 and 6. The above

examples show that different wind situations also influence the shape of the Taiwan warm current and the intensity and position of the highly saline tongue front.

Historical materials show that Zhejiang coastal water fronts often appear as highly saline tongue fronts in latitudes north of 29°30'N, and it is formed by the upper layer water of the Taiwan warm current wedging into the Zhejiang coastal water mass. The sharpness of the highly saline tongue fronts are determined by the wedging intensity of the Taiwan warm current upper layer water.

The sea current structure of the Zhejiang coastal rising current area can be seen from Figures 12-14. The sea current in the vicinity of the front face and the geostrophic current direction are extremely uniform. On the two sides of the coast front, the sea current has a clear horizontal shear, the coastal current has the characteristics of a southerly current, and the outer sea Taiwan warm current has the characteristics of a north-northeast current. In August 1981 the coastal current velocity was rather small and in October the coastal current velocity had clearly increased, and was of the same intensity and expanded range toward the south of the Zhejiang coastal waters; on the outer side of the coastal current, from the figures we can see that in June, the current direction in the sea area under study was toward the north (the surface is in a northeasterly direction), the current velocity was small, averaging 9 cm/sec. In August, the upper layer sea current leaves the shore and the maximum current velocity reaches 40 cm/sec, but the lower layer current velocity diminishes and there is a component which climbs the shore, showing that the upper layer sea water is characterized by offshore radiation, and the lower layer sea water, by shoreward compensation. In October, the middle layer offshore current has a certain intensity, and the lower layer sea current still has a shoreward component. The average velocity of the sea current in October is 18 cm/sec, clearly smaller than in August. All of these circumstances indicate that the shoreward rise of the Zhejiang coastal rising current front is inseparable from the offshore radiation of the upper layer sea water and the upwelling of the lower layer sea water. The greater the offshore radiation of the upper layer sea water, the higher the rise of the rising current front layer; the smaller the offshore radiation of the upper layer sea water, the lower the rise of the rising current front layer. As concerns the intensity of the offshore radiation of this upper layer sea water, on the basis of observation results, it can be seen as primarily determined by the direction and current velocity of the Taiwan warm current axis. In fact, from Figures 12-14, it seems that the left side flow of the Taiwan warm current axis is characterized by flow north north-northeast, northeast, and north-northeast in August and October, and the current velocity is small in June, fastest in August, and diminishes again in October, indicating the uniformity of upper level sea water offshore radiation and the height of the rising of the rising current front layer in June, August, and October.

In addition, the Taiwan warm current also is characterized by flow along depth curves. The June, August, and October upper layer sea current surface distribution reveal this phenomenon, thus also verifying the views stated in Reference 5.

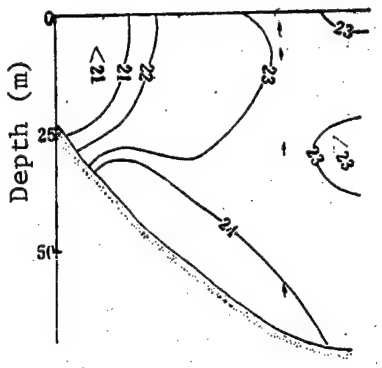

Figure 12. Vertical Distribution of σ_t and Horizontal Current Vectors of Cross Section No 4 in June 1981

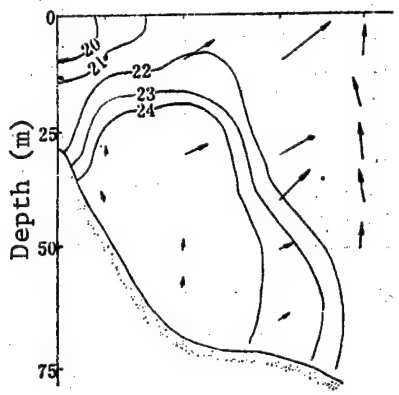

Figure 13. Vertical Distribution of σ_t and Horizontal Current Vectors of Cross Section No 4 in August 1981

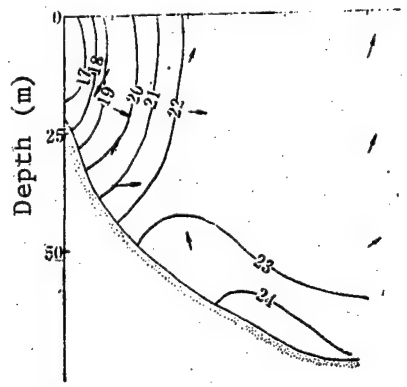

Figure 14. Vertical Distribution of σ_t and Horizontal Current Vectors of Cross Section No 4 in October 1981

III. Hybrid Condition in an Area Where Three Water Masses Join

The area where three water masses join here actually refers to the area adjacent to the coastal front and the rising current front. The analysis will rely mainly on the temperature-salinity point cluster chart and static and dynamic stability. The cross section studied is the No 4 cross section near 29°N latitude.

1. t-S Point Cluster Chart

Figures 15-17 are the results obtained by three sailings in June, August, and October 1981. The basic characteristics of the hybrid of the three water masses in the seas near Zhejiang reflected in these three figures are: the hybrid at the interface between the Zhejiang coastal water mass and the upper layer water mass of the Taiwan warm current is primarily a lateral hybrid, and between the upper and deep layer waters of the Taiwan warm current the hybrid in this area is primarily a vertical hybrid. The lateral hybrid in the nearshore section is clearer in June and August and the lateral hybrid is very clear in October. As for the vertical hybrid, in June it only appears in the farshore section, by August this phenomenon extends to the nearshore section, and in October again retreats to the farshore section, revealing the characteristic of the vertical hybrid in the cross section studied that it expands toward the shore with the rising current; the lateral hybrid expands out to sea as the intensity of the deep layer upwelling retreats.

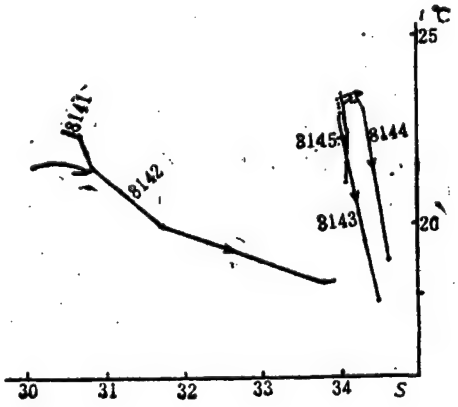

Figure 15. Collection Graph of t-S Points of Cross Section No 4 on 17 June 1981

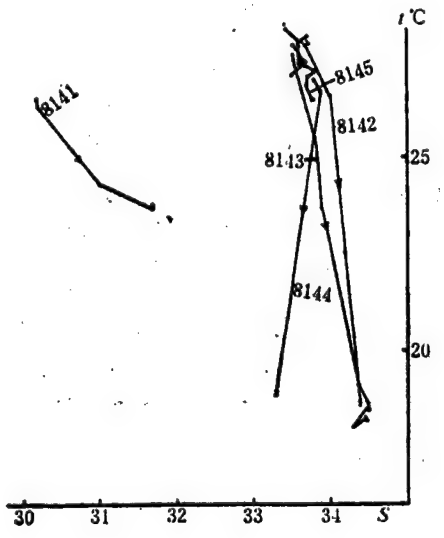

Figure 16. Collection Graph of t-S Points of Cross Section No 4 on 7 August 1981

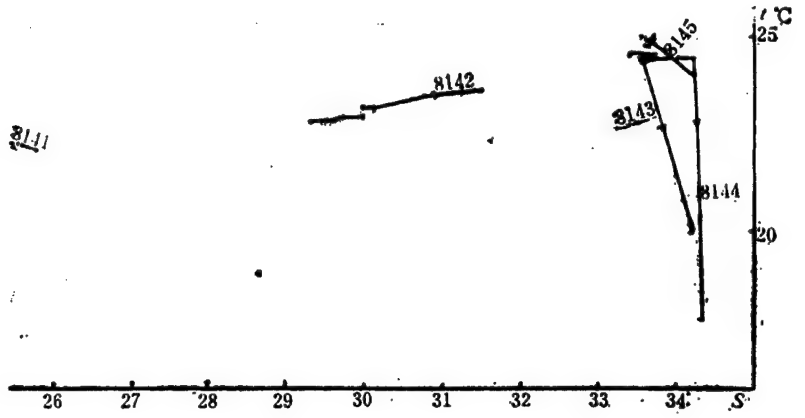

Figure 17. Collection Graph of t-S Points of Cross Section No 4 on 11 October 1981

2. Vertical Stability

We calculated the vertical stability of the sea area studied. The results show that the monthly variation characteristics of the vertical stability of the sea area studied are: in winter it is zero, in spring it gradually increases, in summer it is at its maximum, and in autumn it decreases again.

The distributional characteristics of vertical stability in the lateral cross section can be seen in Figures 12-14. The vertical stability in the rising current front layer generally should be greater than the vertical stability in the coastal front. As concerns the vertical stability distribution in the rising current front layer, the vertical stability of the rising current front layer near the outer sides of the coastal front (conditional density isoseismic line level distribution section) generally is greater than its two sides. This phenomenon seems to indicate that the rising current front layer in this area can form a cross-over screen for the upper and lower level water bodies, and in addition may intensify the development of the lateral hybrid in the coastal front area.[8] As concerns the reasons why the stability of this area tends to be greater, our understanding from the analysis is that it is because the speed of the upwelling of the deep layer water in this area is greater than the sea area's slope toward the outer side.[2]

3. Estimated Results of the Richardson Number (R_i)

The equation for calculating the Richardson Number[8] is

$$R_i = g\frac{\partial \rho}{\partial z} \Big/ \rho\left(\frac{\partial U}{\partial z}\right)^2$$

in which, g is gravitational acceleration, ρ is average density, U is horizontal flow velocity, z is vertical direction of the axis. Figure 18 is the calculation result. From Figure 18 it can be seen that the R_i value is at its maximum between stations 8142 and 8143 and that the R_i value suddenly

decreases between stations 8143 and 8145, this situation means that the rising current front layer between stations 8142 and 8143 is highly dynamically stable, but the dynamic stability of the area between stations 8143 and 8145 is not great. Connecting this with the static stability distribution discussed above, from the calculation results it seems we can learn that however great the rising velocity of the water body below the rising current front, it is generally difficult to penetrate the rising current front layer entering the offshore front area. This is because, between stations 8142 and 8143, this water layer not only has considerable static stability, but also very great dynamic stability. This conclusion can be verified by the results of observations that the Taiwan warm current deep layer water which has low temperature, high salinity, high phosphorous content and low oxygen content does not penetrate the coastal front area.

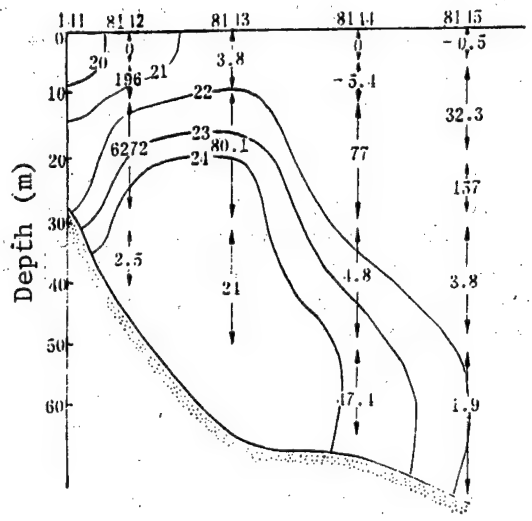

Figure 18. Cross Section No 4 R_i Distribution in August 1981

Solid lines are equal condition density lines, numbers between arrow heads indicate the R_i values in the observed layers.

IV. The Causes of Variation Occurring in the Zhejiang Coastal Rising Current Area Front Surface

On the basis of analysis of historical materials, the causes of variations which occur in the coastal front (including its tongue portions) depend primarily on the axis of the Taiwan warm current and the wind. Generally speaking, when the axis of the Taiwan warm current is narrow and close to the shore, the intensity of the coastal front increases, and fish school; when the current is wider and gradually moves away from the coast from south toward the north, the intensity of the coastal front diminishes, and fish scatter. A long period of east-northeast winds can cause the Zhejiang coastal water to extend along the coast to the south, and the warm current width becomes smaller and slightly closer to the coast, the intensity of the coastal front increases; long periods of west-southwest winds can cause the

Zhejiang coastal waters to shrink toward the north, the width of the warm current axis increases and leaves the shore, the coastal front intensity diminishes. The formation and advance and retreat of the highly saline tongue fronts are determined by the influence of the Taiwan warm current and the intensity of its axis: as the intensity of the Taiwan warm current increases, its northerly advance is further; in the opposite case, it retreats toward the south. The role of the wind generally can promote the lateral shift of the highly saline tongue front, especially north of 29°30'N, and because the bottom in this area is flat, the tongue front's lateral fluctuation is greater.

For the causes of the variation in the height of the Zhejiang coastal rising current front layer we must start with the formation of the rising current in this area. This is because the rising current front layer's inclination toward the shore in the final analysis is because of the rising of the Taiwan warm current deep layer water. However, in terms of the rising mechanism of the Taiwan warm current deep layer water, current explanations are not in agreement. Some feel that the wind is primary, others feel that it is primarily the after pulses of the north Kuroshio climbing the continental shelf sea bottom along the East China Sea. On the basis of historical materials and the actual observational results of the surveys conducted by the Second Oceanologic Institute, State Oceanologic Bureau we feel that scattering of the depth contours of the central Zhejiang offshore waters' sea bottom and the Taiwan warm current are an important factor. This is because with an unfavorable wind (east-northeast wind) the Taiwan warm current deep layer water in this area still has traces of upwelling (see Figures 13 and 14 and the State Oceanologic Bureau cross section survey materials of June 1977 and June 1978 at the 29°N cross section); in addition, the winter sea current observation materials (late 1982) show that even with a prevailing northeasterly wind the bottom layer current of this area still has a slope climbing component.

The theory from this point of view which is presented in this paper is based on the topographical rising current theory proposed by Janowitz, et al.[6] This theory holds that when the boundary sea currents which have weak variable current natures along the depth contours flow up on sloping variable continental slope (Rossby number $R_0=\frac{V_M}{fL}<<1$, in which V_M is the characteristic velocity, f is the Coriolis parameter, and L is the horizontal length), the rising current produced can be expressed with the following equation

$$W_1(x,y,-h)=-\frac{h}{f}\left(\frac{V_M}{a}\right)^2\left|\nabla h\right|\frac{\partial}{\partial S}\nabla^2 h,$$

in which

$$\frac{\partial}{\partial S}\nabla^2 h=\frac{\partial}{\partial S}\left(\frac{\partial^2 h}{\partial n^2}\right)+\frac{1}{r^2}\frac{\partial h}{\partial n}\frac{\partial r}{\partial S}-\frac{1}{r}\frac{\partial}{\partial S}\frac{\partial h}{\partial n}.$$

When the curve radius of the depth contour is very great (the central Zhejiang offshore seas belongs to this condition)

$$\frac{\partial}{\partial S}\nabla^2 h \doteq \frac{\partial}{\partial S}\left(\frac{\partial^2 h}{\partial n^2}\right).$$

in which W_1 is the vertical upward velocity, V_u and a are the deep contour slope and the upward velocity of the boundary sea current, $|\nabla h|$ is the absolute value of the downward deep contour slope, and r is the curve radius.

This means that there is a relationship between the upwelling current velocity caused by topography and the boundary sea current velocity and the variations in the upward and downward topographical slope.

On the basis of the above equations and the maximum current velocity of the Taiwan warm current on the one hand and the minimum possible velocity and the distributional characteristics of the deep water contours in the sea area under study (see Figure 19 for the calculation sea area) we calculated the upwelling velocity of the Taiwan warm current deep layer water in the sea area under study and the values we obtained were, when the Taiwan warm current velocity was 40 cm/sec, the deep layer water rising velocity was 6×10^{-3} cm/sec; when the Taiwan warm current velocity was 10 cm/sec, the deep layer water upwelling velocity was 4×10^{-4} cm/sec (see Table 1).

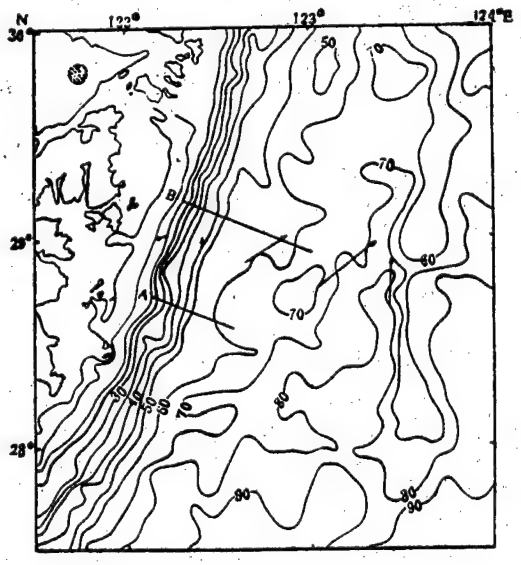

Figure 19. Zhejiang Offshore Sea Bottom Topography and Flow Characteristics of the Taiwan Warm Current

Table 1. Vertical Velocity West of 60 m Depth Contour at 28°40'-29°10'N

α	V_M (cm/s)	f (1/s)	h (cm)	$\lvert\nabla h\rvert$	$\frac{\partial}{\partial s}\left(\frac{\partial^2 h}{\partial n^2}\right) = \frac{\left(\frac{\partial^2 h}{\partial n^2}\right)_B - \left(\frac{\partial^2 h}{\partial n^2}\right)_A}{\Delta S}$ (1/cm²)	w_{-h} (cm/s)
1×10^{-3}	40	7×10^{-5}	45×10^{2}	6×10^{-4}	-1×10^{-16}	6×10^{-3}
	10					4×10^{-4}

$R_O = 0.05$ in which $V_M = 40$ cm/s, $f = 7 \times 10^{-5}$/s, L = 100 km

This result indicates that in the Zhejiang coastal seas the deep layer water upwelling velocity caused by the Taiwan warm current and the sea bottom deep contour divergency is of rather large magnitude. This paper also estimates the velocity value of wind driven rising front current and we discovered their magnitude is considerable, with a value of $5 \times 10^{-3} - 4 \times 10^{-4}$ cm/sec. Thus on the basis of the results we feel that topography and wind make a sizable contribution to the Zhejiang offshore coastal rising current, therefore, apart from the wind force the role of topography and the Taiwan warm current must be taken into account. The above-described observed phenomena can be seen as, under certain combined circumstances, such as when topography and current are in the dominant position, it can cause the deep layer water to upwell under unfavorable wind conditions. But the above-described distributional traits of the height of the rise in the lower front layer may amount to a clear scattering of the deep contours (40-60 m) in the vicinity of 29°N latitude. In the northern part there is a slight convergence.

We are indebted to Professor Su Jilan [5686 4764 5695] for reading this paper and providing valuable opinions and we express our profound thanks.

REFERENCES

1. Hu Dunxin [5170 2415 2946], GUANYU ZHEJIANG YANAN SHANGSHENGLIU DE YANJIU [ON THE STUDY OF THE ZHEJIANG COASTAL RISING CURRENT], Kexue Tongao, 1980, 3:131-133.

2. Pan Yuqiu [3382 3768 3808], ZHEJIANG YANAN SHANGSHENGLIU FENGQU TEZHENG JI QI CHENGYIN DE CHUBU TANTAO [THE TRAITS OF THE ZHEJIANG COASTAL RISING CURRENT FRONT AND PRELIMINARY EXPLORATION OF ITS CAUSES], Haiyang Hushao Tongbao, 1980, 3:1-7.

3. Ding Zongxin [0002 1350 0207], FENG DUI ZHEJIANG YANAN HAIYU XIAJI WENYAN ZHUIZHI JIEGOU HE SHANGSHENGLIU DE YINGXIANG [THE INFLUENCE OF WIND ON THE RISING CURRENT AND SUMMER TEMPERATURE-SALINITY VERTICAL STRUCTURE OF THE ZHEJIANG COASTAL SEAS], Haiyang yu Hushao, 14 (1983), 1:14-21.

4. Weng Xuezhuan [5040 1331 0278], et al., TAIWAN NUANLIU SHENCENGSHUI BIANHUA TEZHENG DE FENXI [ANALYSIS OF THE VARIATION CHARACTERISTICS OF DEEP LAYER WATER IN THE TAIWAN WARM CURRENT], Haiyang yu Hushao, 14 (1983), 4:357-366.

5. Guan Bingxian and Mao Hanli, A NOTE ON CIRCULATION OF THE EAST CHINA SEA, C.J. of Oceanology and Limnology, 1 (1982), 1:5-16.

6. Janowitz, G.S. and Pietrafesa, L.J., THE EFFECTS OF ALONG SHORE VARIATION IN BOTTOM TOPOGRAPHY ON A BOUNDARY CURRENT (TOPOGRAPHICALLY INDUCED UPWELLING), Continental Shelf Research, 1 (1982), 2:123-141.

7. Guan Bingxian [4619 4426 6343] and Chen Shangji [7115 0006 0644], ZHONGGUO JINHAIDE HAILIU XITONG [China's Offshore Seas' Current System], 1964.

8. Nakao Tetsu, tr. by Wang Yuan [3769 0337], Zou Emei [6760 1230 2734], HUANGDONGHAI HAIYANG HUANJIN BIANHUA YU YUYE DE GUANXI [RELATIONSHIP OF VARIATION IN THE MARINE ENVIRONMENT IN THE EASTERN YELLOW SEA AND FISHERIES].

8226/6091
CSO: 4008/1097

STRUCTURAL FEATURES OF OKINAWA TROUGH BY SEISMIC REFLECTION

Beijing HAIYANG YU HUZHAO [OCEANOLOGIA ET LIMNOLOGIA SINICA] in Chinese
Vol 16, No 6, Nov 85 pp 481-487

[Article by Jin Xianglong [6855 5046 7893], Zhuang Jiezao [8369 2638 2764], Tang Baojue [0781 1405 3778], Mu Dunshun [3664 2415 7311], Fan Shouan [5400 1343 1344], and Wang Shaozhi [3769 4801 2535], Institute of Oceanology, Chinese Academy of Sciences, Qingdao; Contribution No 1113 from the Institute of Oceanology, Chinese Academy of Sciences; This paper is the seismic reflection portion of a paper read at the annual meeting of the China Marine Geology Association in 1982; paper received 3 November 1984; first two paragraphs are source-supplied English abstract]

[Text] A seismic reflection survey for investigating the structure of the Okinawa Trough was carried out in June 1982. The seismic strata in the Trough are divided into three layers: the upper layer, the middle layer and the lower layer, they are Pleistocene, Pliocene and Miocene, respectively. The upper layer is of parallel or subparallel seismic reflection configuration. The reflection interfaces keep primary sedimentary structure, and are easy to track continuously, the energy reflection from which is intensive. The middle layer is folded slightly. The seismic interface of the middle layer appears mostly in short curves due to faulting and folding, the energy from which is either strong or weak. The interface cannot be tracked in a wide area, because the seismic sequences lost primary sedimentary structure already. The lower is a deformed layer. The interface of the lower layer is rough and obscure, the reflected energy from which is so weak that the lower layer is even reflection-free or with chaotic seismic reflection configuration.

There are several seismic onlaps of stratal configuration for each layer, implicating relative changes of sea level in geological time. Three important sedimentation cycles were found in the upper layer, and the progradational reflection configuration can be distinguished in seismic profile DSIII. Numerous contemporary structures, such as growth faults and roll-over structures, are produced in the sedimentation process.

The trench-arc-basin system of the Western Pacific is structurally a violently active zone. The Okinawa Trough is a dorsal arc basin on the inner side of the Ryukyu Island arc. The Western Pacific (Philippine Sea)

Plate has had a big influence on the geological formation and structural activity of the Ryukyu Trench, Ryukyu Arc and Okinawa Trough, and research on the structure of the Okinawa Trough will be of help in revealing the history of the development of this trench-arc-basin system. According to research,[1] there are clear differences between the northern and southern parts of the Okinawa Trough in crustal configuration, sea bottom heat flow, and structural activity. The southern section of the Okinawa Trough has a thin crust, high heat flow value, and violent structural activity; the northern section has a thicker crust, lower heat flow value, and weaker structural activity. The Okinawa Trough not only has significance topographically, but more importantly, it is a dorsal arc basin or peripheral basin, structurally. Studying the structural geology of the southern section of the trough is especially important for understanding the structural characteristics of the Okinawa Trough.

In June 1982, the research vessel "Kexue No 1" of the Institute of Oceanology, Chinese Academy of Sciences, measured five seismic reflection sections (Figure 1) of the southern section of the Okinawa Trough to study the geological characteristics of the trough.

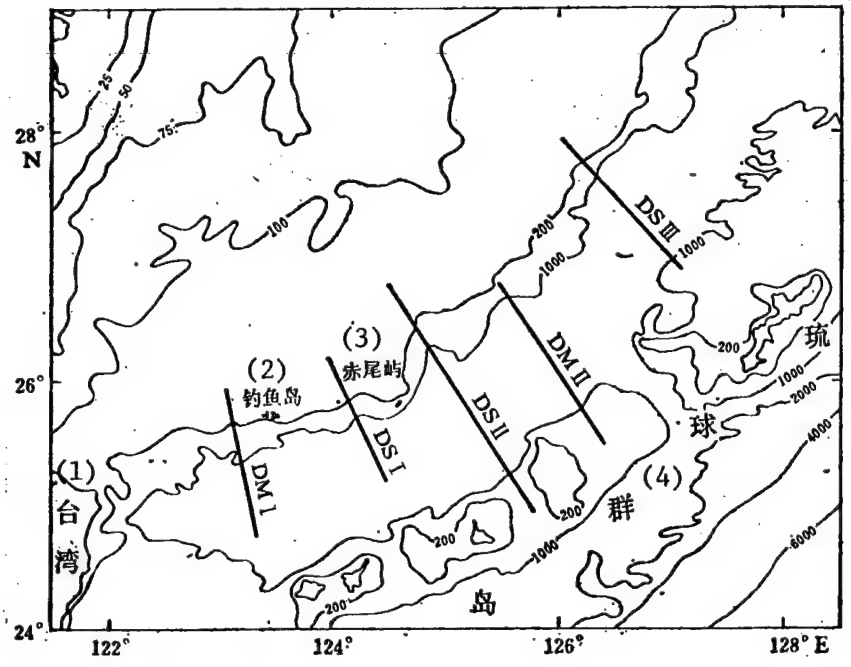

Figure 1. Map of Seismic Measurement Line Positions

Key:

1. Taiwan
2. Diaoyudao
3. Chiweiyu
4. Ryukyu Archipelago

I. Geophysical Work Method

Navigational positioning was carried out by a compound satellite navigational system made up of satellite receiver, Laolan [0525 5695] C and doppler sonar. The average position error was 45 m. Due to the influence of the doppler sonar work state (on traces of water masses or the sea bottom), we calculate the ship's position error to be at the most 2 nautical miles and at the least, 0.5 nautical miles, and the maximum measurement line deviation to be 3 nautical miles.

All geophysical measurement was under the unified management and automatic control of a geophysical materials collection system made up of a three-level computer. An HP2112B computer directed the compound satellite navigation system and the geophysical measurement systems. For the seismic system, PEC peripheral controller received instructions from the HP2112B, then controlled the entire seismic measuring system, which included an Aircon-3 gas gun controller, DFS-V digital seismograph, ERC photographic recorder and EPC 3200 electrostatic plotter. An SE148-channel seismic floating towed cable was used as receiving equipment. The towed cable depth was generally held at 10 m under water. Its attitude was determined by an automatic depth controller (AC/DC) and from shipboard the depth could be changed as necessary by issuing a command at any time. The sound source was a gas gun array with a capacity of 1820 in^3 (30L) and pressure of 1898 lbs/in^2 (130 kg/cm^2). The array was made up of 7 gas guns (610, 400, 250, 190, 150, 120 and 100 in^3), controlled by the Aircon-3 gas gun controller, with a trip synchronization error held at ±1 ms. The gas gun array was submerged at a depth of 10 m. The research vessel's operating speed was 4-5 knots, and the gas gun firing interval was 50 m.

II. Seismic Measurement Results

The five seismic measurement lines distributed in the southern section of the Okinawa Trough are, from south to north, DM I, DS I, DS II, DM II, and DS III, the measurement lines being nearly perpendicular to the direction of the trough.

The DM I cross section enters the Okinawa Trough on the southwest side of Diaoyudao. DS I crosses between Diaoyudao and Chiweiyu, reaching a point 40 nautical miles northwest of Shiyuandao. DS II passes to the northeast side of Chiweiyu and to a point 30 nautical miles east of Gonggudao. DM II is located between Jiumidao and Gonggudao. DS III goes from southeast of the continental shelf to 60 nautical miles northwest of Okinawa Island.

According to the analog recording of the seismic jindao [6602 6670] reflection (corresponding to the vertical incidence and reflection), the seismic reflection waves of the trough area can be divided mainly into three groups, part of the area can be divided into four groups, each corresponding to a definite layer position. The upper layer (layer A) is made up of undeformed reflection interface, which is mostly parallel or subparallel relations, basically maintaining the primitive configuration. This interface is flat, reflection energy is strong, and can be tracked continuously; the layer

thickness is different in different places, the thickest reflection travel time was nearly 2 seconds, and the thinnest was about 0.3 seconds. The southern section of the trough is thick, becoming thinner toward the north. The middle layer (layer B) is made up of microdeformed reflection interface, the layer has undergone slight bending, this layer's reflection interface is slanted or shows arc-shaped short line segments, reflection energy is medium, it is not easy to track over a large range, the layer thickness varies the reverse of layer A, thinner in the south of the trough and thicker toward the north. In a transverse direction across the trough, the thickness of the central part is greater, becoming smaller toward the two sides. The bottom layer (layer C) is made up of severely deformed reflection layers; the bottom layer interface curvature is very varied or abruptly faulted, its undulations are very large, reflection energy is extremely weak, with the reflection even disappearing, the interface is not continuous, and it is very hard to track and contrast. The lower interface of the layer is frequently not visible and its thickness is hard to estimate. Below layer C in some areas another layer (layer D) can be faintly distinguished.

The basic characteristics of the measurement lines are as follows:

DM I (Figure 2, Plate I:A) There are three configuration layers in the cross section. Layer A has a divergent configuration toward the center of the trough, the bottom curves downward, the spacing of the reflection interface in the central part of the trough is thin, becoming denser on the two sides. This layer is very thick, the maximum travel time in the trough being as much as 1.5 seconds, on the western slope it was about 1 second, the central part of the trough is thick, the two sides are thinner. The interfaces of layer A in the trough appear as onlap reflection terminals. This layer can be divided into three sublayers, representing three large sedimentation cycles. Layers B and A are in a disconformity relationship. In the trough, layer B is filling shape, its thickness is uneven, with a maximum travel time of not more than 1 second, but off the margin of the continental shelf it becomes more stable, and the thickness also increases. In this layer there is partial covering and onlap, which appears at the periphery of the continental shelf and at the edge of the B layer sedimentation basin. They may be a rock bulge. Layer C basically has no reflections, and the bottom interface is not visible.

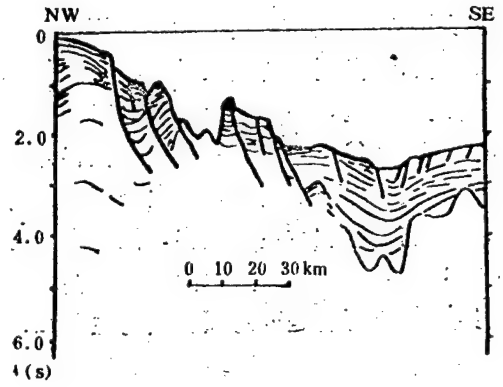

Figure 2. DM I Geological Cross Section
(For seismic record see Plate I:A)

On the trough slope the layer is cut by many normal faults, with the fault surfaces inclined toward the center of the trough, rather steeply, but generally the steepness tapers off downward, the rock layers have been tilted in the opposite direction by the fault action, manifesting large-scale block sliding, two reflections appeared in the trough.

DS I (Figure 3, Plate I:B) The trough center is intensely depressed, and has three reflection layers: A, B, and C. Layer A is an undeformed reflection layer, energy is strong, interface is distinct and rather regular, it can be tracked and compared in large section, between the interfaces is a secondary parallel relationship, the layers within the trough exhibit dispersion toward the center of the trough. The continental shelf region layer A is dispersed toward the west. Layer A suffered damage from a multitude of faults, the faults are nearly erect, incline toward the center of the trough, a large amount of sliding construction appears. This layer is very thick, the travel time exceeds 1.5 seconds, it also can be divided into three sublayers, between each of which is an overlap relationship, which indicates that the sea surface had changed several times; the uppermost sublayer also can be divided into two groups, between which there is a strong reflection interface, divided into different sedimentation cycles. In the trough there are valleys which are filled with horizontal modern deposits. Layer B is a microdeformed layer, reflection interface is slightly curved, it is in disconformity contact with the covering A layer interface (layer A overlaps B layer), and in discordance contact with the underlying C layer interface. C layer interface is severely deformed geometrically, the bottom interface is not clear. On the trough slope there may be some magma intrusion activity.

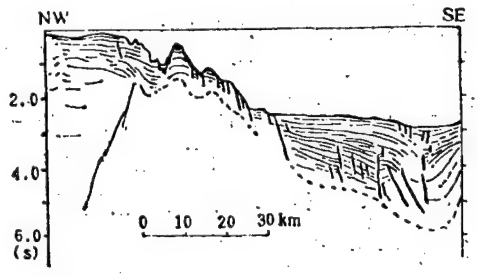

Figure 3. DS I Geological Cross Section
(For seismic record see Plate I:B)

DS II (Figure 4, Plate I:C) Primarily three layer configurations, but a D layer can be seen faintly. Layer A is level, thickness is less than 1 second (travel time), toward the island arc it becomes thinner or missing, toward the continental shelf it is not easy to separate it from layer group B, the two become a subparallel relationship, yet in part of the area layer A can be seen to overlap layer B. Layer A was damaged by a great many nearly vertical faults, the fault faces are slightly inclined toward the trough center, these are contemporaneous faults of gravitational sliding, and the layer A some rolling folds were also created. Within layer A one can distinguish at least two onlap configurations, which means that when layer A was

formed at least two fluctuations occurred. Layer B is microfolds, thickness within the trough is 0.4-1.1 seconds (travel time). Layer B reflection interface in the trough mostly exhibits curved arc sections forming a (dieluanzhuang) configuration. They may represent the sliding of turbidity current accumulation of sediments. But in the trough some large amplitude brief reflections and diffractions and covering phenomena outside the margin of the continental shelf may indicate that layer B was penetrated by some rock bulge. Layer C in the trough basically has no reflections, but in the cross section folding near the island arc section is clear. It is the main body which makes up the sea bottom in this section. In the eastern part of the trough appears an enormous sliding block which is made up of layer C and part of layer B, with a nonconformity relationship between them. Layer D also appears in the western part of the trough bottom, it is very clear and needs further study.

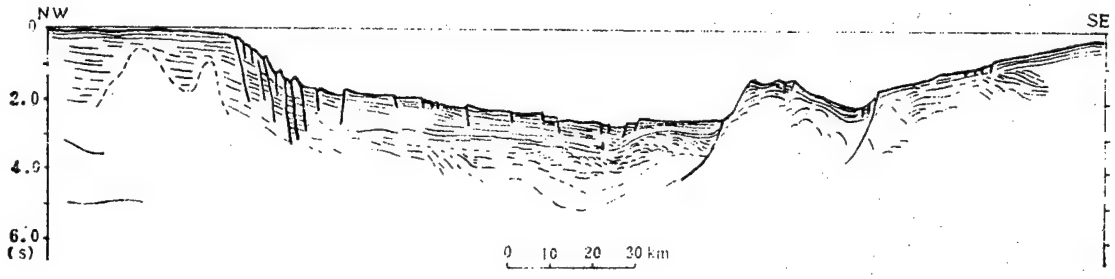

Figure 4. DS II Geological Cross Section
(For seismic record see Plate I:C)

The two trough valleys at the bottom of the trough are both filled by layer A, the fullest valley has 0.5 second (travel time) thick deposits. Toward the two sides they diminish progressively, and with the underlying interface form an onlap configuration. These two valleys may have been one unified deposit basin which later was cut in two by a rock bulge. Outside the margin of the continental shelf there is a large area without reflections, and this very well might be a rock intrusion.

DM II (Figure 5, Plate II:D) Still a three-layer structure. The cross section of layer A discussed above is thin, although the central part of the trough is thick, its travel time is only about 0.5 seconds. The top of this layer has been damaged by many simultaneous normal faults, and created sliding toward the center of the trough. The cross section of layer B discussed above is thick, can be reached in 1.2 seconds, deformation is also severe, and it has been cut by a great number of microbent vertical faults toward the center of the trough. The faults may cut across layers B and A so that the reflection interface is sloped, showing clear block sliding and collapse; when layer B was formed, it was accompanied by a mass of simultaneous faults, rock formation sliding and rolling, so that many fine short arc reflection configurations appeared on the cross section. Layers B and A in the trough are deposited in two basin valleys. The basin valley near the island arc is a narrow structural valley, matter fills the valley to a thickness of 2.5

seconds (travel time) and the reflection interface is clear. One side of the valley is a large fault, the other side may be a rock bulge. One basin valley in the central part of the trough is large. It is the main basin of the bottom of the trough but has been punctured by a volcanic cone and rock bulge so that the sides of this basin valley have been separated into two small valleys, which are filled with the material of layers A and B, but primarily of layer B. Layer C at the bottom of the trough exhibits a non-reflecting configuration. It may be the primary constituent matter of the near island arc slope, but above it is the thick layer B.

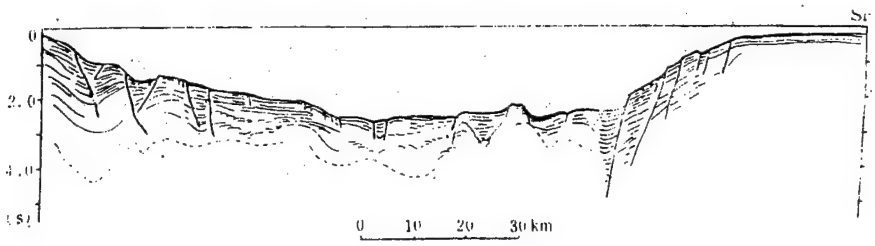

Figure 5. DM II Geological Cross Section
(For seismic record see Plate II:D)

DS III (Figure 6, Plate II:E) This cross section is a three-layer structure. Layer A is very thin, with a travel time generally of 0.3-0.5 seconds, and has an onlap or underlap relationship with the underlying reflection layer surface. Generally speaking, layer A is characterized by the preaccumulation configuration (oblique or S shaped) and sometimes exhibits a transitional relationship with layer B. The top of layer A has some gravity sliding simultaneous faults. Layer B is thick, travel time can reach 1-1.6 seconds, and its top is very like the top sets. In the trough, layer B forms a trough basin of the sedimentation center toward the southeast, it is in contact with the island arc slope as a fault, here the sediments are more, but there may be rock bulge thrust into the bottom so that they are separated from the main trough basin. The reflection interface of layer B in the main is toward the northwest and cut off by faults, forming a block sliding structure. Layer B in the center of the trough and on the outside of the continental shelf periphery also has some puncturing, possibly still caused by rock bulge. The side slope of the island arc is mainly composed of layer B. The top of layer C is not clear, but the main body is still of a nonreflecting configuration.

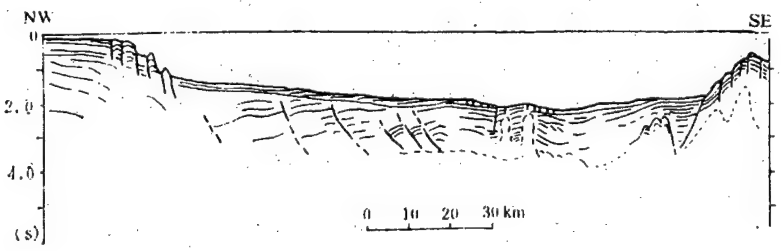

Figure 6. DS III Geological Cross Section
(For seismic record see Plate II:E)

III. Conclusion

1. The Okinawa Trough can generally be divided into three reflection layers A, B, and C. Layer B is generally the top layer of the island arc slope rock, and in cross section DS III formed the main body of the island arc border slope but DS III's eastern section approaches Okinawa Island. The primary rock layer on the island's basic rock system is Pliocene (daokaoqun), which is broadly distributed throughout the entire Ryukyu Islands, the (daokaoqun) has slight folds[2,3] and its characteristics are extremely similar to layer B, thus the age of layer B should be Pliocene. On layers A and B the surface layer of the sea bottom was formed, thus its age is Pleistocene or Modern. Layer C which is seriously deformed below the nonconformity surface on the bottom of layer B should correspond to Miocene series or strata even older than Miocene. Layer D is an older strata than layer C, but there is no way to date it (Table 1).

Table 1. Comparison of Strata Eras

Layer	Era	Comparison with Ryukyu Archipelago strata
A	Modern to Pleistocene	Ryukyu (or nabazu)
B	Pliocene	Daokaoqun
C	Miocene or older	Bazhongshanqun or older
D	Undetermined but older than C	

2. In the direction stretching along the axis of the trough there are changes in the distribution of the thickness of layers A and B. Layer B (Pliocene) is thicker in the northern part of the trough, with a maximum (both paths) reflection travel time of 1.6 seconds, the thickness of the southern part of the trough is smaller, with a reflection travel time of 1 second; it is just the opposite with layer A (Pleistocene): in the northern part of the trough it is 0.3-0.5 seconds, and in the southern part of the trough reaches 1.5 seconds or slightly more (Table 2).

Table 2. Comparison of Variation in Thickness (Reflection Travel Time) of Layers A, B, and C in Cross Sections

Time (s) / Cross section / Layer	DM I	DS I	DS II	DM III	DS III
A (Pleistocene)	1.5	>1.5	<1	0.5	0.3-0.5
B (Pliocene)	<1	*	0.4-1.1	1.2	1-1.6

*Bottom interface not clear, hard to measure.

Layer B is thicker in the north and thinner in the south, layer A is thicker in the south and thinner in the north indicating that from the end of the Pliocene to the beginning of the Pleistocene there were changes in structural activity and the sedimentation environment in the Okinawa Trough or that

relative differences appeared in the rate of fissure subsidence in the southern and northern parts of the trough with different eras or that the pattern of the fissure subsidence varied with time.

Some rock bulges frequently appear in layer B and from configuration identification a few were created by volcanic action, but the majority are reef shaped bodies or salt domes which appeared when layer B was formed and require further study.

In layer A there are many onlap configurations, which indicates the numerous sea level changes which occurred since the Pleistocene, and in the cross section at least three major sedimentation cycles can be identified. A pre-accumulation sedimentation layer appears in DS III cross section.

3. Normal faults developing fully along the direction of the trough in the center of the trough are important evidence of the cause of the trough fissure subsidence. From the configuration of these layers we see that the maximum location (the center) of the fissure subsidence is toward the eastern half of the trough indicating the asymmetrical nature of the trough fissure subsidence.

Many simultaneous faults appear in both layer A and layer B, and some large-scale gravitational slide structures appear in layer B in particular, the collapse fissure surfaces generally are steep at the top and gradual at the bottom, and can be viewed as evidence of trough edge filling and marginal fissure subsidence.

4. The identification of the appearance of many deep reflection layers which seriously interfere with reflection in the strata cross sections, depending on the time of appearance and frequency, may be judged to be multiple reflections of the sonar waves between the sea surface and sea bottom or sea bottom strata, the frequency of reflection is in direct proportion to the extreme density (reflection coefficient) of the rocks of the sea bottom strata. According to statistics, the number of reflections in the trough generally were only two, on the marginal slope of the continental shelf were three, but on the island arc slope could be as many as eight or nine. The overall sequence of sea bottom strata rock density from large to small is island arc slope, continental shelf slope, and trough. This situation indicates that the occurrence of multiple reflections in the trough can be controlled.

Yu Puzhi [0827 2528 0037], Yu Jianjun [0060 1696 6511], Du Quansheng [2629 0356 0524], Wang Gang [3769 0474], Sui Yiyong [7131 0110 0516], Yu Tao [0060 3447], Zhang Baolu [1724 1405 4389], Li Benzhao [2621 2609 0340], Lu Chengfu [0712 2052 1381], Li Changzhen [2621 1603 3791], Wang Huiqing [3769 1920 0615], and Li Naisheng [2621 0035 0524] also participated in the work at sea.

REFERENCES

1. Jin Xianglong [6855 5046 7893], Yu Puzhi [0827 2528 0037], Lin Meihua [2651 5019 5478], et al., 1983. "Chongsheng Haizao Dike Jiegou Xingzhi De Chubu Tantao" [Preliminary Discussion of the Structural Nature of the Okinawa Trough Crust], HAIYANG YU HUZHAO 14(2): 105-116.

2. Kisaki Kanero, Oki Itsuro, 1977. "Ryukyu Gunto Teki Ko Chiri" [Ancient Geography of the Ryukyu Archipelago], (Japanese) KAIYU GAGKUSEI 9(8): 38-45.

3. Yan Lunbo [7346 3229 3134], 1978. "Taiwan Beibu Yu Liuqiu Qundao Nanbu De Dizhi Guanxi" [Relationship of the Geology of the Northern Part of Taiwan and the Southern Part of the Ryukyu Islands], TAIWAN HAIYANG XUEBAO 8: 1-21.

8226/6091
CSO: 4008/1004

NEUTRON ACTIVATION ANALYSIS OF THE SEDIMENTS AND GEOCHEMISTRY STUDY OF ELEMENTS IN THE OKINAWA TROUGH

Beijing HAIYANG YU HUZHAO [OCEANOLOGIA ET LIMNOLOGIA SINICA] in Chinese
Vol 16, No 6, Nov 85 pp 461-474

[Article by Li Peiquan [2621 1014 3132], Yu Yinting [0578 6892 0080], Ren Guangfa [0117 1639 3127], Institute of Oceanology, Chinese Academy of Sciences, Qingdao, Li Xiuxia [2621 1485 7209], Qian Xingzhen [6929 2622 3791], and Mao Xueying [3029 7185 3841], Institute of High Energy Physics, Chinese Academy of Sciences, Beijing: "Neutron Activation Analysis of the Sediments and Geochemistry Study of Elements in Okinawa Trough: 1. The Contents and Distributions of 29 Elements"; Contribution No 1239, Institute of Oceanology, Chinese Academy of Sciences; paper received 15 March 1983; first three paragraphs are source-supplied English abstract]

[Text] Abstract: The contents of 29 elements in sediments in Okinawa Trough have been determined with neutron activation analysis. The distributions of all elements have also been discussed. The elements can be divided into seven sorts. The contents of more than 80 percent of the elements approximate to that of Clarke's value. The distribution of the above-mentioned elements may be related to their physio-chemical property, redox state, biotic action, volcanic activity and sedimentation type.

The analysis of procedures including the preparation of the samples and the standard samples, radioactive determination and data processing are described in detail.

The neutron activated samples are counted directly by Ge (Li) gamma spectrometer with a large volume and high resolution after optimizing decay periods.

Research on the content, distribution, state, and transformation mechanism of elements in the oceans is very important for revealing the laws of movement of matter in the oceans, sediment composition and its changes, the relationship between the ocean and the land, the relationship between the composition of sediments on the sea bottom and the covering water, and the problem of pollution of the oceans brought on by industrial development. Updating and developing element analytical testing methods is one key to resolving the above-mentioned problems. The neutron activation method which

has the advantages of high sensitivity, strong selectivity, and can determine the many elements in a single sample has become an effective analytical technique in ocean research.[5-7,9] In recent years, there have also been some application of this work in China.[1,4] Recently we used this method to measure the content of 29 elements in sediments from the Okinawa Trough, and on this foundation carried out preliminary discussion on the influence of the interrelationship of the elements and the sedimentation types on the element content, the relationship of the source of the sediment and continental geology, the relationship of the enrichment coefficient and element stationary time and related factors which influence element distribution.

I. Analytical Method

1. Preparation of Samples

After being ground fine through a sieve (200 mesh) and mixed uniformly in 85°-90°C heat, the sediment samples from the Okinawa Trough were placed in a dryer for preservation. Before analysis, the samples were weighed into two groups (approximately 20 mg) and wrapped in two layers of pure aluminum foil.

2. Preparation of Standards

The elements were divided into 10 groups on the basis of the chemical and nuclear properties of the elements to be tested. The spectral compounds or metals of each element were weighed, the appropriate high purity acid or base solution was used to mix the standard solution, the breakdown of the elements and the prepared concentrations are listed in Table 1. The radiation standard used was: the mixed standard solution of each group was dropped on polyethylene film (ϕ6 mm) of known weight, then weighed precisely, and after being dried in a dryer, was wrapped in pure aluminum foil. From the weight of the solution and the density of the elements in the solution we can calculate the irradiation of the elements.

3. Irradiation

The two sets of standards were placed on the top and bottom of the sample, wrapped in aluminum foil and placed in the radiation container. They were irradiated for 15 hours in the central passage of the reactor at Qinghua University, and the neutron flux was about $1 \times 10^{13} n \cdot cm^{-2} \cdot s^{-1}$.

4. Radioactive Measurement

After radiation, they cooled for 3 days then the aluminum foil was removed from the sample and the standard and they were transferred to a polyethylene measurement bottle, and placed in the measurement gamma spectrum in a Ge(Li) detector. The detector used was a SCORPIO-3000 program controlled gamma spectrometer, the Ge(Li) detector sensitive volume was 136 cm^3, the energy resolution of 1.85 KeV had a relative efficiency of 28 percent, a fengkang [1496 1660] ratio of 55:1 (all of the above refers to the ^{60}Co 1332 KeV gamma rays). The sample and the standard were measured under identical conditions, and from the ratio of the radioactive intensity of the two we could calculate

Table 1. Concentration and Classification of Mixed Standard Solutions

(1)分 组	(2)元素	(3) 照射量 (g)	(4)化 合 物	(5)介 质	浓度 (g/ml) (6)
1	As	3.17×10^{-7}, 3.21×10^{-7}	As_2O_3	HNO_3	1.84×10^{-5}
	Na	1.26×10^{-5}, 1.28×10^{-5}	NaCl	H_2O	7.32×10^{-4}
	K	5.54×10^{-4}, 5.61×10^{-4}	KCl	H_2O	3.22×10^{-2}
2	Fe	3.10×10^{-4}, 2.69×10^{-4}	Fe 粉 (7)	HCl	2.01×10^{-2}
	Co	1.01×10^{-6}, 8.76×10^{-7}	Co 粒(12)	HCl, H_2O_2	6.53×10^{-5}
	Ni	1.55×10^{-4}, 1.35×10^{-4}	海棉 Ni (8)	HNO_3	1.00×10^{-2}
	Sb	4.74×10^{-6}, 4.12×10^{-6}	Sb 金属(9)	HCl, HNO_3	3.07×10^{-4}
	Th	1.54×10^{-7}, 1.34×10^{-7}	—	50%HCl	1.00×10^{-5}
3	Rb	2.13×10^{-5}, 1.99×10^{-5}	RbCl	H_2O	1.11×10^{-3}
	Cs	5.20×10^{-7}, 4.86×10^{-7}	CsCl	H_2O	2.71×10^{-5}
	Sr	1.37×10^{-4}, 1.28×10^{-4}	$SrCl_2\cdot6H_2O$	H_2O	7.15×10^{-3}
	Sc	6.06×10^{-8}, 5.67×10^{-8}	Sc_2O_3	HNO_3	3.16×10^{-6}
	Ba	5.51×10^{-5}, 5.16×10^{-5}	$BaCl_2$	HNO_3	2.87×10^{-3}
4	Zn	2.96×10^{-5}, 2.94×10^{-5}	Zn 粒(12)	HNO_3	1.89×10^{-3}
	Cd	3.66×10^{-7}, 3.64×10^{-7}	Cd 粒(12)	HCl	2.33×10^{-5}
	Se	3.31×10^{-6}, 3.30×10^{-6}	Se 粉 (7)	HNO_3	2.11×10^{-4}
5	Ta	3.91×10^{-7}, 4.18×10^{-7}	Ta 片(10)	2%HF	2.28×10^{-5}
	Hf	2.74×10^{-7}, 2.93×10^{-7}	HfO_2	HF, H_2SO_4, HNO_3	1.60×10^{-5}
	Cr	4.24×10^{-6}, 4.53×10^{-6}	Cr 粉 (7)	HCl	1.97×10^{-4}
6	La	4.24×10^{-7}, 4.15×10^{-7}	La_2O_3	HNO_3	2.18×10^{-5}
	Nd	2.26×10^{-5}, 2.21×10^{-5}	Na_2O_3	HNO_3	1.16×10^{-5}
	Eu	3.78×10^{-7}, 3.70×10^{-7}	Eu_2O_3	HNO_3	1.94×10^{-5}
	Yb	2.03×10^{-7}, 1.98×10^{-7}	Yb_2O_3	HNO_3	1.04×10^{-5}
	Lu	4.86×10^{-8}, 4.75×10^{-8}	Lu_2O_3	HNO_3	2.49×10^{-6}
7	Ce	3.07×10^{-6}, 2.83×10^{-6}	CeO_2	HNO_3	1.49×10^{-4}
	Sm	2.93×10^{-8}, 2.69×10^{-8}	Sm_2O_3	HNO_3	1.42×10^{-6}
	Tb	2.87×10^{-7}, 2.64×10^{-8}	Tb_4O_7	HNO_3	1.39×10^{-5}
8	U	1.01×10^{-6}, 1.11×10^{-6}	—	1%HCl	5.57×10^{-5}
9	Zr	1.44×10^{-4}, 1.32×10^{-4}	$ZrOCl_2\cdot8H_2O$	H_2O	6.85×10^{-3}
10	Ca	8.59×10^{-3}, 4.62×10^{-3}	$Ca(OH)_2$	固体(11)	

Key:

1. Class
2. Element
3. Irradiation volume (g)
4. Compound
5. Medium
6. Concentration (g/ml)
7. Powder
8. Sponge nickel
9. Metal
10. Plate
11. Solid
12. Granules

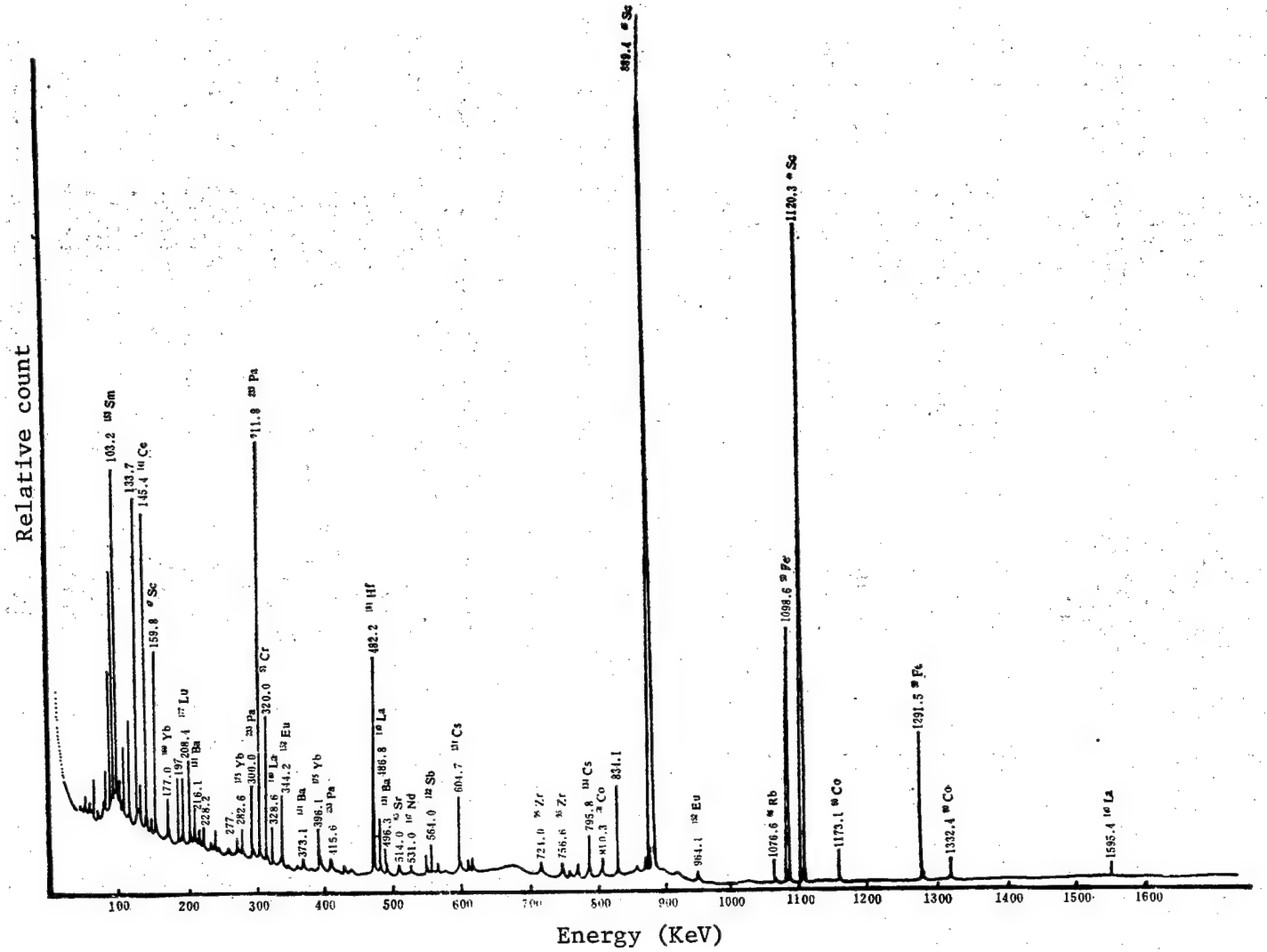

Figure 1. Gamma Ray Spectrum of Okinawa Trough Sediments (Spectrum After Cooling Samples for 15 Days)

the content of the elements. From the measured shorter half-life decay period nuclides after 3 days' cooling we obtained the content of the elements K, Na, As, Br, La, Sm, and U; after about 15 days' cooling we measured a second time (each sample was measured for 3,000 seconds) and we obtained Rb, Ba, Ca, Lu, and Nd content; after 30 days' cooling we measured a third time (each sample measured for 5,000 seconds) and this time, based on the long life isotopes we obtained the content of the elements Ce, Co, Cr, Cs, Eu, Fe, Hf, Ni, Sb, Sc, Sr, Ta, Tb, Th, Yb, Zn, and Z. Figure 1 is a typical gamma energy spectrum diagram of a 15 day cooling measurement.

5. Data Processing

The energy spectrum data obtained from the SCORPIO processor was transferred to the system's hard disk, then according to the Ge(Li)-F program on a PDP 11/04 computer energy spectrum analysis, peak area calculations and corrections were carried out on the samples and standard automatically, then a printer listed the content of the samples.

To verify the accuracy of the method, we irradiated with the sample at the same time standard reference coal powder from the U.S. National Bureau of Standards (NBS SRM 1632a). See Table 2 for the test results. From Table 2 it can be seen that the data obtained in this test is believable.

Table 2. Comparison of Reference Values and Measurement Results Using Standard Reference Coal Powder 1632a

Element	Measurement value (g/g)	Reference value (g/g)
Ba	1.35×10^{-4}	1.00×10^{-4}
Ce	3.03×10^{-5}	2.85×10^{-5}
Co	6.98×10^{-6}	6.53×10^{-6}
Cs	2.4×10^{-6}	2.3×10^{-6}
Eu	5.9×10^{-7}	5.1×10^{-7}
Fe	1.29×10^{-2}	1.11×10^{-2}
Gd	4.06×10^{-6}	4.41×10^{-6}
Hf	2.00×10^{-6}	1.44×10^{-6}
La	1.71×10^{-5}	1.46×10^{-5}
Lu	1.65×10^{-7}	1.9×10^{-7}
Nd	1.61×10^{-5}	1.56×10^{-5}
Pa	4.6×10^{-6}	4.5×10^{-6}
Rb	3.18×10^{-5}	2.82×10^{-5}
Sb	6.3×10^{-7}	6.2×10^{-7}
Sc	7.4×10^{-6}	6.7×10^{-6}
Se	2.36×10^{-6}	2.67×10^{-6}
Ta	3.87×10^{-7}	4.5×10^{-7}
Tb	3.4×10^{-7}	2.9×10^{-7}
U	1.34×10^{-6}	1.28×10^{-6}
Yb	1.06×10^{-6}	9.8×10^{-7}

II. Results and Discussion

1. Content and Distribution of Elements in Okinawa Trough Sediments

Figure 2 shows the stations for sampling Okinawa Trough sediments. Station 903 is not in the trough area and the data it measured was used for reference. These stations are primarily between 26°-31°N and 124°-129°E. The samples all were surface layer sediments. Table 3 gives the measurement results of the 29 elements in Okinawa Trough sediments.

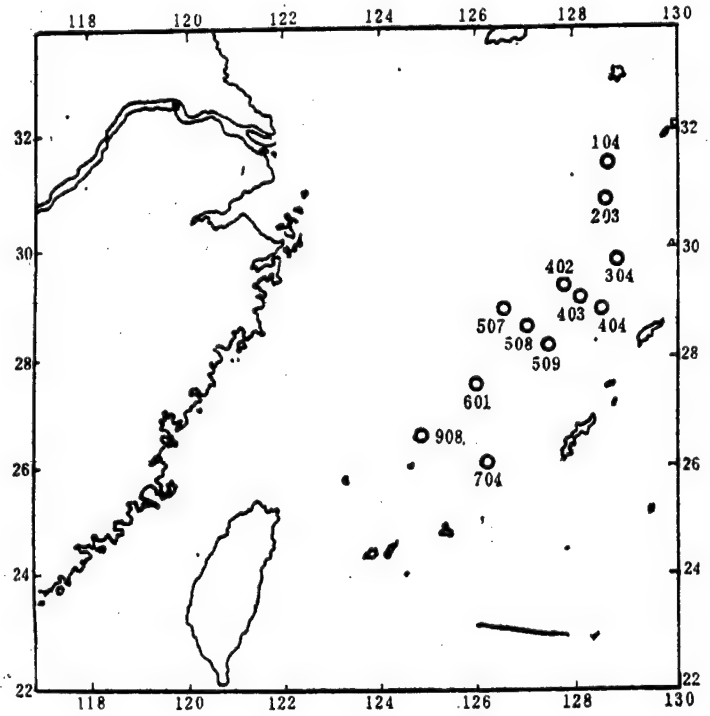

Figure 2. Okinawa Trough Sediment Sampling Stations

Neutron activation analysis primarily included constant quantity elements and trace elements among some of the metals in the sediments.

There is an intimate relationship between the laws of activity of the elements in the natural world and their own atomic structure, and the periodic table also was established on the foundation of atomic structure, thus most classifications are based on the periodic table. We feel that A. (Chawaliciji) classification method is better.[2] This method is based on the relationship of the element's crystal chemical characteristics, electron layer structure, ion radius and the element's geochemical nature and the combination of elements in the natural world and classifies on the basis of the periodic table. This method is divided into 12 classes but in our measurement work we included only 7 of the major classes.

Table 3. Measurements of 29 Elements in Okinawa Trough Sediments (ppm or %)

Element \ Station No. / Cross section No.	104	203	304	402	403	404	507	508(1)	508(2)	509	601	704	908	Average
	1	2	3	4			5				6	7	9	
As	3.5	—	3.9	3.5	3.1	8.6	3.0	9.5	2.7	6.1	3.7	3.3	12	5.5
Ba	(4.5±0.4)×10²	(4.8±0.8)×10²	(5.0±0.1)×10²	(5.6±0.8)×10²	(5.0±0.1)×10²	(6.6±0.6)×10²	(3.8±0.1)×10²	(6.7±0.1)×10²	(4.8±0.2)×10²	(5.2±0.1)×10²	(2.8±0.5)×10²	(4.4±0.1)×10²	(6.8±0.2)×10²	5.1×10²
Br	12	7.4	7.6	9.4	7.2	7.5	6.6	8.0	11	6.2	6.4	3.8	6.5	7.7
Ca(%)	9.4±0.2	9.8±0.4	7.0±0.1	5.8±0.6	8.6±0.2	6.8±0.4	10.0±0.2	7.1±0.8	7.3±0.5	8.8±0.4	15±1	3.3±0.3	2.5±0.1	7.8
Ce	53±1	47±1	76±16	61±1	52±1	57	74±5	54±1	68±1	57±1	59	86±1	63±1	62.1
Co	10.5±0.1	9.0±0.4	14.1±2.4	12.7±0.1	10.4±0.2	19.1±0.2	10.4±0.2	18.6±0.1	12.2±0.1	12.5±0.1	7.3±0.1	10.4±0.1	21.2±0.1	12.9
Cr	59±0.1	45±0.1	79±1.9	69±0.1	55±0.1	69±0.1	6.5±0.1	6.4±0.1	70±0.1	6.5±0.1	67±1.2	6.9±0.1	7.8±0.1	65.7
Cs	6.7±0.1	6.2±0.1	9.2±0.9	8.8±0.1	6.8±0.1	8.6±0 2	7.5±0.1	8.3±0.1	8.7±0.1	7.6±0.1	3.2±0.1	5.7±0.1	9.0±0.1	7.4
Eu	0.95±0.02	1.01±0.01	1.34±0.38	1.11±0.01	1.12±0.03	1.13±0.01	1.14±0.03	1.17±0.02	1.19±0.04	1.12±0.04	0.96±0.32	1.39±0.13	1.36±0.02	1.2
Fe(%)	2.94±0.02	2.87±0.11	3.93±0.50	3.54±0.01	3.13±0.08	3.86±0.05	3.11±0.08	3.81±0.04	3.51±0.02	3.62±0·01	2.35±0.03	3.04±0.03	4.28±0.09	3.4
Hf	4.9±0.1	4.5±0.2	8.1±4.3	5.1±0.4	5.5±0.2	4.5±0.8	6.9±0.7	4.4±0.1	6.0±0.7	5.2±0.5	9.6±2.3	10.5±0.5	5.1±0.3	6.2
K(%)	1.5	1.5	1.5	1.7	1.3	1.4	1.5	1.5	1.5	1.4	1.0	1.5	1.6	1.5
La	24±1	20±1	28±1	27±1	24±1	27±1	32±2	27±1	33	29	—	—	27	27.1
Lu	0.32±0.03	0.34±0.01	0.48±0.20	0.36±0.02	0.38±0.01	0.36±0.02	0.33±0.03	0.34±0.01	0.30±0.01	0.34±0.01	0.30±0.03	0.39±0.01	0.39±0.21	0.36
Na(%)	1.03	1.35	1.11	1.34	1.16	1.06	0.94	1.04	1.00	0.95	1.26	1.02	1.14	1.11
Nd	27±7	23±1	47±1	28±0	28±0	26±3	37±10	32±1	36±5	39±1	29±4	47±2	37±2	33.54
Ni	65±4	51±2	65±6	74±13	120±20	93±1	53±5	91±3	61±6	55±1	36±8	54±1	92±5	70.0
Rb	(0.95±0.4)×10²	(0.96±0.01)×10²	(1.31±0.01)×10²	(1.26±0.02)×10²	(1.05±0.01)×10²	(1.16±0.02)×10²	(1.12±0.04)×10²	(1.20±0.01)×10²	(1.31±0.01)×10²	(1.13±0.01)×10²	(0.59±0.01)×10²	(1.06±0.01)×10²	(1.26±0.02)×10²	1.10×10²
Sb	1.0±0.3	1.0±0.2	1.6±0.3	1.6±0.1	1.2±0.2	3.8±0.4	0.84±0.21	3.8±0.1	0.84±0.01	1.2±0.3	0.61±0.01	0.62±0.06	4.2±0.1	1.72
Sc	9.2±1.3	7.9±0.1	13.0±0.5	15.0±0.1	13.4±0.1	15.8±0.2	12.4±0.2	15.7±0.1	13.9±0.1	14.4±0.1	8.0±0.1	12.1±0.4	17.1±0.1	12.92
Sm	3.2	2.5	3.6	3.4	3.3	3.6	4.1	3.4	3.9	3.4	3.2	4.7	4.1	3.57
Sr	(4.9±0.1)×10²	(4.6±0.2)×10²	(2.4±2.1)×10²	(2.9±0.6)×10²	(3.9±0.4)×10²	(4.3±0.4)×10²	(6.4±0.4)×10²	(4.1±0.3)×10²	(3.9±0.2)×10²	(4.5±0.4)×10²	(7.6±0.5)×10²	(1.9±0.4)×10²	(2.6±0.1)×10²	4.15×10²
Ta	0.64±0.03	0.56±0.06	1.5±1.2	0.80±0.04	0.63±0.08	0.67±0.08	0.81±0.05	0.70±0.04	0.89±0.05	0.67±0.06	0.80±0.10	1.7±0.8	0.79±0.05	0.80
Tb	0.66±0.04	0.63±0.02	0.92±0.30	0.68±0.10	0.64±0.08	0.66±0.10	0.76±0.10	0.73±0.04	0.34±0.06	0.76±0.03	0.60±0.18	0.92±0.01	0.77±0.07	0.69
Th	9.2±0.6	8.4±0.2	13.5±4.0	11.1±0.3	9.36±0.06	10.3±0.03	12.0±0.5	10.5±0.2	12.1±0.5	10.3±0.4	9.7±0.6	14.8±0.1	11.5±0.3	10.98
U	2.3±0.1	1.6±0.1	2.2±0.1	2.1±0.1	1.3+0.1	1.5±0.2	1.3±0.4	1.3±0.3	2.5	1.8	—	—	2.4	1.85
Yb	2.1±0.1	2.4±0.1	3.3±1.5	2.5±0.1	2.5±0.1	2.4±1.6	2.2±0.1	2.5±0.2	2.3±0.1	2.5±0.1	2.0±0.1	3.0±0.3	2.7±0.1	2.49
Zn	76±1	67±1	89±2	110±1	74±2	99	69±1	82	86±7	120±1	210	91±6	97±11	97.69
Zr	(2.4±0.1)×10²	(1.7±0.2)×10²	(3.4±1.8)×10²	(2.3±0.1)×10²	(2.5±0.3)×10²	(3.3±0.1)×10²	(2.9±0.3)×10²	(2.1±0.3)×10²	(2.7±0.3)×10²	(2.2±0.1)×10²	(4.0±1.3)×10²	(4.5±0.7)×10²	(1.6±0.3)×10²	2.74×10²

Note: Cross section number is the cross section number used in the figures in this paper; 4, 5 are the average values of several stations.

(1) Lithophile elements: including Na, Ca, K, Sr, Rb, Cs, and Ba;

(2) Ferrous class elements: Cr, Fe, Co, Ni;

(3) Sulphophile element: Zn;

(4) Rare and rare earth element classes: Sc, Tr, Zr, Hf, and Ta;

(5) Radioactive elements: U, Th;

(6) Semimetal and heavy mineralizer class: As, Sb;

(7) Heavy halogen class: Br.

Now they are simply described as follows:

(1) Content and distribution of lithophile elements:

Na: Na is an important constant quantity element in sea water, its density is 10 g/kg. In the Okinawa Trough sediments, the distribution of Na is comparatively homogeneous, its average content being 10.9 g/kg·d·W (fluctuates between 9.4 g/kg and 13.5 g/kg), and density in sea water corresponds in quantity. However, the fluctuation of some numerical values may be related to the type of sediments and the water content.

K: The average density of K in the Okinawa Trough sediments was about 14.7 g/kg (varies between 10 g/kg and 17 g/kg). The variation in density of the K in the sediments in this area was very small, and the distribution exhibits homogeneity in the entire sea area. Unlike Na, the proportion of the K content in the sediments is 39-fold higher than in sea water. This indicates that the chemical properties and transformation process of this element are different and that K is more easily enriched in the sediments.

Cs and Rb: These belong to the trace elements in sea water. The Cs content of sea water is 5.5×10^{-4} mg/l, the average content in the Okinawa Trough sediments is 7.4 mg/kg (fluctuates between 3.2 mg/kg and 9.2 mg/kg). The content of Rb in sea water is 0.12 mg/l, in the Okinawa Trough sediments it is 110 mg/kg (fluctuates between 59 mg/kg and 131 mg/kg). The distribution of these two elements in this area is as illustrated in Figure 3.

From Figure 3 it can be seen that the variation of Cs and Rb in the Okinawa Trough sediments is unusually similar. They are not controlled by K and Na elements, which indicates that Cs and Rb may still be restricted by some other factors (such as clay constituents).

Ca and Sr: The average content of Ca in Okinawa Trough sediments is 78 g/kg. Figure 4 is the curve of variation of Ca content in the sediments from this area (in a northeast-southwest direction along the trough).

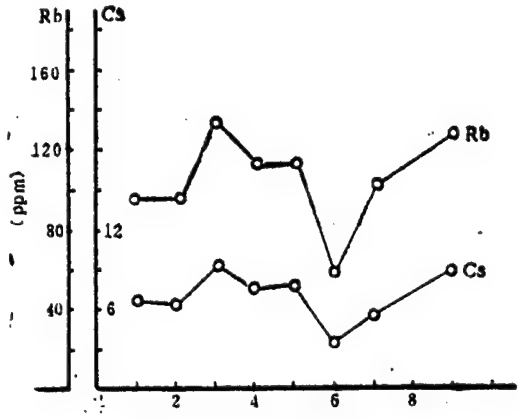

Figure 3. Variation in Content of Cs and Rb in Okinawa Trough Sediments (northeast to southwest direction)

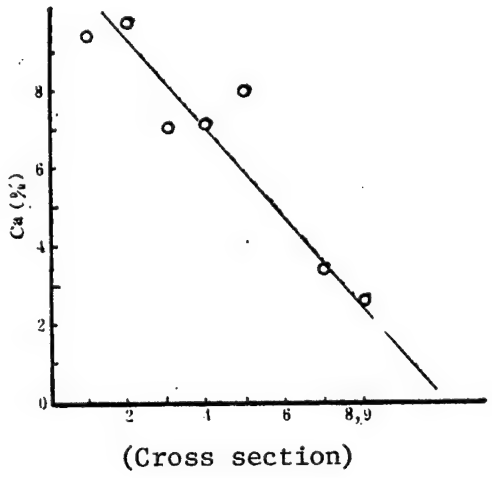

Figure 4. Variation in Ca Content in Okinawa Trough Sediments (northeast to southwest direction)

From Figure 4 it can be seen that the distributional feature of Ca in the trough sediments exhibits a trend to go from high in the northeast to low in the southwest. This is due to the fact that the organic content in the northeast area is higher than in the southwest. Due to the influence of rising current in the northeast area there are abundant nutritional salts in the sea water which leads to reproduction of organisms in great quantity. After death they can create organic sediments on the sea bottom and thus increase the Ca content. Yet in the southwest area, due to volcanic activity and no abundance of nutritional salts, biological life and its shell sedimentation is relatively scarce, thus the Ca content declines along the trough from northeast to southwest. According to Shi Liangren's [8902 5328 0088] survey,[3] the organic content in the sediments in the northeast region of the trough may be 15-72 percent, with each gram of sediment containing $n \times 10^3 - n \times 10^4$ biological individuals, primarily foraminifera

and radiolaria. Compared with the northeast area, the organic volume in the southwest area is clearly lower.

The Sr content in the trough sediments averages 415 mg/kg. Figure 5 is the variation of Sr content of the sediments in this area along the trough from northeast to southwest.

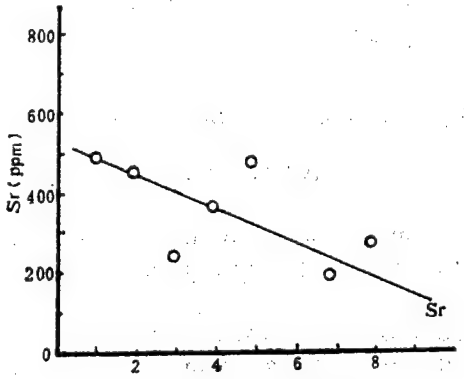

(Cross section)

Figure 5. Variation in Sr Content in Okinawa Trough Sediments (stretching along the survey cross section from northeast to southwest) (Footnote: Survey cross section refers to a survey area made up of several stations in a northwest-southeast direction determined in plans on initially setting out to sea. In actuality, due to limitations on conditions samples were not obtained at all stations, most are only from one station, but here we are still accustomed to treating it as a cross section.)

A comparison of Figures 4 and 5 makes it clear that the variation of Sr and Ca is unusually similar. This means that they are close accompanying elements, and the transformation mechanism in the trough and the geochemical processes are also similar, though the variation of Sr is a little slower than that of Ca.

Ba: Figure 6 is the curve of the distribution of Ba in the Okinawa Trough sediments (in a northeast to southwest direction).

From Figure 6 we see that the variation of Ba is different from that of Ca and Sr, it almost goes through the opposite geochemical processes of Ca and Sr. The tendency of the Ba in the trough to increase progressively from northeast to southwest may be related to the progressive increase of S in the southern part. In the southern volcanic area rather more SO_4^{2-} combines with the Ba^{2+} in the water and is deposited. The low value of station 601 may be related to the type of sediment. This is the shallowest (140 m) border area of the trough and many elements exhibit low values here.

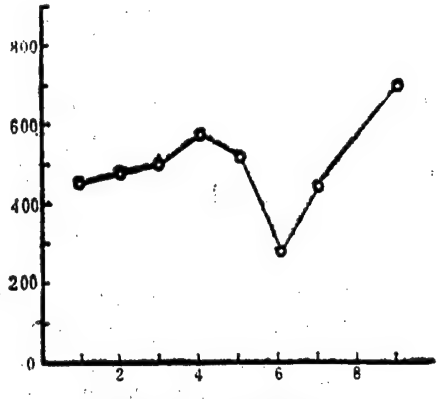

(Cross section)

Figure 6. Variation in Ba Content in Okinawa Trough Sediments (northeast to southwest direction)

(2) Ferrous class elements: Primarily includes the elements Ti, Mn, Cr, Fe, Co, and Ni. We measured the average content of Fe, Co, Ni, and Cr in the trough sediments, 3.4 percent, 12.9 mg/kg, 70.0 mg/kg, and 65.7 mg/kg, respectively. Figure 7 is the curve of the variation of these elements in the trough sediments.

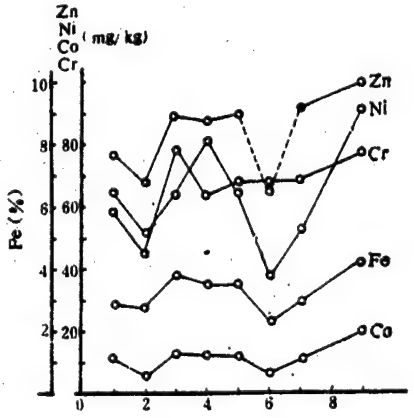

(Cross section NE-SW)

Figure 7. Curve of Variation of Fe, Co, Ni, Cr, Zn (Footnote: Zn is a sulphurophilic element and is placed here for ease of comparison) in Okinawa Trough Sediments
(northeast to southwest direction)

From Figure 7 one sees the tendency of Fe, Co, Ni, and Cr to increase slightly in the trough area in a northeast to southwest direction (station 601 is an exception) and their variation in content at different stations is a mutual fit, which indicates that there is a definite similarity in their properties and variation. The content of Fe among these elements is the highest, and the great variation of the other elements is the influence of variation in Fe content. It can be inferred that Fe may play an important role with regard to their absorption.

(3) Sulphurophilic elements: We measured only Zn and studied its variation along with that of Fe, Co, Ni, and Cr (see Figure 7). Its content averaged 97.69 mg/kg. In a northeast to southwest direction, Zn also had a tendency to increase which may be related to the ease of ZnS formation in this region.

(4) Rare and rare earth elements: Including the elements Sc, TR (element No 57-71), Zr, Hf, Nb, and Ta, we measured four rare elements and eight rare earth elements. Since arrangement of the peripheral electron layer of the rare earth elements was $4f^{0\to14}5d^{0\to1}6S^2$, their properties are unusually similar. For this reason we discuss them together. Figure 8 is the variation in the content of the eight rare earth elements in the Okinawa Trough sampling station.

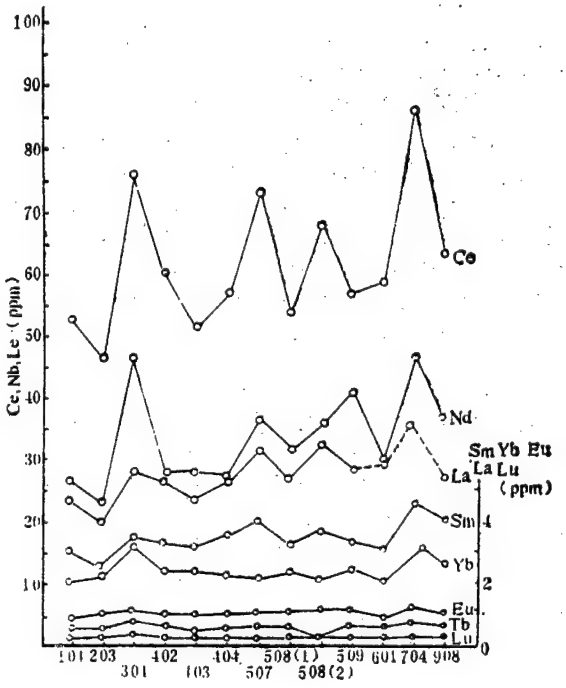

Figure 8. Variation in Content of Eight Rare Earth Elements in Okinawa Trough Sediments
(northeast to southwest direction)

Figure 8 shows that the variation of the eight rare earth elements in the trough sediments was rather uniform: they all change with changes in Ce (or La). Thus, study of the variation in distribution of the Ce in the sediments one can basically understand the variation of the other rare earth elements. On the basis of our analysis, differentiation of rare earth elements in the trough was not clear.

Figure 9 is the distribution of average content of the eight rare earth elements in the sediments at the measured stations in the Okinawa Trough.

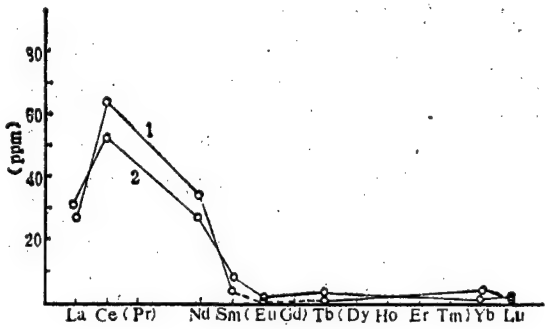

Figure 9. Distribution of Average Content of Some Rare Earth Elements in Okinawa Trough Sediments
(1) Test value; (2) Clarke value

From Figure 9 one sees that the Ce content is highest, averaging 62 mg/kg (fluctuating between 52 mg/kg and 86 mg/kg); Nd is in second place, averag-aging 34 mg/kg (fluctuating between 23 mg/kg and 47 mg/kg); La averages 27 mg/kg (fluctuating between 20 mg/kg and 30 mg/kg). In addition, the Sm, Eu, Tb, Yb, and Lu content was very low, Lu being the lowest, averaging 0.36 mg/kg (0.30-0.48). Sc, Zr, Hf, and Ta content in the trough was, respectively, 13 mg/kg (8-17); 274 mg/kg (160-450); 6 mg/kg (4-11); and 0.80 mg/kg (0.56-1.7). Figure 10 is their variation in the trough sediments.

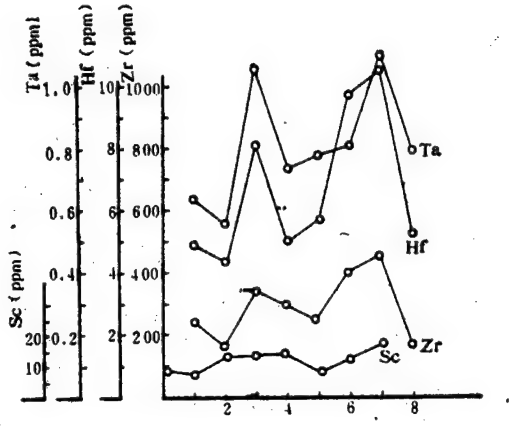

Figure 10. Variation of Sc, Ta, Hf, Zr in Okinawa Trough Sediments (northeast to southwest direction)

From Figure 10 we see that these four elements are going through very similar geochemical process, especially Ta, Hf, and Zr. Experiments revealed that their high values all are related to muclinagenous sediments and silty soft-mud; their low values are related to sand, fine sand, and silt clay. Evidently, they are clearly influenced by the granularity of the sedimentation material. At the same time, we can also deduce that their movement in sea water is very much influenced by suspended particles.

(5) Radioactive elements U and Th: The average content of U and Th in the trough sediments was 1.9 mg/kg and 11.0 mg/kg, respectively. This value is close to the gamma spectrum directly measured value, which was 2.2 mg/kg and 9.1 mg/kg. Figures 11 and 12 are the variation of U and Th content in the trough sediments.

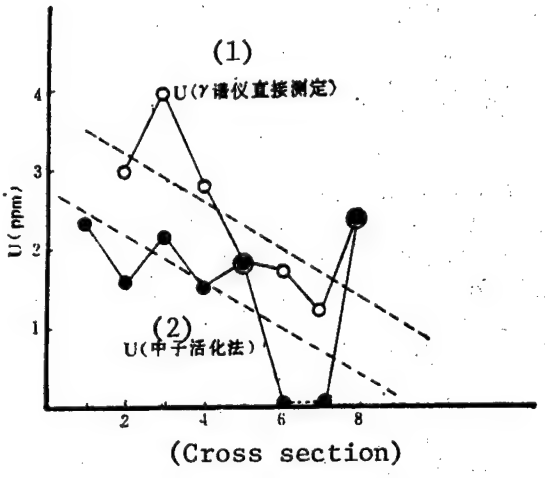

Figure 11. Variation of U Content in Okinawa Trough Sediments (measurement values of two methods; northeast to southwest)

Key:
1. Gamma spectrometer direct measurement
2. Neutron activation method

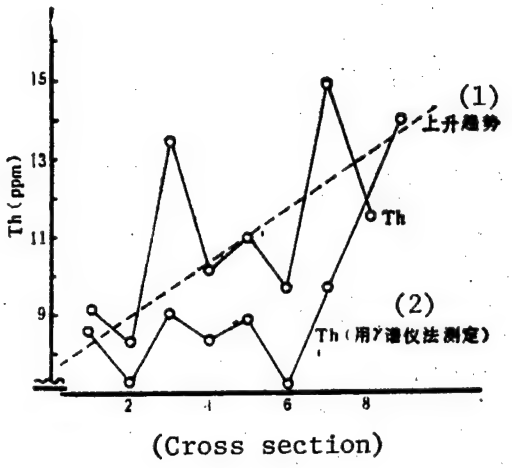

Figure 12. Variation of Th Content in Okinawa Trough Sediments (measurement values of two methods; northeast to southwest)

Key:
1. Rising tendency
2. Measured using gamma spectrometer method

From Figures 11 and 12 we see that U and Th are opposites: U decreases progressively in a northeasterly to southwesterly direction in the trough and Th increases progressively in a northeasterly to southwesterly direction. The former may be because in the northeast area there are more organisms and their reductivity is still strong, thus it is easy for enriched U and to cause U^{6-} to turn into U^{4-}, and increase the U volume in the sediments. [sentence as published]

$$U^{6-} + S_3^{2-} \rightleftharpoons U^{4-} + 5S^0$$

The southwest area of the trough becomes an oxidation area or an area of weak oxidation due to volcanic activity. Thus, on the one hand the ferro-manganese oxides produced by the volcano cause S^{2-} to be oxidized into S^0, and on the other hand, the volcano itself also puts out S^0. The existence and increase of S^0 promotes the change of U^{4-} in the sediments into U^{6-} and its dissolution in sea water and this may cause a decline in the volume of U in the southwest area.

Th is not affected by the oxidization reduction environment, and the slightly high content of Th in the southwest area may be related to volcanic activity. When there is lava or hot liquid ejected from the sea bottom, the number of suspended particles increases greatly, which aids in the absorption of the Th in the sea water and its sedimentation on the sea bottom. Of course there is also a certain amount of Th in the volcanic matter. This mechanism still awaits further study. The dotted line in the figure is drawn on the basis of the data obtained by the gamma spectrum direct measurement method. From comparison one sees that the regularity and trends obtained by the two methods is uniform.

(6) Semimetals and heavy mineralizer class: We only measured the two elements As and Sb. Figure 13 is the variation in content of As and Sb in the Okinawa Trough. For ease of comparison we have also drawn the variation of Fe at the stations. The As content is 5.5 mg/kg (2.7-12); Sb content was 1.7 mg/kg (0.6-4.0).

From Figure 13 one sees that the variation in these two elements have many similarities, and that there is a definite relationship with Fe, rising and falling as Fe volume increases and decreases. S. Kanamori discovered the direct ration between variation in As and Fe.[8]

(7) Heavy halogen class: We only measured Br in the sediments. Its average content was 7.7 mg/kg (3.8-12). The Br content had a tendency to decrease progressively in the trough from northeast to southwest. We know that Br^- in different sea areas also differs, and its transportability is not great. We still do not have a fully rational explanation for the decline of Br in the sediments from northeast to southwest, because there may be a pollution problem of large quantities of Br in the sediments.

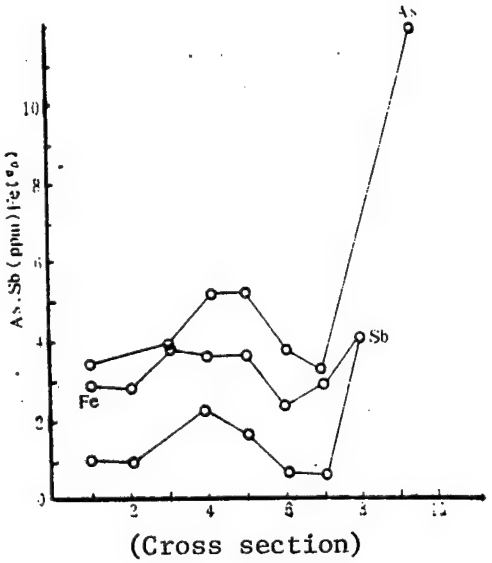

Figure 13. Variation of As, Sb Content in Okinawa Trough Sediments (northeast to southwest)

2. Comparison of Average Content of Elements in Okinawa Trough Sediments With Clarke Value

Table 4 gives the average content of the elements in the sediments in the survey area of Okinawa Trough and the Clarke value.[2]

From Table 4 we see that 28 of the 29 elements measured can be compared and that 22 come close or correspond to the Clarke values; 2 (Na, Ta) are smaller than the Clarke value; 4 (Zr, Hf, As, Sb) are greater than the Clarke value. Clearly the differences are not great. Over 80 percent of the elements come close to or fit the Clarke value which means that the sediments in this area are characterized as rather typical continental source materials. The fact that some of the elements which appear to be higher or lower may be related to the influence of the properties of the elements or environment, or may be related to deviations of the measured value (including the Clarke value). Those abnormal phenomena which appear in some elements must be explained by further study. However, with regard to the causes of the higher or lower values for some elements, this can now be analyzed on the basis of relevant materials. For example, the fact that Ca content increases may be due to organic sediments; variation in U may be related to reduction conditions and the existence of life.

III. Conclusion

1. Using neutron activation technology to study the element content and distribution in marine sediments is an advanced method which is both rapid and accurate. Its advantages are that it does not damage the samples and analysis of many elements can be carried out simultaneously.

Table 4. Comparison of Clarke Value and Average Content of 29 Elements in Okinawa Trough Sediments

(1)元素	(2)平均含量 (mg/kg)		(3) 克拉克值 (mg/kg)	(1)元素	(2) 平均含量 (mg/kg)		(3) 克拉克值 (mg/kg)
Na	10009	<	22000—25000	Zn	97.7	≐	40—150
K	15000	≃	16000—28200	As	5.5	>	1.8—3
Rb	110	≐	90—150	Br	7.7	≃	2.1—5.7
Cs	7.48	≐	1.1—10	La	27.1	≐	20—44
Ca	78000	≃	28000—60000	Ce	62	≐	32—75
Sr	415	≐	100—480	Nd	33.5	≐	19—37
Ba	510	≐	250—650	Sm	3.6	≃	4.7—8.6
Sc	12.9	≐	10—42	Tb	0.69	≃	0.9—7.2
Zr	274	>	130—170	Eu	1.15		
Hf	6.2	>	0.87—3	Yb	2.5	≐	0.16—3.4
Ta	0.80	<	2—7.5	Lu	0.36	≃	0.50—1.1
Cr	66	≐	70—110	Th	11	≐	2.6—13
Fe	34000	≃	35000—65000	U	1.85	≐	0.76—3.5
Co	12.9	≐	17—27	Sb	1.72	>	0.2—0.53
Ni	70.0	≐	44—89				

Key:
1. Element
2. Average content (mg/kg)
3. Clarke value (mg/kg)

2. We discussed the content and distribution of 29 elements in Okinawa Trough; experiments discovered that: 1) Over 80 percent of the element content is close to the Clarke value; less than 20 percent of the elements were higher or lower than the Clarke value; 2) the distribution of some elements exhibited a homogeneous or fairly homogeneous state, such as Na, K, Cs, and Rb, which although of the same class, are not entirely uniform in terms of distribution, Cs and Rb are even closer; 3) the distribution of elements is not sufficiently homogeneous, but variations between them are clearly interrelated, for example, Fe, Co, Ni, Cr; Sc, Ta, Hf; and rare

earth elements; 4) the distribution of elements has a clear pattern, such as Ca, Sr, U, and Th. The above phenomena may be related to the influence of different conditions such as oxidation reduction state, organic sediments, volcanic activity, element chemical properties and types of sediments.

REFERENCES

1. Li Youxia [2621 1485 7209], Qian Xingzhen [6929 2622 3791], Mao Xueying [3029 7185 3841], 1984. "Haishui Xuanfuwu He Chenjiwu De Duo Yuansu Zhongzi Huohua Fenxi" [Neutron Activation Analysis of Multiple Elements in Seawater Suspensions and Sediments], HAIYANG YU HUZHAO, 15(4): 365-370.

2. Nanjing Daxue Dizhi Xibian, 1979. "Diqiu Huaxue (Xiuding Ben)" [Geochemistry (Revised Edition)], Kexue Chubanshe, pp 123-125.

3. Shi Liangren [8902 5328 0088], 1981. "Chongsheng Haicao De Jige Chenji Tezheng" [Characteristics of Several Sediments in Okinawa Trough], HAIYANG DIZHI YANJIU, 1(1): 69-74.

4. Qian Xingzhen [6929 2622 3791], Mao Xueying [3029 7185 3841], and Chai Zhifang [2693 0037 5364], 1983. "Haishui Zhong Weiliang Yuansu De Huoxingtanxifu Yu Nongji He Zhongzi Huohua Fenxi" [Activated Carbon Adsorption of Trace Elements in Seawater Preconcentration and Neutron Activation Analysis], HAIYANG KEXUE, 2: 25-27.

5. Kusaka Yujuru, Tsuji Haruo, Imai Sakingo, and Omori Sayoko, 1979. "Kaisuinaka No Biryo Genso No Chuko Hoshaka Bunseki" [Neutron Radiation Analysis of Trace Elements in Seawater], RADIOISOTOPES, 28(3): 139-145.

6. Grancini, G.M., B. Stievano, F. Girardi, et al., 1976. "The Capability of Neutron Activation for Trace Element Analysis in Sea Water and Sediment Samples of the Northern Adriatic Sea," JOURNAL OF RADIOANALYSIS CHEMISTRY, 34: 65-78.

7. Hirose, A., D. Ishii, 1978. "Determination of Uranium in Sea Water by Preconcentration on Chelex 100 and Neutron Activation," JOURNAL OF RADIOANALYSIS CHEMISTRY, 46: 211-215.

8. Satoru Kanamori, 1965. "Geochemical Study of Arsenic in Natural Water. The Signification and Sedimentation of Arsenic in Lake Water," reprinted from JOURNAL OF EARTH SCIENCES, 13(1): 46-57.

9. Wijkstra, J., H.A. Van Der Sloot, 1978. "The Determination of Manganese in Seawater, Surface Water and Rainwater by Neutron Activation Analysis," JOURNAL OF RADIOANALYSIS CHEMISTRY, 46: 379-388.

8226/6091
CSO: 4008/1004

MODEL HJ-82-1 FILTER AND MARINE SEISMIC TRAILING ARRAY

Beijing HAIYANG XUEBAO [ACTA OCEANOLOGICA SINICA] in Chinese Vol 7, No 4, 15 Jul 85 pp 513-519

[Article by Jie Baoxing [6043 1405 5281] and Zhu Houqing [2612 0624 0615], Institute of Acoustics, Chinese Academy of Sciences, Beijing, and Tu Benliang [3205 2609 5328] and Shi Xiaolin [0670 4607 7792], Geophysical Exploration Company of the Bohai Petroleum Company, Tianjin: "Development of Model HJ-82-1 Filter and Marine Seismic Trailing Array"; paper received 24 February 1984; first paragraph is source-supplied abstract]

[Text] Abstract: This paper describes the structure and principles of a new seismic exploration filter for use at sea and the properties of a trailing array made with it. The filter is made up of a piezoelectric ceramic tube and two piezoelectric ceramic plates. It has very high sound reception voltage sensitivity, low acceleration sensitivity, and a certain pressure resistance and a very broad frequency band. This filter was used in several trailing arrays at equal intervals. Tests show that this array doubled the sound reception sensitivity over foreign equipped trailing arrays.

Increasingly, people are now using long arrays widely for obtaining acoustical information, and especially with the development of hydroacoustic and geoacoustic research, line trailing base arrays are being used more widely daily.

Underwater receiver sound systems ("equidistant floating cable," for short) which are made up of line trailing arrays as long as several thousand meters are crucial equipment in marine seismic exploration. The technology is complex, involving a wide range of scientific fields and they are high in cost. The filter (hydrophone) is the major component of the "cable." It can convert weak sound waves reflected from deep strata into electrical signals. The filter must: have high sensitivity to sound reception, low self-created noise, low impedance, a broad frequency, and low acceleration sensitivity.

The filters produced in China and abroad currently can be divided into two classes on the basis of structural principles. One class is the curved plate type, such as the model HJ-79-1; the other is the ring filter, the U.S. Multidyne filter is of this class. The production technology for the HJ-79-1 filter is complex, the use depth is shallow (less than 50 m) and the sound

reception voltage sensitivity is only 23 x 10^{-5} μV/μPa. The Multidyne filter's sensitivity is higher and impedance is moderate, but the voltage gain at the two ends of the filter is hard to control, and it is difficult to manufacture.[1,2]

Tests of high acoustic reception voltage sensitivity, broad band, and the HJ-82-1 filter which has suppression of acceleration response and new trailing arrays made with it show that the new "cable" developed in this paper has about a 6 dB higher sound reception voltage sensitivity than the French AMG-96 channel "cable" which has a similar array.

I. Filter Structure and Principles

The model HJ-82-1 filter is a complex filter. It is made up of two radially polarized piezoelectric ceramic thin wall tubes and two piezoelectric ceramic round plates with stainless steel plates (see Figure 1). To satisfy filter demands a "two series-one parallel" method was used to connect the components, i.e., two piezoelectric cylinders and two piezoelectric round plates are connected in series and then output in parallel. The piezoelectric ceramic is wrapped in a layer of tightly sealed rubber which serves as insulation and damper, generally polyurethane rubber can be used. The filter is fixed to the "cable" with a nylon framework (see Figure 2).

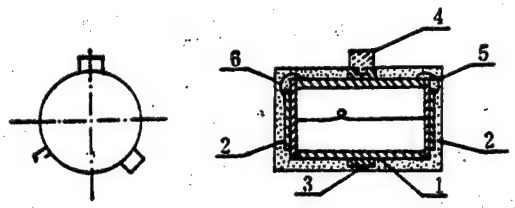

Figure 1. Structure of the HJ-82-1 Filter

1--Piezoelectric ceramic tube; 2--Piezoelectric ceramic plate; 3--Fixed ring; 4--Electrode post; 5--Link; 6--Acoustical rubber

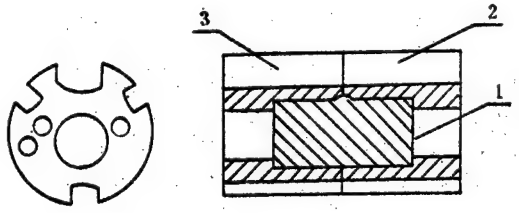

Figure 2. Filter Installed in Nylon Framework

1--Filter; 2--Nylon support; 3--[Omitted in source]

The piezoelectric tube and round plate both are made from PZT-5 piezoelectric ceramic material. The outer poles of the tube are divided into two sections with a 1.5 mm gap in the center, the entire inner surface is covered with silver, and under these conditions it is equivalent to two radially polarized tubes in series (see Figure 3).

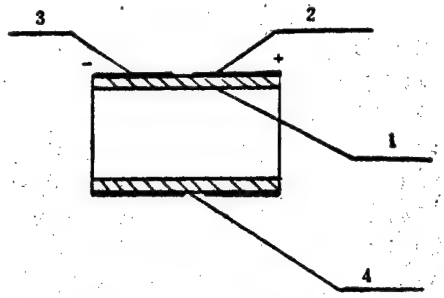

Figure 3. Electrodes of Piezoelectric Ceramic Tube

1--Inner electrode layer; 2--Positive electrode; 3--Negative electrode; 4--Gap

Clearly there is a contradiction between the resistance to pressure ability of the piezoelectric round plate and its sensitivity to sound reception, thus the ceramic round plate is adhered to a stainless steel plate 0.25 mm thick. The serially connected piezoelectric round plates are cemented concentrically to the two ends of the piezoelectric tube.

In the above arrangement, the piezoelectric round plates at the two ends of the tube create bending oscillation under edge-fixed boundary conditions and the tube creates radial oscillation under exposed ends conditions. According to the related theories of Wollett[4] and Langeven[5] the parameter design and computation formula of the HJ-82-1 filter can be obtained.

1. Frequency Bandwidth

The HJ-82-1 filter is a hydroacoustic transducer for aharmonic uses and the frequency range it uses is between distant resonant points and the cut-off frequency. Since externally identical piezoelectric thin-wall tubes and piezoelectric round plates were used to make the oscillating components in the design, according to oscillation theory the determinant of frequency limitation on the filter should be the harmonic frequency of the curved round plate. The harmonic frequency of the edge-fixed double stack type curved round plates in air is:

$$f_{r.a} = \frac{1}{\pi}\sqrt{\frac{\Lambda^D}{3K}}\, C_p \frac{h}{a^2}\sqrt{\frac{\Lambda^E}{\Lambda^D}}, \tag{1}$$

in which, energy factor is $\Lambda^D = 4/3$; kinetic energy factor is $K = 1/5$; $\Lambda^E/\Lambda^D = 1-0.4875\ k_p^2$, k_p is the plane coupling coefficient; the longitudinal wave sound velocity is $C_p = [\rho_c S_{11}^D\ (1-\sigma^2)]^{-\frac{1}{2}}$; a is the radius of the round plate, h is the thickness of the stack; if the ceramic density $\rho_c = 7.5\ g/cm^3$, the elasticity coefficient $S_{11}^D = 11.1 \times 10^{-13}\ cm^2/dyn$, the Poison ratio $\sigma = 0.3$, and $k_p = 0.5$ are substituted in Eq. (1), then

$$f_{r.a} = 161.6\frac{h}{a^2}\ (kHz). \tag{2}$$

in which, h and a are both calculated in centimeters.

When the filter is placed in the water, the round plates at the two ends of the tube vibrate at the same amplitude, equivalent to the transmission and reception in air, thus it can be seen as being in an infinite rigid obstruction, and at this time, the harmonic frequency in the water is

$$f_{r.w}=f_{r.a}\left[1+\frac{8\rho_w\Theta}{3\pi\rho_c k\frac{h}{a}}\right]^{-\frac{1}{2}}, \tag{3}$$

in which Θ is the near field kinetic energy factor, and with water density ρ_w = 1 g/cm^3, h = 0.05 cm, a = 0.8 cm, Θ = 0.1577, we have

$$f_{r.w}=0.64f_{r.a}=8.1(\text{kHz}).$$

and this is the upper cut-off frequency of the filter.

The lower cut-off frequency of the filter is

$$f_L=\frac{1}{2\pi CR}, \tag{4}$$

in which, C is the low frequency free capacitance of the filter, R is the input impedance of the receiver, generally, several megaohms.

Letting $C=5500\text{pf}$, $R=3\times10^6\Omega$, then

$$f_L=9.6(\text{Hz}).$$

From the above calculations we can see that the HJ-82-1 filter has a bandwidth of from several Hz to several thousand Hz and can satisfy the bandwidth demands of from several Hz to several hundred Hz in marine seismic exploration.

2. Sound Reception Voltage Sensitivity

The HJ-82-1 filter is a composite receiver. Its sound reception voltage sensitivity is the weighted superposition of the sound reception sensitivity of its tube and round plates. Their relationship is

$$M=\frac{C_1}{C_1+C_2}M_1+\frac{C_2}{C_1+C_2}M_2, \tag{5}$$

in which M_1 and C_1 are the sound reception voltage sensitivity and serial capacitance of the round plates; M_2 and C_2 are the sound reception voltage sensitivity and serial capacitance of the tube.

The sound reception voltage sensitivity of the serial curved vibration round plate is:

$$M_1 = 2\left(\frac{3}{8}\, g_{31}\frac{a^2}{h}\right), \tag{6}$$

in which a and h are calculated in centimeters.

The serial sound reception voltage sensitivity of the tube is:

$$M_2 = 2a\left[\, g_{33}\left(\frac{1-\rho}{1+\rho}\right) + g_{31}\left(\frac{2+\rho}{1+\rho}\right)\right], \tag{7}$$

in which a and b are the outer and inner radii of the tube and the round plates; $\rho = b/a$; h is the thickness of the curved round plate; g_{31} and g_{33} are the ceramic piezoelectric coefficients.

Letting $g_{31} = -11.4 \times 10^{-3}$ Vm/N, $g_{33} = 24.8 \times 10^{-3}$ Vm/N, h = 0.5 mm, a = 8 mm, b = 7 mm, C_1 = 2500 pf, and C_2 = 3000 pf, then the acoustic reception voltage sensitivity of the filter is

$M = 46.8 \times 10^{-5}$ μV/μPa, i.e., -186 dB (reference level relv/μPa).

3. Acceleration Response Suppression

The filter's acceleration response is an interference output produced by the action of acceleration force on the piezoelectric components. When the filter is trailed, the acceleration force on the trailing body acts on the filter through the connections and thus causes the filter to produce acceleration response interference which severely influences the signal. Present methods of suppressing acceleration response use compensation and damping methods in filter design and manufacture. This is the object of the symmetrical structural rubber damping used in the HJ-82-1 filter. As soon as an acceleration force acts on the two ends of the tube a certain charge is produced on the round plate on each end. If the characteristics and capacitance of the material of the two round plates is basically the same, since the magnitude of the action of the acceleration force on the two end plates is opposite in equal directions (pull and pressure), the charge polarity produced at the two round plates is opposite, and the numerical values are equal. When the two round plates are connected in serial, the overall voltage output caused by the acceleration force is zero (see Figure 4). For sound signals, the force acting on both end plates is pressure, so what is produced on both end plates is an equal charge of identical polarity, and when the two plates are connected serially the overall output voltage is a superposition of the voltage on each plate.

Since the piezoelectric tube has a symmetrical structure, it is easy to know the principles and structure of its acceleration suppression.

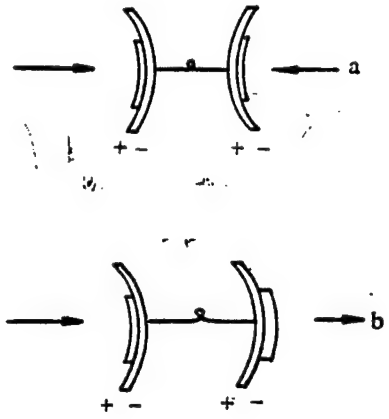

Figure 4. Diagram of Acceleration Force Action Compensation Principle

a. Sound voltage action

b. Acceleration force action

+−

± +− indicates load polarity

+−

II. Trailing Array Arrangement and Characteristics

There are many ways of arranging the trailing arrays used in marine seismic exploration, but most of the ones currently used are arranged with equal spacing, i.e., they are equally spaced to form a long line array, 24 filters spaced at 1 meter intervals form a straight line, the filters are connected in a "8 parallel-3 serial" fashion, i.e., each 8 filters are first connected in parallel and then output in cross serial (see Figure 5). The trailing array is filled with oil, the outer shell is casing of acoustically transparent plastic, the several steel cables in the center can both fix the filters as well as withstand the drag when the line array is being trailing.

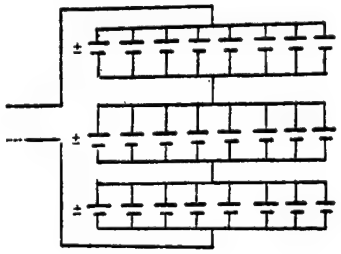

Figure 5. Connection of Filters in Trailing Array

On the basis of Figure 5, the primary technical norm of the trailing array, the sound reception voltage sensitivity is:

$$M_L = 3M \tag{8}$$

in which M is the sound reception voltage sensitivity of the filter. The sound reception voltage sensitivity of the HJ-82-1 filter is 46×10^{-5} μV/μPa,

but the sound reception voltage sensitivity of the filters in the French-manufactured AMG trailing array is 23 x 10^{-5} μV/μPa. The sound reception voltage sensitivity of the new trailing array equipped with the HJ-82-1 filters is about 6 dB higher than an AMG trailing array with similar arrangement.

III. Test Results and Analysis

To prove our theory we carried out a series of tests and calibrations on the HJ-82-1 filter for sound reception voltage sensitivity, ability to resist pressure, and acceleration response. We carried out calibration of sound reception voltage sensitivity and phase on the new trailing array both in the Institute of Acoustics' pond and in the laboratory.

Figure 6 is the curve of HJ-82-1 filter sound reception voltage sensitivity with changes in frequency measured by the "comparative method" in an oil chamber. It can be seen that sound reception voltage sensitivity within the range 10-500 Hz is -187 dB (reference level 1 V/μPa), i.e., 44.7 x 10^{-5} μV/μPa, which is basically the same as the theoretical calculations. Actually, the flat part of the HJ-82-1 filter's reception voltage frequency response is far from limited to 500 Hz, but can reach several thousand Hertz, and this is very significant for expanding the use range of the HJ-82-1 filter.

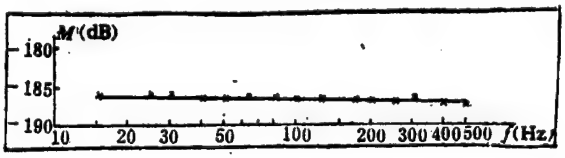

Figure 6. Curve of HJ-82-1 Filter Sound Reception Voltage Sensitivity Frequency Response

When the filter acceleration response curve was measured on the vibration machine (see Figure 7), within the range 10-500 Hz the acceleration sensitivity was lower than -75 dB (reference level 1 v/g), which completely satisfies the demands of trailing use. In addition, the pressure resistance performance of the HJ-82-1 filter was measured with a pressurizer. At 20 atmospheres the filter did not leak water in 12 hours of pressurization, performance did not change, thus this filter could be used at water depths of less than 150 meters, and this is very important in its application.

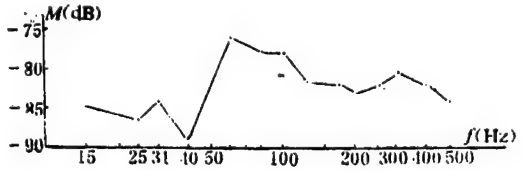

Figure 7. HJ-82-1 Filter Acceleration Response Curve

Measurement and calibration of the trailing array is a very difficult task,[8] mainly because the trailing array is more than several tens of meters long, the measurement frequency is also low, and it is extremely difficult to obtain an open homogenous sound field. To calibrate the trailing array in the pond, the "comparative method" was used for this paper. The two lines to be compared were interlaced and wound on a cylindrical holder, thus reducing the space occupied by the trailing array. When the wave length of the measured acoustical signal was much larger than the dimensions of the outside of the tube, the two arrays were in similar homogenous sound fields and the output of comparing the two lines could accurately determine the difference between their reception performance. A "dynamic transducer" was used in the tests as a sound source. It could transmit a low frequency acoustical signal of sufficient signal-noise ratio. Using a "7T08S signal analyzer" we collected and processed the signals received by the array. Figures 8 and 9 are curves of phase difference and comparison of the acoustic reception voltage sensitivity response of the new and old trailing arrays, respectively. From these two curves it can be seen that the new array equipped with the HJ-82-1 filter is much superior to the old AMG trailing array. Acoustic reception voltage sensitivity was higher by 4-5 dB, and phase nonuniformity was less than 15 degrees, which is consistent with design.

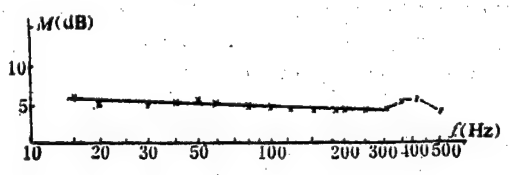

Figure 8. Curve Comparing Reception Voltage Response of Two Arrays

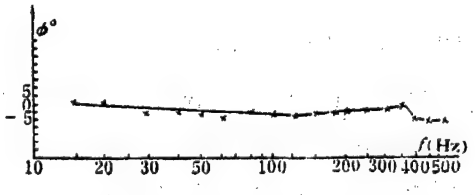

Figure 9. Curve of Phase Difference in Received Signal of Two Arrays

Figure 10 is the solo calibration sound reception voltage sensitivity response curve of the new trailing array. Within the 20-500 Hz range, the sound reception voltage sensitivity of the new trailing array was -179 ± 1.5 dB, i.e., 112 x 10^{-5} μV/μPa, which fits rather well with the theoretical values. It is not difficult to calculate the AMG trailing array's sound reception voltage sensitivity as 63 x 10^{-5} μV/μPa.

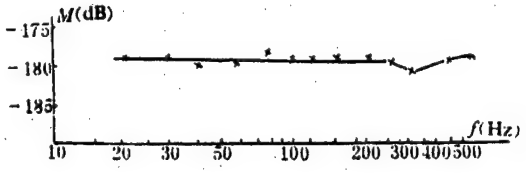

Figure 10. New Trailing Array Sound Reception Voltage Sensitivity Response Curve

IV. Conclusion

1. Test results show that the HJ-82-1 filter is simple in construction and easy to produce. Its performance indicators reach or approximate the levels of the advanced "Multidyne" filter. Not only can it be used for marine seismic exploration, but it can also serve as a general purpose array element for use in other underwater sound systems. The performance of the new trailing array in which it was installed is superior to the AMG trailing array currently in use and we predict that the use of the new array for seismic exploration can improve the quality of seismic materials.

2. The design thinking and design formulas of the filter in this paper can be used to design various filters for different needs. The measurement method for the trailing array has a certain reference value for persons working in aquatic sound measurement.

REFERENCES

1. Wo Site [3087 2448 3676], K.H. FANSHE DIZHEN YU NENGYUAN KAN-TANDE GONGJU [REFLECTION SEISMIC AND ENERGY EXPLORATION TOOLS], Shiyou Chubanshe, 1983, 3.

2. Patent, U.S., 3660809, 1972, 5.

3. Langeven, R.A., ELECTROACOUSTIC SENSITIVITY OF CERAMIC TUBES, J.A.S.A., 26 (1954), 3.

4. Wollett, R.S., THEORY OF PIEZOELECTRIC FLEXURAL DISK TRANSDUCER WITH APPLICATION TO UNDERWATER SOUND, PB 154257.

5. Patent, U.S., 4205954, 1980, 5.

8226/6091
CSO: 4008/1097

APPLIED SCIENCES

PROCEEDINGS OF NATIONAL SYMPOSIUM ON APPLICATION OF ION IMPLANTATION TO NON-SEMICONDUCTORS

Shanghai HE JISHU [NUCLEAR TECHNIQUES] in Chinese No 8, Aug 86

[English Table of Contents]

9717
CSO: 4008/2

THE EXPERIMENTAL DATA PROCESSING METHOD OF DYNAMIC CALIBRATION IN TIME DOMAIN

Beijing LIXUE XUEBAO [ACTA MECHANICA SINICA] in Chinese Vol 18, No 6, Nov 86 pp 553-557

[English abstract of article by Huang Junqin [7806 0193 2953], Miao Tong [5379 1749], and Wang Xiaokui [3769 2400 5525] of the Beijing Institute of Aeronautics and Astronautics]

[Text] A set of experimental data processing method of dynamic calibration in time domain is presented in this paper. It can give parametric models (difference equation, discrete transfer function and continuous transfer function), nonparametric models (frequency response and unit-step response) and dynamic performances of transducer (or system) using experimental data of dynamic calibration in time domain. At the same time it has the function of testing the model efficiency, the model calculated transient response and the experimental data of dynamic calibration draw in the same coordinate, it is easy to identify whether the quality of the mathematical model is good or not.

There are some methods of eliminating the measurement noise when the parametric model is built up whether in frequency domain or in time domain. Therefore, the frequency response calculated from parametric model more coincides with the linear model characteristics than the frequency response calculated from experimental data using FFT algorithm. It is more reasonable that the dynamic performance index both in frequency domain and in time domain should be calculated from model calculated frequency response and unit-step response. The experimental data processing results of the dynamic calibration of a transducer with amplifier are given in this paper. (Paper received 10 September 1984, revised 15 December 1985.)

REFERENCES

[1] Bowersox, R. B. & Carlson, J., Digital Computer Calculation of transducer frequency response from its response to a step function, JPL, Pasaclena, California, JPL Progress Report 20-331, July, (1957).
[2] 马彭骥,高一飞,华师韩,动压传感器的校验,计量工作, 3(1974).
[3] 马彭骥,华师韩,测力传感器的校验计量工作, 3(1976).
[4] 黄俊钦,由过渡过程求频率特性的阶梯线法,计量技术, 2(1978).
[5] Waston, W. H. & Federman, C., Fourier Transform Techniquer for the Calibration of Shock Accelerometers, *Instrumentation in the Aerospace Industry*, **21**, *Advancfs in Test Measurement*, **12**, 315—320.
[6] 黄俊钦,侯连生,余辉里,付里叶变换的一种近似算法,中国仪器仪表学报告, 4(1983)413—422.
[7] 黄俊钦,张继志,加速度传感器动态数学模型研究,中国航空科技文献 HJB830086, 航空工业部 (1983).
[8] 张继志,黄俊钦,线性系统传递函数频域辨识的一种方法,北京航空学院学报, 2, (1983), 37—51.
[9] 黄俊钦,张继志,能同时辨识线性差分方程模型阶次和参数的算法,仪器仪表学报, 4(1984).
[10] 黄俊钦,张继志,苗彤,一种特殊白化滤波器的广义最小二乘法,航空学报, 6(1985).

THE STRUCTURE OF SHOCK-WAVE FRONT IN CALIBRATION OF SHOCK-TUBE AND THE PRESSURE TRANSDUCER WITH NANON-SECOND RESPONSE

Beijing LIXUE XUEBAO [ACTA MECHANICA SINICA] in Chinese Vol 18, No 6, Nov 86 pp 558-560

[English abstract of article by Fan Liangzao [5400 5328 5679], Li Guobin [2621 0948 1755], and Li Guangda [2621 1639 6671] of the Institute of Mechanics, Academia Sinica]

[Text] This paper deals with the relation between the response character of a pressure transducer for calibration usage and the structure of shock-wave front in a calibration shock-tube. A new approach is introduced which could minimize the thickness of the shock-wave front. The nanon-second response pressure transducer has been elaborately made in laboratory and its reliability is discussed. (Paper received 22 February 1984, revised 14 August 1985.)

REFERENCES

[1] Markus W. Sigrist and Fritz K. Kneubühl, Laser-generated Stress waves in Liquids, *Journal of the Acoustical Society of America*.
[2] Baganoft, D., *Rev. sci. Instr.*; **35** (1964), 288.
[3] 王竹溪著,统计物理学导论, 186. 高教出版社 (1955)

/6091
CSO: 4009/1041

IDENTIFICATION OF 2 MAJOR COMPONENTS IN CHINESE NYSTATIN

Beijing YAOXUE XUEBAO [ACTA PHARMACEUTICA SINICA] in Chinese Vol 21, No 6, 29 Jun 86 pp 454-457

[Article by Ling Dakui [0407 1129 1145], Chen Su [7115 5685], Wang Shaowen [3769 4801 2429], and Sun Zengpei [1327 2582 1014], Bureau of Pharmaceuticals and Biological Products Control, Ministry of Health, Beijing, and Ma Jianwen [7456 0494 2429], Drug Control Bureau, PLA, Beijing; paper received 3 September 1985]

[Text] Abstract: The two major components in the Chinese nystatin products were identified as nystatin A_3 and polyfungin B by ultraviolet, proton nuclear magnetic resonance and fast atom bombardment mass spectroscopy.

Key Words: Nystatin; Nystatin A_3; Polyfungin B; Fast atom bombardment mass spectroscopy

Nystatins were first isolated from the fermentation broth of Streptomyces noursei by Hazen and Brown in 1959.[1] Commercial nystatin products are generally a mixture of many related compounds including nystatin A_1, A_2, and A_3.[2] Polyfungin, another tetraene family antibiotic that is similar to the nystatins, is composed of four major components--nystatins A_1, A_2, A_3 and polyfungin B.[2,3] The structure of nystatin A_1 has completely been elucidated.[4,5] The structures of nystatin A_3 and polyfungin B have also been determined. Compared with A_1, they both contain an extra digitoxose moiety in addition to the common mycosamine.[6-8] But the structure of nystatin A_2 has not been reported.

In 1959, Cai Runsheng [5591 3387 3932] and coworkers isolated the Actinomyces A-94 strain from the soil of Guangdong. The crystalline powder extracted from the mycelia showed a strong anti-fungal activity.[9,10] Subsequently, Bao Qinzhu [0545 3830 3796] and others suggested, based on the physico-chemical properties, UV and IR spectra and direct comparison with an authentic sample, that the fermentation products of A-94 were nystatins.[10,11]

Based on the results of several tests, our agency has pointed out that the Chinese nystatin products are different in terms of biological potency and chemical stability when compared with foreign products. There are so much controversies about the quality of Chinese nystatins that they have even

drawn international attention. Using thin layer and high performance liquid chromatography (HPLC), Thomas et al. have analyzed the nystatin products from many countries and found that A_1 is the major component, about 70 percent, in the U.S., Italian, and Hungarian products. But the Chinese products generally contain no more than 12 percent of A_1. Their major ingredients are two other compounds whose abundance, approximately 20-50 percent, vary from lot to lot. He has also compared the chromatographic behaviors of the Chinese nystatin products and polyfungin and proposed that the two major ingredients in Chinese products are probably nystatin A_2, A_3 or polyfungin B, based on their Rf values and retention times.[12,13] Ma Jianwen et al. have further refined the separation condition of high performance liquid chromatography and found that the major ingredients of domestic and foreign products are indeed different. They have been unable to detect the presence of A_1 in Chinese products. They have isolated the major components in Chinese products, namely peak No 9 and No 13 (from now on referred to as C_1 and C_2), by preparative HPLC.[14] In order to look further into the quality issue of Chinese manufactured nystatins, we have carried out the structural analysis of C_1 and C_2 by means of proton nuclear magnetic resonance (^{1}HNMR) and fast atom bombardment mass spectroscopy (FABMS) techniques.

Experimental

The ^{1}HNMR and FAB mass spectra of C_1, C_2, international nystatin standards (lot No 2), Chinese standards (801210), and the HPLC purified A_1 (a product of the U.S. Squibb Co.), were taken. The HPLC purifications of C_1, C_2 and A_1 will be reported elsewhere.

The proton NMR spectra were recorded at room temperature by a Varian XL200 NMR spectrometer, using deuterated-DMSO as a solvent and TMS as an internal standard.

The fast atom bombardment mass spectra were recorded by a NEC double-focusing mass spectrometer (Model JEOLDX 300). The instrument was equipped with a JAM3500 data processing system, an add-on FAB06-C ion source, and a stainless steel target. The angle between the target and atom beam is about 70°, bombarding atom Xe, resolution 1000, and acceleration potential 1.5 kV. Adequate amounts of samples (about 10 µg) were placed on the target and protonated by adding 0.4 µl of 0.1 N HCl solution dropwise. Measurements were made after they were thoroughly mixed with 0.6-1 µl of high grade glycerol.

Structural Analysis and Identifications

Samples C_1, C_2 and nystatin A_1 all display very similar ultraviolet absorption characteristics. Their absorption maxima in methanol occur at 230, 291, 304 and 318 nm. This indicates that they contain a common chromophore (a conjugated polyene). The proton NMR data of the three also support the above conclusion (see Table 1, peak assignments were based on literature report[1]). They have a common vinyl proton resonance signal in the 5.4-6.4 ppm range. The integration gives a total of 12 protons, which is consistent with the alkene structure shown in Figure 2. In general, there are many

Table 1. ^{1}HNMR Data for C_1, C_2 and Nystatin A_1

Group	Chemical shift (ppm)			Protons	Multiplicity
	C_1	C_2	A_1		
Methyl	0.89(6 Hz)	0.90(6 Hz)	0.87(6 Hz)	3	Doublet
Methyl	0.96(6 Hz)	0.97(6 Hz)	0.97(6 Hz)	3	Doublet
Methyl	1.11	1.12	1.16	9 (C_1&C_2) 6 (A_1)	Multiplet
Methylene and methine	1.3~4.5	1.3~4.5	1.3~4.5		
Methine-dioxy	4.71	4.72	—	1	Multiplet
Methine-dioxy	4.93	4.92	5.06	1	
Olefinic proton	5.50, 5.73 5.92, 5.98 6.22	5.50, 5.74 5.92, 5.98 6.20	5.50, 5.71 5.90, 5.97 6.20	12	

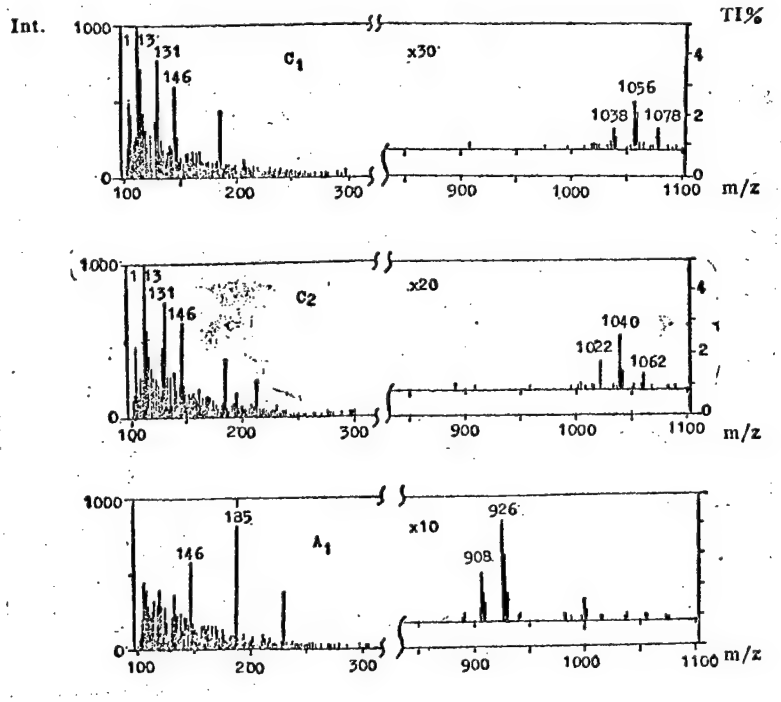

Figure 1. FAB Mass Spectra of C_1, C_2 and Nystatin A_1

similarities among the NMR data of the three. The major differences are: 1) In the methyl group range of 0.8-1.2 ppm, samples C_1 and C_2 have 3 more protons than A_1, which implies an extra methyl group. 2) C_1 and C_2 display a proton signal of dioxygenated methylene (-O-CH-O-) at 4.71 and 4.72 ppm, respectively, a signal not present in A_1. These suggest that C_1 and C_2 molecules have one more sugar moiety than A_1. This is completely confirmed by the FAB mass spectra as shown in Figure 1.

Nystatin A_1 has the molecular formula $C_{47}H_{75}NO_{17}$ and a molecular weight of 925. Its FABSM (Figure 1-A_1) shows the molecular ion peak $(M + H)^+$ at m/z 926. In the low mass region, the fragmented mycosamine ion peak at m/z 146 is observed. The molecular ion peak of sample C_1 is at m/z 1056, 130 mass units greater than that of A_1. And there is a fragment peak at m/z 131 in the low mass region, which is not present in A_1. Together with the NMR data that suggest the presence of an additional sugar moiety in C_1, it can be established that m/z 131 fragment derives from a sugar moiety other than mycosamine. Its mass number is the same as the sugar (L-digitoxose) Zielinski[8] obtained from the hydrolysis of nystatin A_3 and polyfungin B. By further consulting the chromatographic data of Thomas,[12,13] it is clear that C_1 is nystatin A_3. The characteristic peaks of C_1 are m/z 1078 $(M + Na)^+$, 1056 $(M + H)^+$, 1038 $(M-H_2O+H)^+$, 146 (mycosamine)$^+$, 131 (digitoxose)$^+$ and 113 (digitoxose-H_2O)$^+$.

The FABSM of C_2 is very similar to that of C_1. Its characteristic peaks are m/z 1062 $(M + Na)^+$, 1040 $(M + H)^+$, 1022 $(M-H_2O+H)^+$, 146 (mycosamine)$^+$, 131 (digitoxose)$^+$, and 113 (digitoxose-H_2O)$^+$. It can be seen that both C_1 and C_2 contain mycosamine and digitoxose. But C_2 is 16 mass units less than C_1, indicating C_2 is one oxygen less. Based on this as well as the NMR and ultraviolet data, the chromatographic analysis results of Thomas' and the fact that C_2 and polyfungin B display similar biological activities,[2,14] it is concluded that C_2 is polyfungin B.

Their structures and fragmentation mechanisms are shown in Figure 2.

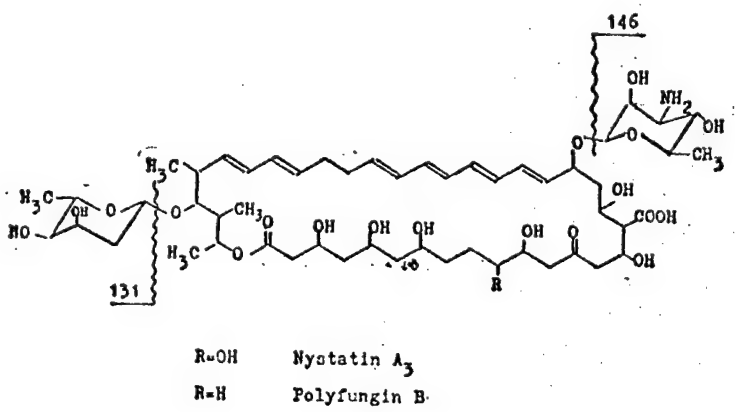

Figure 2. Structures of Polyene Macrolide Antibiotics and Their Fragmentation Mechanisms

Summary

The two major components of Chinese produced nystatins are identified as nystatin A_3 and polyfungin B by ultraviolet, proton NMR and FABSM analysis. Thomas et al. have pointed out that the commercial nystatins from different sources all give positive results in the test based on the procedure of the British Pharmacopoeia (1980 edition), even though their compositions vary widely. Therefore, he suggested that the specification of A_1 content be used for the quality control of the product.[13] The British Pharmacopoeia clearly states that the nystatins should be A_1 based. The semi-quantitative analysis by Ma Jianwen and others shows that the presence of A_1 is not detected among the various lots of Chinese products. Furthermore, the compositions of the products from different sources are not the same. Among them, the products from Jiangsu contain mainly A_3, whose relative abundance is about 30 percent and those from Hubei contain mainly polyfungin B, whose relative abundance is about 40 percent.[14] Therefore, all these products do not meet the specifications of the British Pharmacopoeia. However, we believe that they can be renamed according to their actual compositions.

Acknowledgement: Comrades Liu Yubo [0491 3768 3134] and Zhu Fengjuan [2612 7685 1227] of the Bureau of Drug Control, PLA, supplied the purified nystatin A_1 and the two major components of the Chinese nystatins. Comrade Wang Shaohua [3076 1421 5478] and others at the Institute No 703 made the NMR measurements.

REFERENCES

1. Florey, K., ed. ANALYTICAL PROFILES OF DRUG SUBSTANCES, Vol 6, New York; Academic Press, 1977:341.

2. Polowska, N., et al. Components of polyfungin--a new antifungal antibiotic complex. ADV ANTIMICROBIOL ANTINEOPLASTIC CHEMOTHER 1972; 1:1031.

3. Plociennik, L., et al. Polyfungin, a new fungicidal antibiotic. IV. Use of thin layer chromatography for the evaluation of qualitative composition of the polyfungin complex. CHEM ANAL 1973; 18:151.

4. Chong, C.N., et al. Macrolide antibiotic studies XVI. The structure of nystatin. TETRAHEDRON LETT 1970; (59):5145.

5. Pandey, R.C., et al. Carbon-13 nuclear magnetic resonance evidence for cyclic hemiketals in the polyene antibiotics amphotericin B, nystatin A_1, tetrin B, lucensomycin and pimaricin. J ANTIBIOT 1976; 29:1035.

6. Borowski, E., et al. The structure, modification and biological properties of antibiotics from group of polyene macrolides. KHIM FARM ZH MOSCOW 1977; 11:57.

7. Porowska, N., et al. Composition of polyfungin, a new antifungal agent. REC TRAV CHEM 1972; 91:780.

8. Zielinski, J., et al. The structure of a noval sugar component of polyene macrolide antibiotics: 2,6-dideoxy-L-ribohexopyranose. J ANTIBIOT 1979; 32:565.

9. Cai, Renshen, et al. The study of nystatin A-94, Part I--Nystatin A-94 and the biological characterization of its producing strain. KEXUE TONGBAO [SCIENCE COMMUNICATIONS] 1959; 23:795.

10. Cai, Renshen, et al. The polyene antibiotics produced by the three actinomyces strains isolated from the soils of southern China. YAOXUE XUEBAO [ACTA PHARMACEUTICA SINICA] 1960; 8:47.

11. Bao, Qinzhu, et al. The study of nystatin A-94, Part II--The preparation and characterizations of nystatin A-94. KEXUE TONGBAO [SCIENCE COMMUNICATION] 1959; 24:825.

12. Thomas, A.H., et al. Identification and determination of the qualitative composition of nystatin using thin-layer chromatography and high-performance liquid chromatography. J CHROMATOGR 1981; 216:367.

13. Thomas, A.H., et al. The heterogeneous composition of pharmaceutical grade nystatin. ANALYST 1982; 20:294.

14. Ma, Jianwen, et al. The composition study of domestic and foreign nystatin products by high performance liquid chromatography. YAOXUE XUEBAO [ACTA PHARMACEUTICA SINICA] 1985; 20:294.

12922/6091
CSO: 4008/3003

NEUROTOXIN FRACTION IX FROM BUNGARUS FASCIATUS VENOM STUDIED

Beijing YAOXUE XUEBAO [ACTA PHARMACEUTICA SINICA] in Chinese Vol 21, No 6, 29 Jun 86 pp 416-421

[Article by Kong Jianqiang [1313 0256 1730] and Wu Xiurong [0702 4423 2837], Department of Pharmacology, Zhongshan Medical University, Guangzhou; paper received 25 July 1985]

[Text] Abstract: A postsynaptic neurotoxin--fraction IX was isolated from the venom of Bungarus fasciatus. Unlike other postsynaptic snake venom neurotoxins, fraction IX showed a non-competitive inhibition pattern on the acetylcholine concentration-response curve on frog abdominal rectus muscle. In the presence of neostigmine, high concentration of acetylcholine caused an opposite effect on the abdominal rectus muscle. Under the experimental conditions, fraction IX did not show any significant effect on the binding of ^{125}I-labelled cobrotoxin to the membrane preparations of the electric organ of Narcine maculata. In the experiments using the clamped potential technique, fraction IX showed that it suppressed the endplate current (EPC), which eventually disappeared, and it was able to shorten the half-life of the EPC and increase the magnitude of the decay rate constant (α). However, the EPC equilibrium potential was not changed. Our results showed that fraction IX blocked neural transmissions not by acting on the acetylcholine receptors, but possibly on the endplate ion channels.

Key Words: Bungarus fasciatus; Neurotoxin; Concentration-response curve of acetylcholine; Acetylcholine receptor; Endplate current.

In the previous paper, we reported the isolation of a postsynaptic neurotoxin, fraction IX, from Bungarus fasciatus. It displays a similar activity to that of a neurotoxin isolated by Bon and coworkers from Indian krait. They both show a long delay-response time.[1] In this paper, we studied further the fraction to determine the possible location where it acts to produce its postsynaptic effect.

Materials

Cobrotoxin was provided by Comrade Chen Ruzhu [7115 3067 4591] of the department. Carbachol was from Sigma and chloroacetylcholine from Shanghai No 3 Reagent Plant. Neostigmine methyl sulfate was the product of Shanghai No 7

Pharmaecutical Factory. Other reagents were the Chinese products of pure analytical or chemical reagents. The FT-603 well-type γ detector and FH-408 automatic counter were the products of the state-owned No 261 Factory.

Methods and Results

I. Effect of Fraction IX (Fra.IX) on the Concentration-Response Curves of Acetylcholine (Ach) and Carbamylcholine (Carbachol) on Frog Abdominal Rectus Muscle

The frog abdominal rectus muscle samples were taken and suspended in 5 ml of oxygen-saturated Ringer's solution (room temperature). Ach in concentrations that increase geometrically were added at intervals of 1 minute until there was no more significant response in muscle contraction. The experiments were carried out in four steps: measuring the normal concentration-response curve; measuring the same curve 80 minutes after addition of Fra.IX; measuring the Ach curve after Fra.IX was removed by washing and neostigmine added; and measuring the Ach curve after repeated washing for 4 hours and fresh stigmines were added. All four were carried out on the same sample.

The procedures for the Carbachol concentration-response curve were the same as above except that only steps 1 and 2 were followed.

Figure 1-a shows the effect of Fra.IX on the Ach concentration-response curve of frog abdominal rectus muscle. A normal response curve, in which logarithmic dosage is plotted versus percentage response, is a symmetrical S-shaped curve. The concentration-response curve shifted right and maximum response dropped 80 minutes after the addition of Fra.IX (10 μg/ml), a non-competitive inhibition pattern. After the addition of neostigmine, the curve showed a biphasic effect. In the low concentration region, the curve shifted left, a sign of partial recovery, while in the high concentration region, the curve was neither rising with increasing concentration nor levelling off at a certain peak value. Rather, it went down with increasing Ach concentration. The same effect did not appear in the control (Figure 1-b). The effect of Fra.IX remained even after the samples were rinsed for 4 hours.

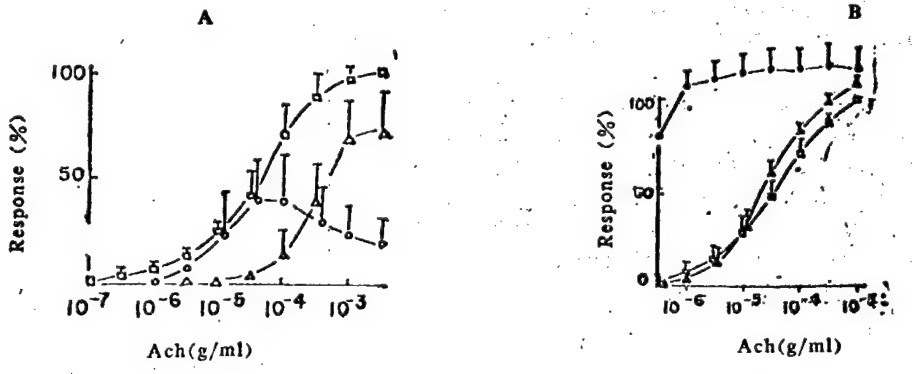

Figure 1. Effect of Fra.IX on concentration response relationship of Ach. A. □: normal; Δ: 80 minutes after Fra.IX (10 μg/ml); o: 10 minutes after neostigmine (2 μg/ml); preparation: frog abdominal rectus. B. Control. □: normal; Δ: normal but 80 minutes later; o: 10 minutes after neostigmine

When Ach was substituted with carbachol, a cholinergic activator that is hydrolyzed more slowly, a similar effect was obtained even in the absence of stigmine (Figure 2).

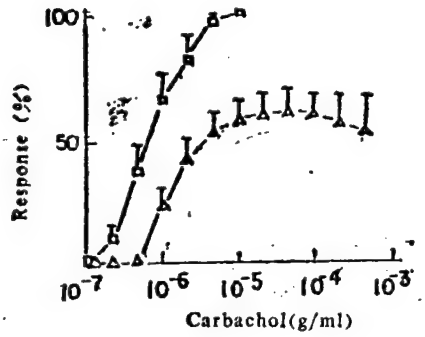

Figure 2. Effect of Fra.IX on concentration-response relationship of carbachol. □: normal; Δ: 80 minutes after Fra.IX (10 μg/ml); preparation: frog abdominal rectus

II. Effect of Fra.IX on the Binding of ^{125}I-labelled Cobrotoxin to the Membrane Preparations Rich in Ach Receptors

Fresh South China Sea electric rays (Narcine maculata) were acquired and the rough membrane preparations of its electric organ were prepared according to the procedure of Hu Benrong [5170 2609 2837] and coworkers.[2] The experiments were divided into the total binding, nonspecific binding, Fra.IX and cobrotoxin control groups. The procedures for each group are listed in Table 1.

Table 1. The Processes of Binding Test of Membrane Rich in Ach-R

Groups	Protective solution(μl)	Membrane preparation(μl)	Cobrotoxin	Fra. IX		^{125}I-cobrotoxin	
Total	200	100	---	---	①	v c 100 μl	②③④⑤
Nonspecific	100	100	15 μg/100 μl	---	①	v c 100 μl	②③④⑤
Fra. IX	100	100	---	v c 100 μl	①	0.48 μg/100 μl	②③④⑤
Cobrotoxin	100	100	v c 100 μl	---	①	0.48 μg/100 μl	②③④⑤

v c: Various concentrations. ①: 24°C incubation for 60 min; ②: 24°C reincubation for 40 min; ③ Reaction stopped by 4°C phosphate buffer 3ml; ④: 4000 r/min. centrifugation for 10 min; ⑤: γ-ray account of sediments

The results are shown in Figure 3. The binding of ^{125}I-labelled cobrotoxin to the rough membrane preparations increased with increasing concentration of the labelled neurotoxin. This is the total binding curve. The labelled toxins bound to the rough membrane preparations were replaced by the unlabelled ones after a large concentration of nonlabelled cobrotoxin was added. The counts measured then was the nonspecific bindings of the toxin to the membrane preparations. The specific binding curve was obtained by subtracting the nonspecific bindings from the total.

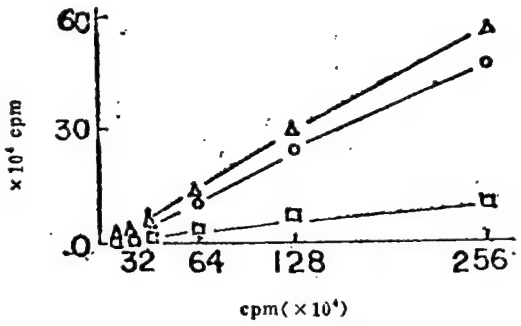

Figure 3. Binding of ^{125}I-cobrotoxin to membrane rich in n-Ach receptor. Abscissa: added ^{125}I-cobrotoxin; ordinate: bound ^{125}I-cobrotoxin; Δ: total binding; ▫: nonspecific binding; o: specific binding

Figure 4 shows that, under the experimental dosage (10 μg/ml)[1] to block the neuron-muscle transmission, Fra.IX does not inhibit to any significant extent the binding of labelled cobrotoxin to the rough membrane preparations. However, at high concentration (100 μg/ml), the binding of labelled cobrotoxin is reduced by 3/4. The nonlabelled cobrotoxin shows a hyperbolic inhibition pattern to the binding of the labelled to the rough membranes.

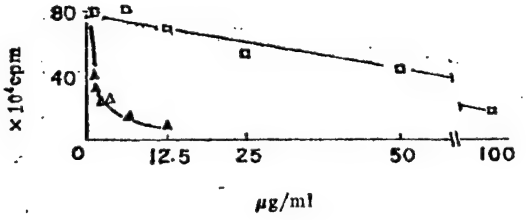

Figure 4. Effect of Fra.IX on the binding of ^{125}I-cobrotoxin to membrane rich in n-Ach receptor. Ordinate: bound ^{125}I-cobrotoxin; abscissa: concentration of nonlabelled cobrotoxin (Δ) or Fra.IX (▫)

III. Effect of Fra.IX on EPC

The endplate potential fixation was based on the procedures of Takeuchi and coworkers.[3,4] Experiments were carried out at room temperature in winter (13-16°C). Samples of nerve ischiadicus-muscle sartorius from frog were prepared, treated for 60 minutes with a Ringer's solution containing 650 mM of glycerol and then suspended in the oxygen-saturated Ringer's solution. The samples were immersed no more than 2 mm deep. The neurons were stimulated with an ultrahigh-intensity square wave, bandwidth 0.1 ms and frequency 1 Hz, through a pair of platinum electrodes. Glass microelectrodes were placed at the endplate region of the surface muscle fibers to record potential. In the same muscle fiber, a microelectrode for the feedback current was placed within 50 μm from the measuring electrode. Both microelectrodes were filled with a 3 M KCl solution. The resistance of the measuring electrode was 2-5 MΩ and that of feedback current electrode 2-3 MΩ. The reference electrode was an Ag-AgCl electrode, which was grounded through a current-voltage converter. The experimental setup is illustrated in Figure 5. The results are as follows.

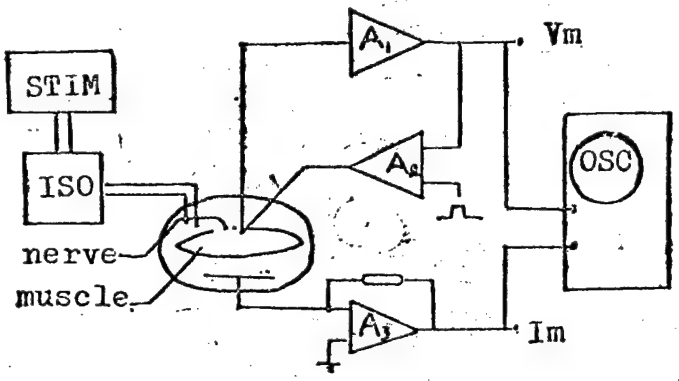

Figure 5. Diagram of EPC measurement. A_1: microelectrode amplifier; A_2: feedback amplifier; A_3: current-voltage converter

1. The blank control: There was no significant difference in the peak intensity (I_0), half-life ($T_{1/2}$) and decay rate constant (α) when EPC data recorded at the beginning and 60 minutes later were compared (Table 2).

Table 2. Effects of Some Factors on EPC. $\bar{X}\pm SD$ (n)

		$T_{1/2}$ (ms)	α (ms^{-1})
Blank	B	4.12±0.37 (6)	0.36±0.023 (6)
60 min.	A	4.35±0.35* (6)	0.372±0.027* (6)
Procaine	B	2.9±0.9 (11)	0.272±0.051 (12)
	A	1.4±0.7**(12)	1.339±0.366**(7)
Cobrotoxin	B	3.7±0.5 (8)	0.333±0.049 (7)
	A	3.4±0.8* (12)	0.318±0.098* (11)
Fra. IX	B	5.0±0.6 (25)	0.256±0.045 (26)
	A	3.6±0.6**(37)	0.311±0.044**(38)

B: before; A: after; *: $P>0.05$; **: $P<0.01$

2. Effect of procaine on EPC: Procaine, a local anesthetic, affects both the amplitude and duration of endplate potential (EPP) and EPC. It binds to the Ach receptor--ion channel complex at a location different from that of the cholinergic activators. We used procaine as a positive control in this paper. As shown in Figure 6, procaine reduces the peak heights of EPP and EPC, accelerates the decay of EPC, and decreases the $T_{1/2}$ of EPC (Table 2). These results agree with those of Deguchi and coworkers.[5]

3. Effect of cobrotoxin on EPC: Cobrotoxin acts on the Ach receptors on the posterior membrane of endplate to block off the action of cholinergic activators. We studied and compared the effect of both cobrotoxin and Bungarus fasciatus Fra.IX on EPC. After the addition of cobrotoxin (2 μg/ml), the EPC gradually diminished and eventually disappeared. But cobrotoxin has no significant effect on the EPC decay rate and $T_{1/2}$ (Table 2).

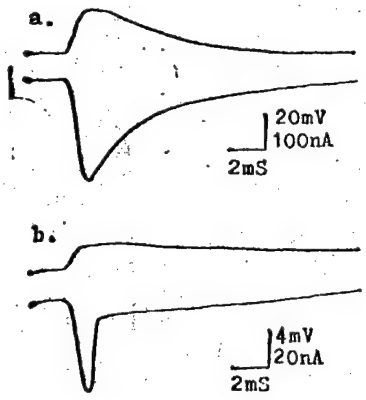

Figure 6. Effect of procaine on EPP and EPC. Upper: EPP; Lower: EPC; clamped potential: -105 mV/ a: before; b: 32 minutes after procaine (100 μg/ml)

4. Effect of Fra.IX on EPC; After the addition of Fra.IX (10 μg/ml), the EPC gradually diminished and eventually disappeared. Fra.IX also affected the duration of EPC, accelerated its decay rate and shortened its $T_{1/2}$ (see Figures 7, 8 and Table 2).

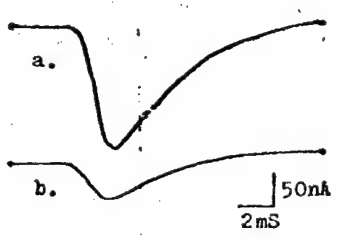

Figure 7. Effect of Fra.IX on the $T_{1/2}$ of EPC. a: before, $T_{1/2}$ = 4.2 ms; b: 38 minutes after Fra.IX, $T_{1/2}$ = 3.4 ms. Clamped potential: -105 mV

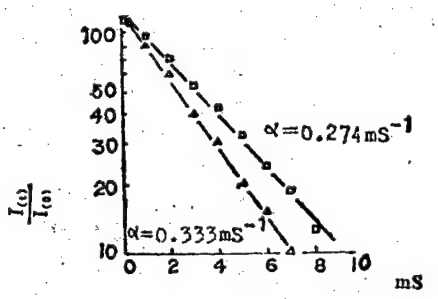

Figure 8. Effect of Fra.IX on EPC decay constant (according to Figure 7). □: before; Δ: 38 minutes after Fra.IX. Clamped potential: -105 mV

5. Effect of Fra.IX on the equilibrium potential of EPC (V_{eq}): The membrane potentials were clamped in a series of different voltages with each lasting 3 s. The neurons were stimulated at each potential to induce a corresponding EPC, which was recorded. A plot with clamped membrane potential as abscissa and peak value of EPC as ordinate was made. Linear regressions were done for each data point and the intercept of the regression line with the abscissa gave the V_{eq} of the endplate. Figure 9a shows a group of normal EPC. After the addition of Fra.IX, their EPC gradually diminish, $T_{1/2}$ are shortened, and their decay rates accelerated. But there is no significant change in their V_{eq} (Figures 9b and 10). The initial V_{eq}: 0.39 ± 2.88 mV (n = 8) and V_{eq} after toxin addition: 0.43 ± 6.97 (n = 30), P > 0.05.

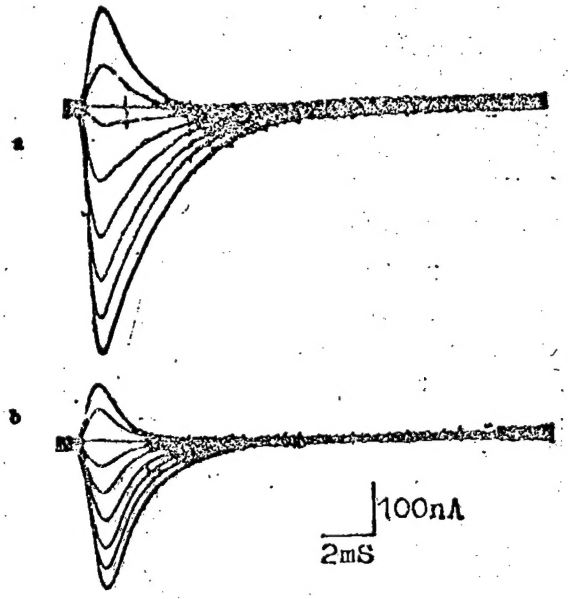

Figure 9. Effect of Fra.IX on EPC equilibrium potential. a: before; b: 55 minutes after Fra.IX (10 µg/ml); Potential series: 34, 14, -9, -34, -57, -81, -103, -127, -151 mV

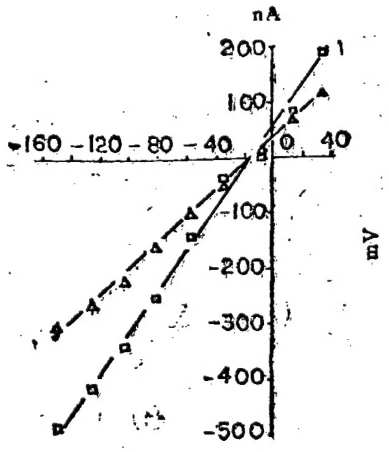

Figure 10. Effect of Fra.IX on EPC equilibrium potential. Ordinate: peak value of EPC; Abscissa: clamped membrane potential; □: before; Δ: 55 minutes after Fra.IX (according to Figure 9)

Discussion

The Ach receptor--ion channel complex is a basic functioning unit that participates in endplate ion activities. It contains at least two distinctive parts: the Ach receptor part and ion transport part. The choline receptor blockers bind to the former and inhibit the activators competitively. The other type of drugs such as local anesthetics and histrionicotoxin (HTX) act on the ion transport part to close off the channel and thus block the action of activators on the receptor--channel complex. This kind of blockage is noncompetitive.[13] They apparently do not affect the binding of activators or inhibitors to the receptor part but do affect, more or less, the duration and decay rate of EPC.[6-8]

From the results of the previous paper,[1] it can be seen that Fra.IX acts on the postsynaptic membrane. But its action is different from that of the regular postsynaptic neurotoxins such as cobrotoxin, Fraction XIII of Bungarus fasciatus venom, Fraction VIII of Ophiophagus hannah venom. The latter toxins inhibit the Ach receptors competitively that can be reversed by neostigmine.[9-11] In the samples of frog abdominal rectus muscle, Fra.IX inhibits the action of Ach non-competitively. After adding neostigmine to raise the activator concentration in the synaptic gap, the response of the samples to high concentration of Ach not only is not restored but instead drops even further, resulting in a bell-shaped curve. The phenomenon cannot be explained totally by non-competitive inhibition. It has been known that butyltrimethylammonium and its derivatives activate frog rectus muscle at low concentration and inhibit at high concentration, resulting in a bell-shaped concentration-response curve. It is believed that butyltrimethylammonium can bind to two types of receptor system. R receptors are activating with an internal activity $\alpha = 1$ and R' receptors are inhibitive with an internal activity $\alpha' = -1$. Butyltrimethylammonium has different affinity toward different receptors. Its dissociation constant for R receptors K_A and for R' receptors K_A' are 0.005 mM and 10 mM, respectively, hence the phenomenon of activation at low concentration and inhibition at high concentration.[12] The mechanism by which Fra.IX alters the response of frog abdominal rectus muscle to high concentration of activator is not clear. But there are two possibilities: a) Fra.IX alters the affinity of activators to R' receptors so that there is an increased binding of the activator to the R' receptors. With a high concentration of activator, the impact of the originally dormant R' receptors becomes noticeable. b) Fra.IX binds better to an open ion channel. High concentration of activator opens up more channels, which results in more channels being blocked and the response of the samples drops.

Hu Benrong and coworkers have reported that the binding of ^{125}I-labelled cobrotoxin to the membrane preparations of the electric organ of South China Sea electric rays is specific, with high affinity, and saturable. They have also described that nonlabelled toxin, carbachol, and tubocuranine can inhibit competitively the binding of ^{125}I-labelled neurotoxin to the membrane preparations of electric organ.[2] The method was used in this paper and the results showed that, with the dosage used in this study, Fra.IX had little effect on the binding of ^{125}I-labelled cobrotoxin to the membrane of the electric organ.

Fra.IX reduces the amplitude of EPC, accelerates the decay rate and shortens its $T_{1/2}$. It is possible that Fra.IX blocks the ion channels by binding to the Ach receptor--ion channel complex and produces the postsynaptic blockage. Fra.IX has no obvious effect on the V_{eq} of EPC, indicating that Fra.IX has no preference over sodium or potassium transport. It is assumed that, during the endplate activity, sodium and potassium ions pass in and out of the membrane through shared channels. Our results are consistent with this theory.

We have pointed out that Fra.IX exerts its blocking effect by a mechanism other than acting on the Ach receptors, possibly on the endplate ion channel. The mode of action of Fra.IX is somewhat similar to that of ceruleotoxin: they both act very slowly, inhibit non-competitively the action of cholinergic activators, do not affect the binding of cobrotoxin to the Ach receptors, and bind tightly that cannot be easily reversed by rinsing. But there are also differences between them: Using the ceruleotoxin provided by Bon in their experiments, Ho and Lee suggested that the toxin also produced presynaptic blockage and muscular toxicity.[14] Therefore, it is difficult to determine at the moment whether the two are the same fraction of the Bungarus fasciatus venom.

REFERENCES

1. Kong Jianqiang and Wu Xiurong. A preliminary study on the separation of Bungarus fasciatus venom and the resulting fraction IX. YAOXUE XUEBAO [ACTA PHARMACEUTICA SINICA] 1986; 21:260.

2. Hu Renrong, et al. The isolation and characterization of the acetylcholine receptors from Chinese electric rays. DONGWUXUE YANJIU [ZOOLOGICAL RESEARCH] 1981; 2 (supplemental):59.

3. Takeuchi, A. and Takeuchi, N. Active phase of frog's endplate potential. J NEUROPHYSIOL 1959; 22:395.

4. Kuba, K., et al. A study of the irreversible cholinesterase inhibitor, Diisopropylfluorophate, on time course of endplate currents in frog sartorius muscle. J PHARMACOL EXPER THER 1974; 189:499.

5. Deguchi, T. and Narahashi, T. Effect of procaine on ionic conductances of endplate membrane. Ibid., 1971; 176:423.

6. Adams, P.R. Drug blockade of open endplate channels. J PHYSIOL 1976; 260:531.

7. Albuquerque, E.X. and Oliveira, A.C. Physiological studies on the ionic channel of nicotinic neuromuscular synapses. In: Ceccarelli, B. and Clementi, F., ed. ADVANCES IN CYTOPHARMACOLOGY, Vol 3. New York: Raven Press, 1979:197-211.

8. Adams, P.R. A model for the procaine endplate current. J PHYSIOL 1975; 246:61.

9. Su C., et al. Pharmacological properties of neurotoxin of cobra venom. In: Russell, F.E. and Saunders, P.R., ed. ANIMAL TOXINS. Oxford: Pergamon Press, 1966:259-267.

10. Kong Jian-qiang and Wu Xiurong. The isolation of Bungarus fasciatus venom and the pharmacological study on its components. YAOXUE XUEBAO [ACTA PHARMACEUTICA SINICA] 1983; 18:97.

11. Ni Huifang [0424 1979 5364] and Wu Xiurong. The isolation of Ophiophgus hannah Canton venom and the study of its components. YAOXUE XUEBAO [ACTA PHARMACEUTICA SINICA] 1983; 18:161.

12. Jin Zhengjun [6855 2973 0971]. "The kinetics of the drug-receptor interaction," Eds. Zhang Changshao [1728 2490 4801] and Zhang Yi [1728 3015], Pharmacology, Vol 1, 1st edition, Beijing, People's Health Publications, 1965: 24-60.

13. Heidmann, T. and Changeux, J.P. Structural and functional properties of the acetylcholine receptor protein in its purified and membrane-bound states. ANN REV BIOCHEM 1978; 47:317.

14. Ho C.L. and Lee C.Y. Mode of neuromuscular blocking action of ceruleotoxin. TOXICON 1983; 21:301.

12922/6091
CSO: 4008/3003

END